

I

THE PREPARATION AND CONFIGURATION OF
LEVOROTATORY 4,5-DIMETHYL-1,3-DIOXOLANE

II

STUDIES OF COLOR CENTERS IN ALKALI
HALIDE CRYSTALS

III

A STRUCTURAL INVESTIGATION OF THE
STRONTIUM-ZINC SYSTEM

Thesis by

Paul Joseph Shlichta

In Partial Fulfillment of the Requirements

For the Degree of

Doctor of Philosophy

California Institute of Technology

Pasadena, California

1956

ACKNOWLEDGMENT

I wish to express my gratitude to Professor Linus Pauling, Professor Howard J. Lucas, and Professor B. Gunnar Bergman for their wisdom and patience in supervising the research reported in this thesis;

to the National Science Foundation and to the Shell Oil Company for their generous fellowship grants which enabled me to pursue my studies free from financial pressures;

to all those who helped me in the final preparation of this thesis, especially Mrs. Margaret Hillman, Mrs. Adelheid Oberhettinger, and Mr. Clive Greenough;

and lastly to the many friends and associates in the California Institute of Technology who have helped to make my stay here both edifying and enjoyable.

FORSAN ET HAEC OLIM MEMINISSE JUVABIT.

- Virgil, Aeneid

ABSTRACT

- I. The configuration of the formal of D(-)-2,3-butanediol has been established unequivocally by reactions of the diol under basic conditions with methylene iodide, methylene chloride, and chloromethyl acetate. The products are optically active, are alike, and are the same as the one obtained in the acid-catalyzed reaction of the glycol with formaldehyde.
- II. The coloration of sodium chloride by white x-radiation has been separated into two distinct types. The intense color at the surface involves the creation of new anionic vacancies by long-wave radiation; aggregate color centers result from optical or thermal bleaching. The less intense coloration throughout the crystal is due to the short-wave radiation; no new vacancies are created and no secondary coloration occurs. Plastic deformation does not affect the overall colorability but greatly enhances the secondary coloration effects. Tentative mechanisms for these processes are discussed.

Studies of the secondary radiative coloration, the so-called colloidal band in additively colored crystals, and the color of blue rocksalt have led to the suggestion that these color centers are members of a continuous series of F center aggregates. The possibility of a true colloidal dispersion in additively colored sodium chloride has been investigated by comparison of these crystals with sodium chloride, known to contain colloidal copper.

Crystals of sodium chloride have been grown containing heavy metal ion impurities. Spectrophotometric studies have been

ABSTRACT (Continued)

II. made of these crystals before and after radiative and additive coloration. The ultraviolet absorption bands in the uncolored crystals have been tentatively explained in terms of V centers. X-radiation and bleaching destroys some of the absorption bands and creates others.

III. An investigation of the strontium-zinc system, using x-ray diffraction techniques, has revealed four intermetallic phases. The compound SrZn_{13} , previously reported elsewhere, has been confirmed with respect to composition and symmetry. The second phase, SrZn_5 , contains 24 atoms in its unit cell, is orthorhombic, and has been tentatively assigned the symmetry Pmnb . The third phase, SrZn_2 , is also orthorhombic, and has 12 atoms in a body-centered unit cell. No single crystals of the fourth phase have been isolated, but the composition has been shown to correspond approximately to Sr_3Zn_2 or Sr_4Zn_3 .

The structure of the SrZn_2 phase has been worked out in detail. It has the space group $\text{D}_{2h}(28)\text{-Imma}$, and corresponds to an orthorhombic distortion of the hexagonal magnesium boride structure.

TABLE OF CONTENTS

<u>PART</u>	<u>TITLE</u>	<u>PAGE</u>
I	THE PREPARATION AND CONFIGURATION OF LEVOROTATORY 4,5-DIMETHYL-1,3-DIOXOLANE	1
	Experimental	2
	D(-)-2,3-Butanediol	2
	Chloromethyl acetate	3
	Discussion of Results	7
	Summary	10
II	STUDIES OF COLOR CENTERS IN ALKALI HALIDE CRYSTALS	12
	Preface	12
	A. Mechanisms of Radiation Coloring	12
	Introduction	12
	Experimental Techniques	15
	Alkali Halide Crystals	15
	X-Radiation	15
	Optical Bleaching	16
	Thermal Bleaching	18
	Plastic Deformation	18
	Absorption Spectra	21
	Results	21
	Coloration by X-Radiation	21
	Bleaching Effects	22
	Filtered Radiation	25
	Plastic Deformation	25

TABLE OF CONTENTS (continued)

<u>PART</u>	<u>TITLE</u>	<u>PAGE</u>
II	Thermal Bleaching	29
	Interpretation of Data	31
B.	Color Center Aggregates in Sodium Chloride	
	Additive Coloration - The Colloidal Band	37
	Introduction	37
	Experimental	38
	Treatment of NaCl with Alkali Vapor	38
	Heat Treatment of Additively Colored Crystals.	45
	Electron Spin Resonance	48
	Electron Microscope	48
	Blue Rocksalt.....	48
	Introduction	48
	Experimental	49
	Specimens	49
	Heating	50
	Plastic Deformation	50
	X-Radiation	50
	Natural Sodium Fluoride	53
	Interpretation of Data	53
C.	Color Centers in Crystals Containing Impurities ..	58
	Introduction	58
	Experimental Techniques	59

TABLE OF CONTENTS (continued)

<u>PART</u>	<u>TITLE</u>	<u>PAGE</u>
II	Growth of Crystals from Solution	59
	Growth of Crystals from Melt	62
	Treatment with Sodium Vapor	68
	Radiation Colors	68
	Experimental Results	68
	NaCl:Ca	68
	NaCl:Rare Earths	69
	NaCl:Cd	69
	NaCl:Ag	70
	NaCl:Mn	70
	NaCl:Cu	72
	NaCl:Cr	73
	NaCl:Fe	73
	NaCl:Ni	73
	NaCl:Pt	76
	NaCl:Au	76
	NaCl:Co	78
	NaCl:Pd	80
	NaCl:Ba	80
	NaCl:O	80
	X-ray Coloration	80
	Secondary Coloration	84

TABLE OF CONTENTS (continued)

<u>PART</u>	<u>TITLE</u>	<u>PAGE</u>
II	Interpretation of Data	88
	The State of the Impurity Ion in the Crystal	88
	Treatment with Sodium Vapor	89
	Ultraviolet Absorption Peaks and x-ray Coloration	90
III	A STRUCTURAL INVESTIGATION OF THE STRONTIUM-ZINC SYSTEM ...	95
	A. Phase Diagram of the System	95
	X-Ray Powder Photographs	95
	Preparation of the melts	95
	Preparation of the x-ray powder photographs	96
	Interpretation of powder photographs	97
	Isolation of the Individual Phases	99
	Experimental	99
	Examination of the melts	99
	X-ray photographs of the pure phases ...	100
	Interpretation of Data	103
	Phase I	103
	Phase II	105
	B. The Structure of Phase III	106
	Experimental	106
	Determination of Structure	109
	Space Group	109

TABLE OF CONTENTS (continued)

<u>Part</u>	<u>Title</u>	<u>Page</u>
III	Layering.....	109
	Composition of the unit cell	109
	The packing of the strontium atoms	110
	Structures Based on Sr_4Zn_6	110
	Previously investigated A_2B_3 structures	110
	A trial structure for Sr_4Zn_6	111
	Trial Structure Based on Sr_4Zn_8	115
	Formulation of the trial structure	115
	Estimate of parameters from interatomic distances	115
	Test of the trial structure	115
	Appendix: Assignment of Powder Lines of Strontium - Zinc Alloys	120
	References	132
	Propositions	135

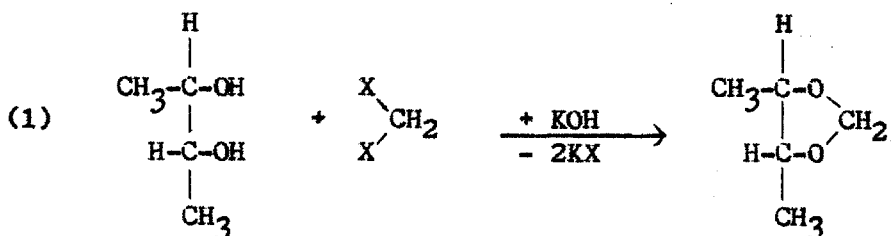
I THE PREPARATION AND CONFIGURATION OF
LEVOROTATORY 4,5-DIMETHYL-1,3-DIOXOLANE

THE PREPARATION AND CONFIGURATION OF
LEVOROTATORY 4,5-DIMETHYL-1,3-DIOXOLANE

D(-)-2,3-Butanediol reacts with formaldehyde in dilute sulphuric acid to form a cyclic formaldehyde-acetal (4,5-dimethyl-1,3-dioxolane)⁽¹⁾. This "formal" is optically active ($\alpha_D^{25} = -23.38^\circ$), thus excluding the possibility of a single Walden inversion, which would produce an optically inactive derivative of the meso-glycol. The D-configuration is not assured, however, since there is a remote possibility of a Walden inversion occurring on both asymmetric carbons, resulting in the L-isomer.

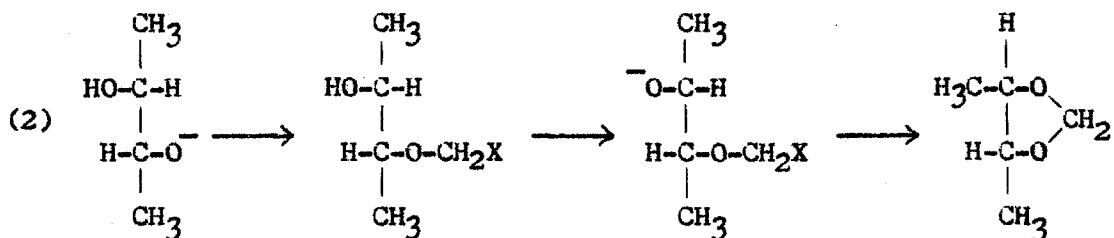
In order to establish the configuration, the formal had to be synthesized in such a way as not to involve at least one of the Alk-O bonds. Since the formal may be regarded as cyclic diether, the Williamson synthesis immediately suggested itself. Three modifications seemed feasible.

A. Methylene halide and glycol in the presence of base:



This method would not be unambiguous, however, since there is a possibility that the methylene halide would be first hydrolyzed to formaldehyde which in turn would react, with or without inversion. Moreover, the KOH tends to dehydrate the glycol to methyl ethyl ketone.

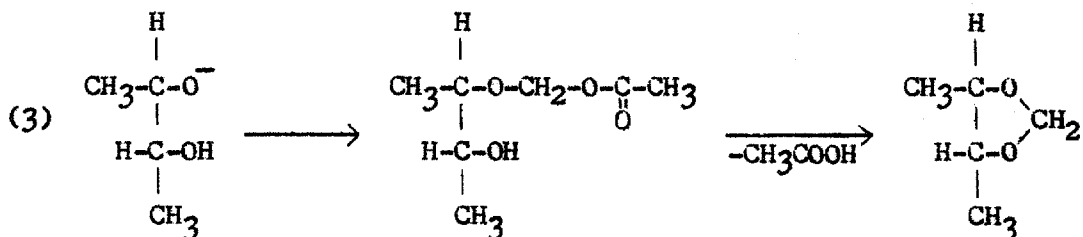
B. Therefore, a direct Williamson synthesis would seem more desirable:



but the pure disodium glycolate is difficult to prepare and has no convenient common solvent with the methylene halide.

Therefore, noting Helmkamp's work on the 2,3-butanediol ethers⁽²⁾, a solution of the sodium glycolate in a five or tenfold excess of the glycol was used. Since this results almost entirely in the monosodium glycolate, a successful reaction would involve either (1), a dynamic equilibrium between the sodium glycolate and glycol adduct, or (2), a single Williamson reaction followed by a condensation with the expulsion of hydrogen halide, with the latter's subsequent neutralization by the unreacted monosodium glycolate.

C. Chloromethyl acetate reacts with alcohols and sodium alcoholates to form oxymethyl acetate ethers. A reaction of this with the sodium salt of the glycol should lead to a mixed hemiacetal-ester which might be susceptible to condensation to the formal and acetic acid:



All of the above methods were tried and all were ultimately successful.

EXPERIMENTAL

D(-)-2,3-Butanediol, a fermentation product of bacillus polymixa, was obtained from the Northern Regional Research Laboratories. The

observed rotation for the pure glycol is $\alpha_D^{25} = -13.02^\circ$. In all experiments here, the stock glycol was distilled in vacuo (75° @ 4 mm) to remove water and biacetyl. Due to the non-critical nature of the work here, glycol having $\alpha_D^{25} = -12.25^\circ$ or better, was considered satisfactory.

Chloromethyl acetate was at first prepared by reacting paraformaldehyde with acetyl chloride. When equimolar quantities are mixed in a reflux apparatus, there is no perceptible reaction, but the addition of a few zinc chloride crystals causes a rapid exothermic reaction leading to boiling; when this subsides, the mixture is refluxed over a water bath at 90° for three hours. The mixture is then distilled at 80 mm (with a dry ice trap to catch unreacted acetyl chloride), the fraction passing over at 50° or higher, being collected. This is redistilled at atmospheric pressure, the 111-113 $^\circ$ fraction being reasonably pure product; the yield is approximately 25%.

A better method, used in later preparations here, is the direct chlorination of methyl acetate in liquid phase at room temperature with constant ultra violet irradiation or, better yet, strong sunlight. A trap is necessary for escaping hydrogen chloride. The chloromethyl acetate is very easily separated from the methyl acetate (b.p. 56°) and higher boiling poly-halogen esters. Before redistilling the remaining hydrogen chloride is best removed with anhydrous potassium carbonate. Three moles (222.2 g.) of methyl acetate, chlorinated for five hours while exposed to long wave ultra-violet radiation, yielded 1 mole (108.5 g.) of pure product (b.p. 112.5-115 $^\circ$ @ 747 mm; Huntress cites 115 $^\circ$ @ 748 mm).

D(-)-4,5-Dimethyl-1,3-dioxolane. In the preparations below, the formal and/or other volatile products were removed from the reaction mixture by partial vacuum distillation and collected in the dry ice trap. Since this procedure sacrifices efficiency for convenience, the true yields

are probably higher than those recorded below.

A. Potassium hydroxide (0.2 mole; 11.2 g.) was added to 1.0 mole (90.1 g.) of D(-)-2,3-butanediol. The solution heated up spontaneously and turned yellow; after cooling 0.2 mole (53.6 g.) of CH_2I_2 was added. The mixture immediately warmed up, turned deep red (due to the liberation of iodine), and boiled gently. It was then refluxed over steam for one hour.

Distillation yielded 1.6 g. (.014 mole; 14% yield) of almost pure formal. Slight contamination of hydrogen iodide caused yellowing on exposure to light. About 0.1 mole of unreacted methylene iodide was recovered.

B. The sodium glycolate solution was prepared by dissolving 0.2 moles (4.6 g.) of sodium (wire or small pellets) in 1.0 mole (90.1 g.) of D(-)-2,3-butanediol. At first there was a moderately vigorous evolution of hydrogen accompanied by heating sufficient to melt the sodium within 2 minutes. A cold water bath was used as a moderator since the reaction is best maintained at 100° . Toward the end, the reaction subsided sharply and the last bits of sodium dissolved only with difficulty. The solution was straw yellow and congealed at 40° - 50° .

Methylene iodide was used at first, it being the most reactive halide. One tenth mole of the iodide was introduced slowly into the glycolate solution at about 100° , the volatile products being immediately distilled over. Although there was immediate darkening (iodine color), and a gradual precipitation of sodium iodide, the distillate was primarily methyl ethyl ketone and similar degradation and oxidation products of the glycol. In a later attempt the reactants were mixed in a reflux apparatus, placed on a steam bath for 2-3 hours, and the volatile products removed as above and fractionated. Only a few drops of product came over at

90°-110° giving a very faint test for formaldehyde (chromotropic acid test). Only one fraction (0.5 g.), passing over at 125°-130°, had the requisite optical activity and gave a very faint chromotropic acid test. This was labeled product #1.

Later, methylene chloride (b.p. 50°) was substituted for the iodide; this formed a clear homogeneous solution with the glycolate with no apparent reaction, but after 2-3 minutes refluxing over a small burner flame, the mixture became turbid and began precipitating sodium chloride. After one hour there was a strong smell of the formal. Stripping of the volatile components, as before, and redistilling yielded 4.9 g. (0.044 mole; 44% yield) of formal with a boiling point of 95.5-96° @ 748 mm. An analysis, by Eleck Laboratories, gave the following:

Calculated for $C_5 H_{12} O_2$: C, 58.80; H, 9.67

Found: C, 58.85; H, 9.70

This, together with the physical constants tabulated in Table I, established the identity of the formal.

C. Chloromethyl acetate was added in a reflux apparatus to 0.1 mole (2.3 g.) of sodium dissolved in 1.0 mole (90.12 g.) of D(-)-2,3-butanediol. Immediately there was a heavy precipitation of sodium chloride. The subsequent course of the reaction depended upon the concentration ratio of the reactants. (1) In equimolar quantities, the reaction apparently proceeded no further; no volatile product could be obtained. Prolonged heating resulted in a faint odor of formaldehyde. (2) When only half as much chloromethyl acetate was added (i.e. basic conditions) the mixture formed a dark brown precipitate and the only volatile product found (approx. 1 g.) boiled at 40°, was optically inactive, gave no halogen test, and had an ester odor. (3) When a strong excess of chloromethyl acetate (0.15-0.2 moles) was added (i.e. acid conditions) and the mixture refluxed

Table I. Properties of D(-)-4,5-Dimethyl-1,3-dioxolane

Reagent	b.p.	α_D^{25}	n_D^{25}	d_4^{25}
Formaldehyde (a)	95.6-.9° @ 746 mm	-23.38°	1.3959	0.9346
CH ₂ Cl ₂	95.5-96° @ 748 mm	-23.40°	1.3978	0.936
Chloromethyl acetate	95.2-96.2° @ 748 mm	-22.40°	1.3970	- - -
CH ₂ I ₂ + KOH (b)	90-92° @ 748 mm	-22.25°	1.4130	- - -

(a) Garner and Lucas, JACS **72** 5498 (1950).

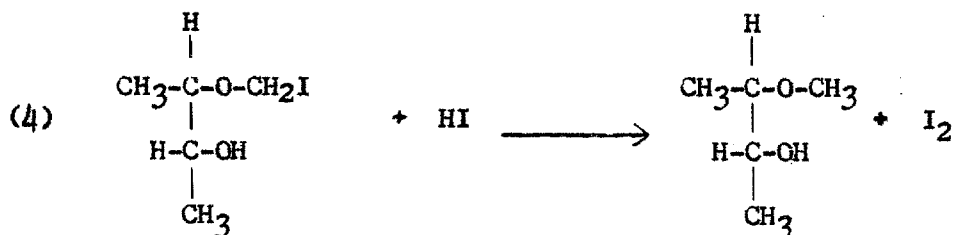
(b) Distilled from reaction mixture, partially as azeotrope.
Dried with K₂CO₃ but not redistilled.

for 1-2 hours, it turned faintly pink and smelled of formal. Stripping and redistilling gave 4.5 g. (.04 mole; 40% yield) of formal boiling at 95.2-96.2° @ 748 mm.

DISCUSSION OF RESULTS

A. Methylene iodide + glycol + potassium hydroxide: The reaction does produce a limited yield of formal, but inasmuch as the initial reaction appears to be rapid, whereas the product is formed slowly, the preliminary criticism is reinforced, and the reaction must be discarded as an unreliable criterion of configuration.

B. Methylene halide + monosodium glycolate: An examination of product #1 with respect to C,H analysis, optical rotation, boiling point, and index of refraction established it almost certainly as threo-2-methoxy-3-butanol (see Table II). Since there is virtually no methyl iodide in the redistilled methylene iodide (b.p. $\text{CH}_3\text{I} = 46^\circ$; $\text{CH}_2\text{I}_2 = 180^\circ$), it seems likely that the initial condensation is with the glycol or sodium glycolate indiscriminately; this would produce a considerable hydrogen iodide concentration which could reduce the iodomethyl group⁽³⁾, and lead to the formation of D(+)-threo-2-methoxy-3-butanol:



The sodium would serve merely to shift the equilibrium. Any unreduced iodomethyl ether is presumably decomposed or oxidized before it can condense to the formal. In any case, the exact nature of the main reaction of the methylene iodide and glycol is unknown, except that it produces iodine and glycol degradation products (methyl ethyl ketone,

Table II. Comparison of Product #1 and D(+)-threo-3-Methoxy 2-Butanol

Mode of Synthesis	b.p.	α_D^{25}	n_D^{25}
<u>Threo D</u> (-)-3Methoxy-2-Butanol (c)	126.4° @ 748 mm	+24.25	1.4067
Product #1	124-127.5° @ 748 mm	+23.35	1.418
Analysis of Product #1:			
Calculated for C ₅ H ₁₄ O ₆ : C, 57.66; H, 11.62			
Found: C, 56.36; H, 11.15			

(c) Helmkamp and Lucas JACS 74 952 (1952).

biacetyl, etc.). A detailed study of this was not considered pertinent to the main problem.

In contrast, the clean reaction with methylene chloride shows the feasibility of a double Williamson reaction when no oxidation is involved and provides an undisputable D formal.

C. Chloromethyl acetate + sodium glycolate: Two reactions may be postulated a priori for the first step of the reaction:

- (1) that the 3-acetoxymethoxy-2-butanol is formed as indicated above,
- (2) that the chloromethyl acetate splits up first into acetyl chloride and formaldehyde, which subsequently forms sodium chloride, butanediol acetate and formal. Since the formation of chloromethyl acetate from acetyl chloride and formaldehyde is rapid and exothermic, the second mechanism seems quite unlikely.

In all proportions, the reactants immediately precipitate sodium chloride, whereas the odors of acetate ester and formaldehyde are present only after considerable refluxing, if at all. Therefore, the first mechanism is almost certainly the correct one.

The presence of a large excess of chloromethyl acetate seems necessary for the formation of formal. In equimolar quantities, the reaction proceeds no further. With an excess of sodium (i.e. basic conditions) the only volatile product is probably an azeotrope of methyl acetate and water, but no positive identification was made.

Therefore, the reaction shown in equation 3 is favored by acidic rather than basic conditions. This is consistent with the need for acid catalysis in the conventional synthesis of acetals.

*

*

*

In all cases the formal was levorotatory (see Table I); therefore, we may conclude that the original synthesis, from the glycol and

formaldehyde under acidic conditions, preserves the D-configuration.

SUMMARY

D(-)-4,5-Dimethyl-1,3-dioxolane, the formal of D(-)-2,3-butanediol, may be prepared in good yields from methylene chloride and the monosodium glycolate, with excess glycol as solvent. When methylene iodide is substituted, only a small amount of the analogous methyl ether is formed; when potassium hydroxide is substituted for the sodium, some formal is formed.

Chloromethyl acetate will also react with the sodium glycolate, but the formal is formed only when a large excess of the chloromethyl acetate is present.

All the above products are levorotatory; therefore, the formal as prepared with formaldehyde preserves the D-configuration.

II STUDIES OF COLOR CENTERS IN ALKALI
HALIDE CRYSTALS

II

STUDIES OF COLOR CENTERS IN ALKALI HALIDE CRYSTALS

PREFACE

The work reported in this section was begun in September, 1953, and terminated in June 1955. Prior to this time the writer had completed a research project of six months duration under Professor Lucas and then had worked for a year with Mr. Floyd Humphrey constructing apparatus for the electron spin resonance spectrograph.

The object of the research was originally to characterize the coloration of blue rocksalt in terms of the various synthetic photostable color centers caused by radiation or alkali vapor treatment. These latter, according to the best reviews then extant^(4,5), were fairly well understood.

The general processes of color center formation and change, as described in the two following sections, have been known long before this work. The experimental results and all of the work in the last section are original unless otherwise noted.

A. MECHANISMS OF RADIATION COLORING

INTRODUCTION

It was first noted over half a century ago that alkali halide crystals subjected to ultraviolet light, x-radiation, or radioactive emanations develop a color characteristic for each alkali halide and identical to the color obtained by heating that crystal in alkali metal vapor. These colors could be bleached by exposure to light or heat, sometimes with the formation of secondary colors. Rates of coloration

and bleaching were studied, together with the secondary coloration process, photoconductivity, migration in electric field, and similar effects. By 1940 it was fairly well established that the primary color is due to an electron trapped in a negative ion vacancy⁽⁵⁾. This has been called the F band.*

Further studies on x-ray coloration initiated by Molnar disclosed many other bands resulting from x-ray coloration and bleaching . These were ascribed to one or more electrons trapped in an aggregate of ion vacancies; for example, 1 or 2 electrons trapped in 2 adjacent negative ion vacancies (the R_1 and R_2 centers), an electron trapped in a negative ion vacancy attached to a vacancy pair (the M center), and a "hole" - the absence of an electron from a normally filled electronic state - trapped in one or more cation vacancies (V centers)⁽⁴⁾. The characteristic absorption frequencies of these color centers for the principal alkali halides are listed in Table III. Various theoretical calculations of the energy and absorption band frequency of the F center have met with a good deal of success⁽⁷⁾.

Hitherto the optical absorption spectra were the only means of characterizing color center bands. In the last 5 years, electron spin resonance has been detected in crystals with additive and radiation induced color centers, with resultant information as to the exact state of the electron⁽⁸⁾.

Work in recent years has concentrated principally upon coloration at liquid helium and liquid nitrogen temperatures⁽¹⁰⁾, and more refined electrical measurements, such as the Hall effect, the A. C. Hall effect, and high frequency dielectric constant⁽¹¹⁾.

* From Farbzentren or color centers.

Table III. The Most Common Color Centers (9)

BAND	MODEL	ABSORPTION PEAK (Å)		
		<u>NaCl</u>	<u>KCl</u>	<u>NaF</u>
F	Electron in anion vacancy	4650	5600	3400
M	Electron in anion vacancy adjacent to vacancy pair	7200	8200	5100
R ₁	Two electrons in two adjacent anion vacancies	5450	6580	--
R ₂	Electron in two adjacent anion vacancies	5960	7270	4150
RT	(Caused by thermal coagulation of F centers)	c.5700*	--	--
Colloidal	Colloidal alkali metal	5800-6300*	7750	--
V ₂	Hole in two adjacent cation vacancies	2230	2320	--
V ₃	Two holes in two adjacent cation vacancies	2100	2160	--

* As reported in this thesis.

Despite all this, the actual mechanisms involved in coloring by radiation have received little attention. The special effects attendant upon radiation of deformed crystals have been likewise neglected. It is precisely these processes which are most important in understanding the nature of the geological coloration of blue rocksalt; therefore our first investigations centered upon these phenomena.

EXPERIMENTAL TECHNIQUES

Alkali Halide Crystals: Transparent cleavages of 99.9% pure alkali halide crystal, obtainable from the Harshaw Chemical Company, are of virtually standard use in this field. These were available only after the first six months of this work. Earlier work was done on colorless rocksalt from Utah - clear, cleavable and free of obvious impurities (99% NaCl). No substantial differences were noted between the colorability of the natural and synthetic material.

The average specimen was a rectangular cleavage, approximately 1/4" to 1/2" square and 2 to 5 mm thick. For cleavage of large blocks of material a special cleaver was designed, employing a blade of high speed steel ground and honed to a 15° bevel edge. The cleaver blade was placed on a diagonal edge of the (100) plane of the crystal, upon a saw or file mark. A sharp blow with a rubber mallet was usually sufficient for a clean cleavage. Smaller pieces, a square inch or less in cross section, were best cleaved by snipping with an ordinary pair of diagonal cutting pliers, and sections less than 5 mm thick were cleaved by steady pressure with a new razor blade. The synthetic material, which generally gave better cleavages, could usually be cleaved down to thicknesses of 0.1 mm.

X-Radiation: All x-rays used were from side portholes of x-ray diffraction camera stands in this department. The earliest work was done

with a molybdenum target Phillips tube by sticking the sample directly over the side x-ray outlet and covering with a lead shield provided by Dr. Sheldon Crane. This gave a small spot of intense radiation about 5 mm in diameter. The tube was operated at 25 to 50 kilovolts with a current of 15 milliamperes. Samples could be changed only when the camera was not in use; thus experiments were very restricted.

Later work was done with a special sample holder, constructed by the instrument shop (see Fig. 1) and attached to a General Electric copper tube. This gave a uniform area of intense radiation, approximately 1 x 2 cm, and samples could safely be put in and removed while the camera was in operation. In the experiments described herein, the tube was operated at 45 to 50 kv. with a current of 15 ma.

Just before the project was terminated an additional sample holder was constructed for the Phillips molybdenum tube, having a similar area of uniform radiation and the same facility for changing samples. No qualitative differences were observed in coloration from these two sources.

Optical Bleaching: Attempts were first made to secure monochromatic light, such as is used for bleaching color centers, by other workers in this field. The two monochromaters available in this department were designed especially for ultraviolet light and gave either very poor resolution in the visible region or such low intensity as to make them unsuitable. Preliminary attempts to make a monochromater using a high dispersion liquid prism showed that, though possible, successful construction would be too lengthy and difficult to be practical.

Since light anywhere in the F band will bleach the entire band⁽⁴⁾, the only essential requirement is that light absorbed by the F band be available while light capable of bleaching other bands is excluded. A series of simple glass filters were therefore quite satisfactory. For

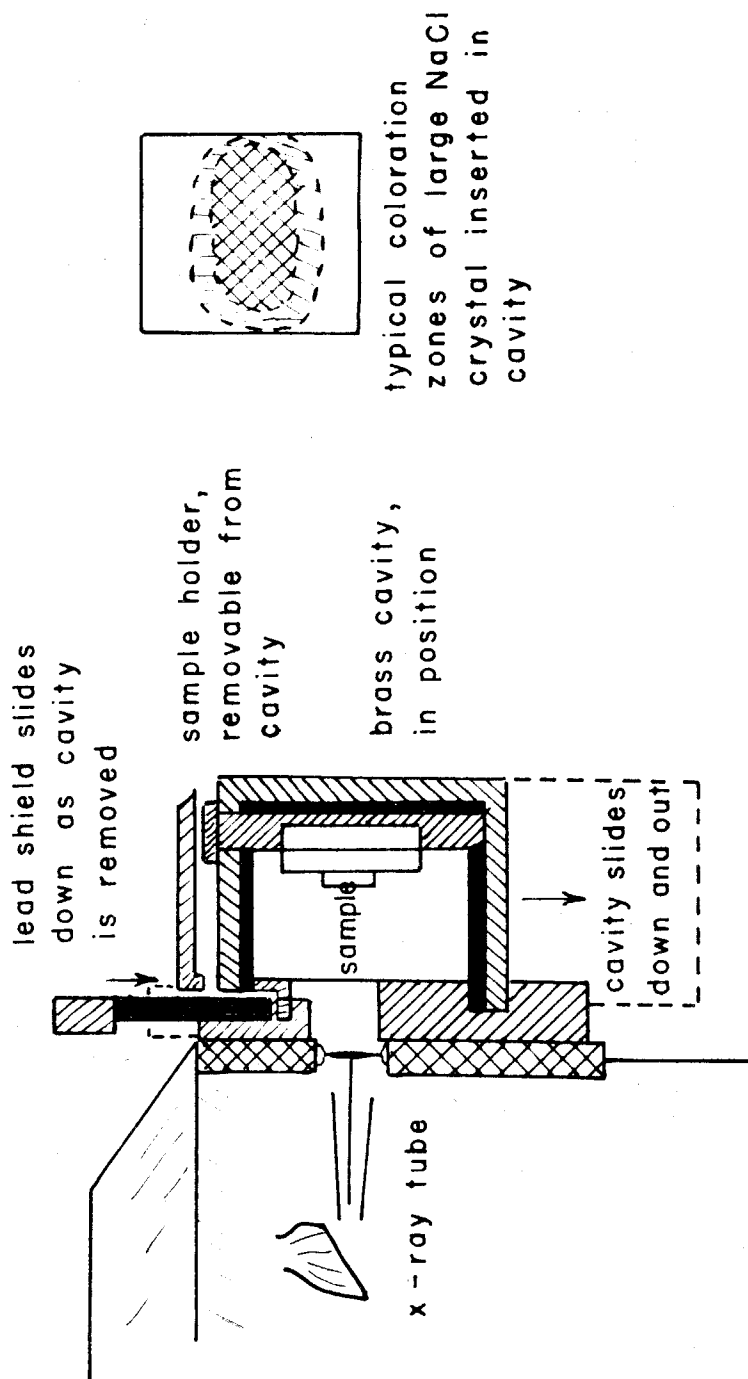


Figure 1. X-Ray Irradiation Cavity (actual size).

the F band in NaCl (4650 Å.) a Wratten filter, transmitting at 4000-5000 Å. (see Fig. 2), was used with a 200 watt incandescent bulb as a standard source of bleaching light. Ordinary cobalt blue glass was used briefly, but was unsatisfactory since it also transmitted light absorbed by the M band (7250 Å.).

The only serious problem was excessive heating of the sample, both by radiant heat from the light source and by absorption of the F light. After several trials of glass and water filters and water cooling of the sample, a compact and practical setup, illustrated in Fig. 3, was adopted as a standard for quantitative work. A sample, after 48 hours continuous exposure to this light, was at a temperature of 45°C.; this does not seem to affect the bleaching, and therefore no additional means of cooling was necessary. No attempt was made to calibrate the absolute energy of the bleaching light absorbed.

Thermal Bleaching: A small muffle furnace was equipped with a rheostat control and thermocouple, the latter being calibrated to the temperature of the sample holder by the melting points of various metals. Samples were placed on a small platform in the center of the furnace, next to the thermocouple, and observed through quartz windows at either end.

Plastic Deformation: The sample, generally 1 cm square and 4 to 10 mm thick, was placed between two hardened and polished steel blocks and set in a hydraulic press, and subjected to pressures of 10,000 to 40,000 lbs. per square inch. The resultant strains were between 50 and 75 percent. Best results were obtained by spreading a drop of lubricating oil on the surfaces of the steel blocks before deformation of the sample. Pressure need not be applied slowly, best results having been obtained by putting on the total force in a matter of seconds and leaving the sample at

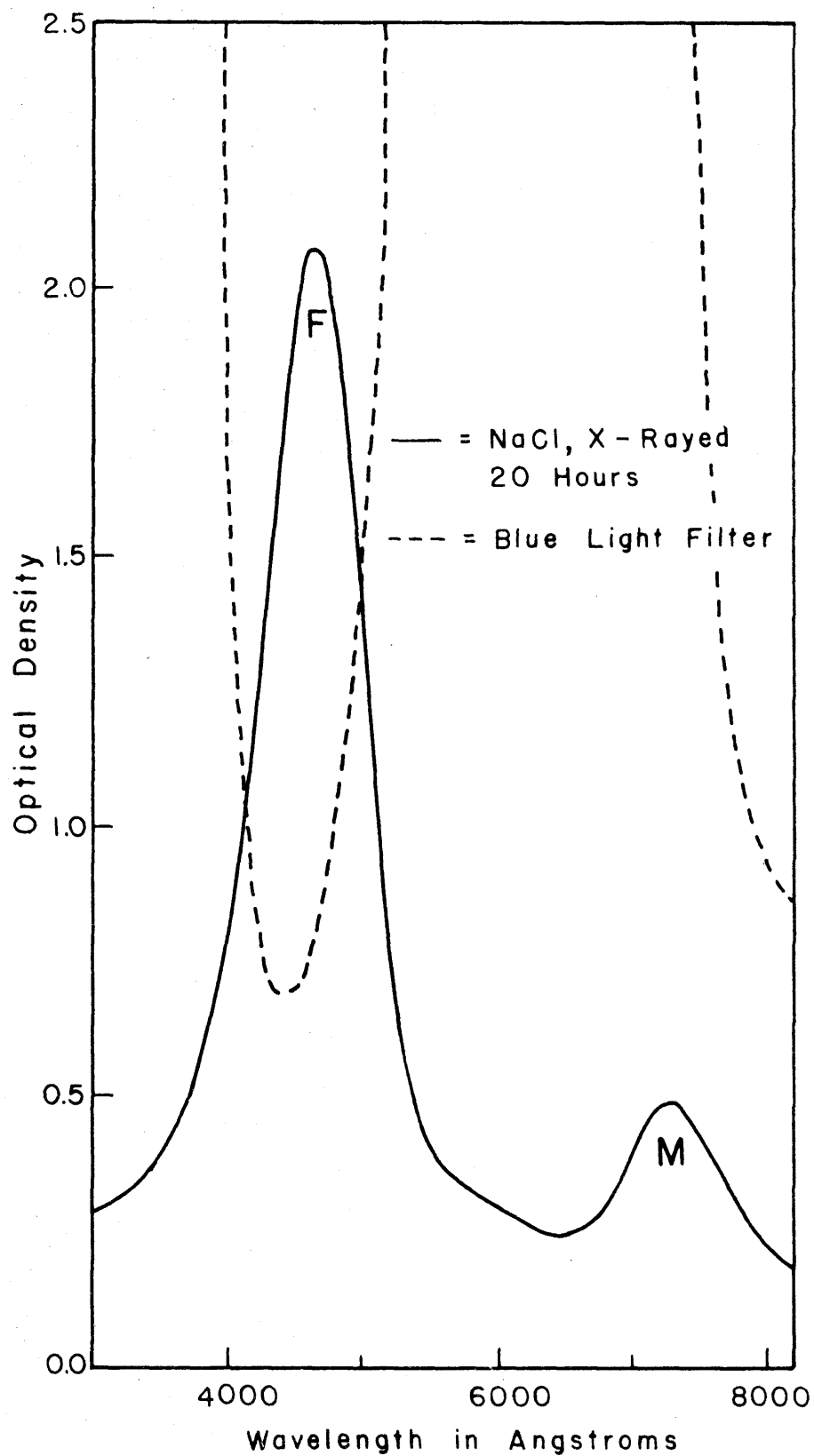


Figure 2. Bleaching Light for F Centers in NaCl.

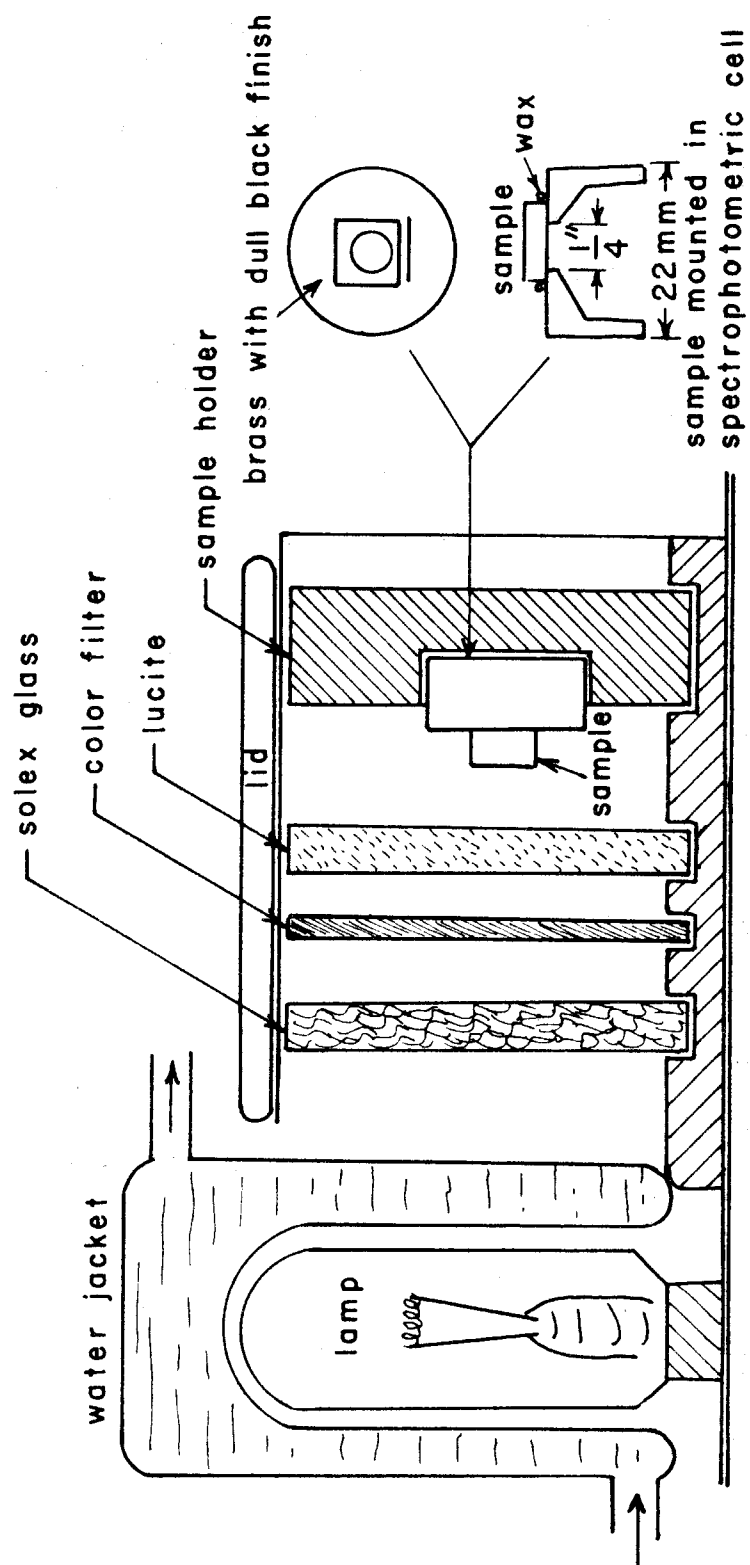


Figure 3. Optical Bleaching Apparatus (actual size).

maximum pressure for about a minute, after which there was no appreciable creep.

The samples, especially the synthetic ones, were quite plastic; fine cracks formed, but the piece as a whole was coherent and transparent. Under a polarizing microscope, birefringent bands were observed along the (110) planes, the usual slip planes for sodium chloride, and also along the (111) planes.

Absorption Spectra: Special spectrophotometer sample holders were constructed, having a 1/4" aperture over which the sample was fastened with wax (see Fig. 3). Occasionally 1/8" apertures were used. The only effect noted was increase in the resolution of the background, i.e., the cells tended to exaggerate any irregularities in the straight line spectra obtained for an air path in both sample and reference chamber. This was compensated for by using largest slit width possible. For absorption bands of extraordinarily high optical density, wire screens were used as gray filters. These were quite satisfactory and gave no distortion.

Provision was made for using the x-ray irradiation cavity and the optical bleaching apparatus with the sample already mounted in the spectrophotometer cell, so as to obtain reproducible results.

RESULTS

Coloration by X-Radiation: Samples of sodium chloride irradiated 1 to 15 minutes show a moderate yellow-brown color which, when viewed in cross section, is strongest at the surface, diminishing continually until it becomes negligible at a depth of 1 to 2 mm. An exposure of 24 hours produces a deep, almost black skin coloration for 1.0-1.5 mm superimposed upon a moderate, gradually diminishing, coloration extending 5 mm or

or more. After a week or more of radiation, the deeply colored skin increases to 2.0-2.5 mm including a rapidly varying transition zone of less than 0.5 mm, while the background color is not appreciably increased or extended. The spectra are shown in Figure 4.

The effect is generally the same for the other alkali halides except that the depth of intense coloration varies; for KCl it is approximately 1 mm for long exposures, with a background color of about 3 mm; for KBr less than 1 mm of skin depth with a background color of less than 2 mm beyond this; for KI 0.5 mm of deep color with no appreciable color beyond.

Prolonged storage of the crystals in the dark caused the color of NaCl to deteriorate slightly, producing a pink or gray tint and an irregular structure of light and dark zones not found in freshly irradiated material. These discolorations are probably due to gradual thermal bleaching (q.v.). The background color seems to bleach more rapidly than the skin, which is virtually unchanged.

Coloration in other alkali halides varies greatly in stability. KBr bleaches a little more rapidly than NaCl, KCl loses its color in a few weeks unless heavily exposed, and KI bleaches completely, leaving behind a pale yellowish tint possibly due to iodine.

Bleaching Effects: Upon optical bleaching, the background color deteriorates rapidly while the deep skin at first becomes even darker, developing a grayish color, which gradually fades to purple. This suggests that the secondary color centers are formed rapidly by a reaction of some of the F centers, while others bleach more slowly, with or without the formation of secondary centers. It has been reported that the secondary band grows at first rapidly and then very slowly⁽¹²⁾. This is also indicated by spectra taken here (see Fig. 5).

The purple color thus formed is confined to the upper part of the

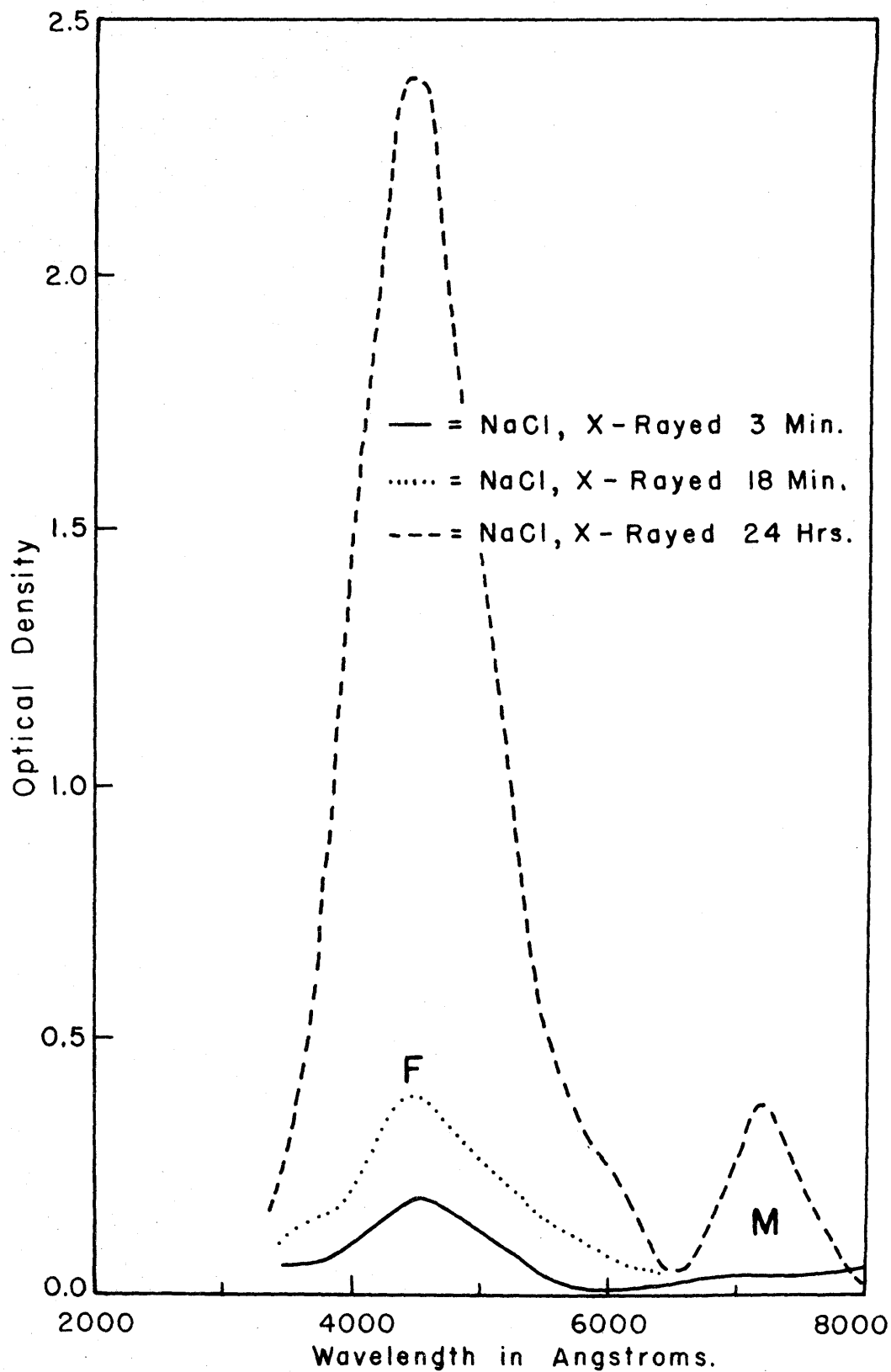


Figure 4. Radiation Colorimetry of NaCl.

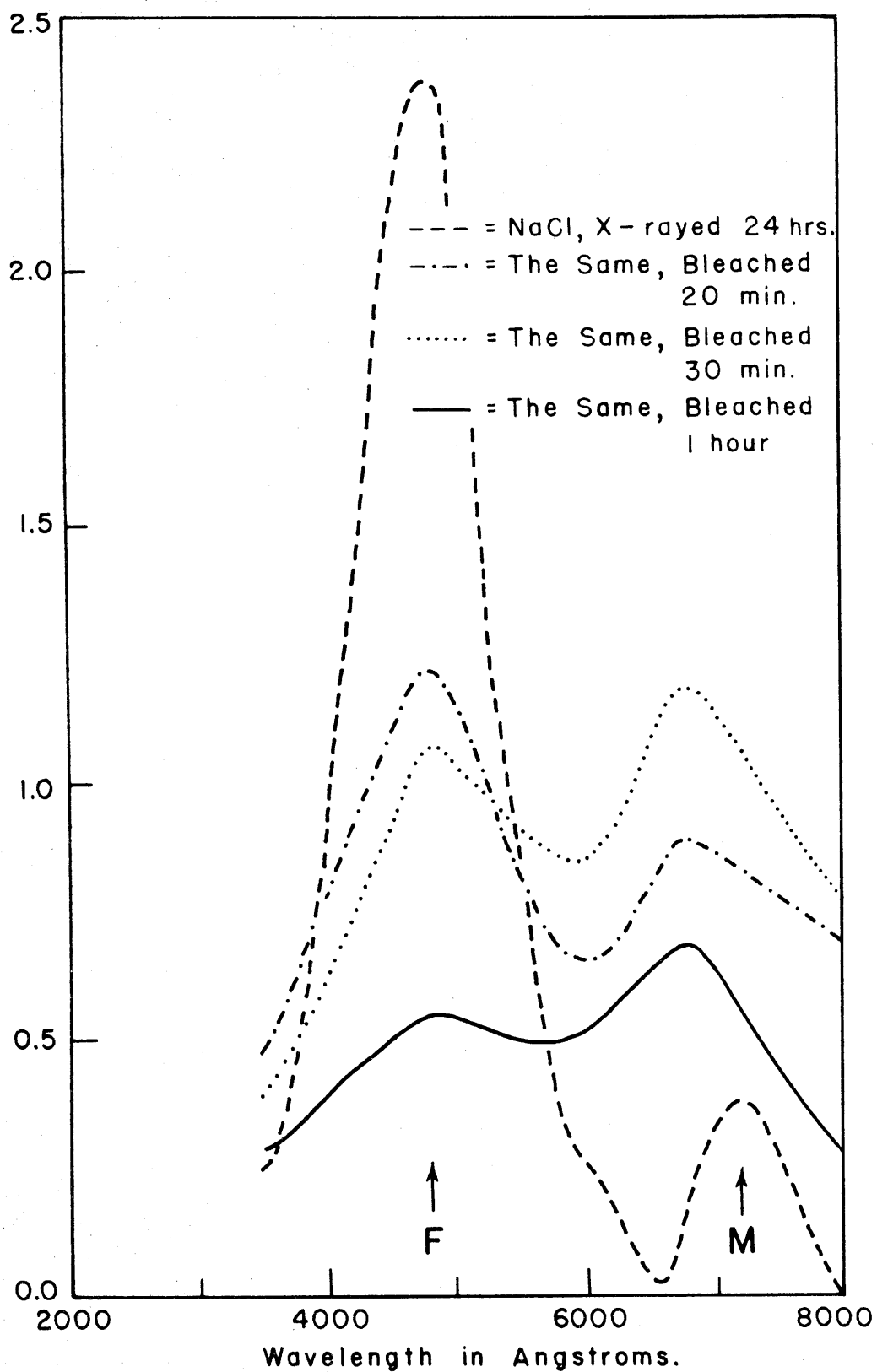


Figure 5. Optical Bleaching of NaCl.

deeply colored skin, being only 0.1 mm deep in crystals radiated 24 hours and occupying the entire skin area in crystals exposed a week or more.

The M band, which is frequently cited as resulting exclusively from the bleaching of F centers, is formed spontaneously upon heavy irradiation (see Fig. 4). Samples wrapped during radiation in black paper, and later in very thin aluminum foil (.002"), show the M band undiminished. Another experiment, described immediately below, indicates that this M band is confined only to the dark skin area. This effect, plus the aforementioned existence of two distinct zones of coloration, has also been reported in a recent paper by Mador, Wallis, et al⁽¹³⁾.

Filtered Radiation: It has been found possible to separate these two zones completely by the use of filters. A 4 mm cleavage of NaCl was radiated for several days, with one half of it covered with a 0.020" aluminum sheet, after which it was cleaved lengthwise into half a dozen thin slices. In all but the uppermost layer (.5 mm thick) the color was identical on the filtered and unfiltered sides; a pure F band which rapidly became colorless upon bleaching. In the uppermost slice, the unfiltered layer had the usual deep skin color (deeper than all the other layers combined) and bleached to a purple color. The filtered half of this layer was only slightly darker than the layers below it, and became colorless upon bleaching. Hence the two types of coloration appear to have been separated.

Plastic Deformation: Samples of NaCl 4 to 8 mm thick were deformed to a strain of 50% in the manner described above. Upon immediate x-radiation, the samples showed increased colorability, being deeply colored after 3 to 5 minutes of radiation. After 24 hours of radiation, however, they were not much darker than the undeformed crystal (see Fig. 6). No skin effect was observed, but rather an almost uniform coloration in

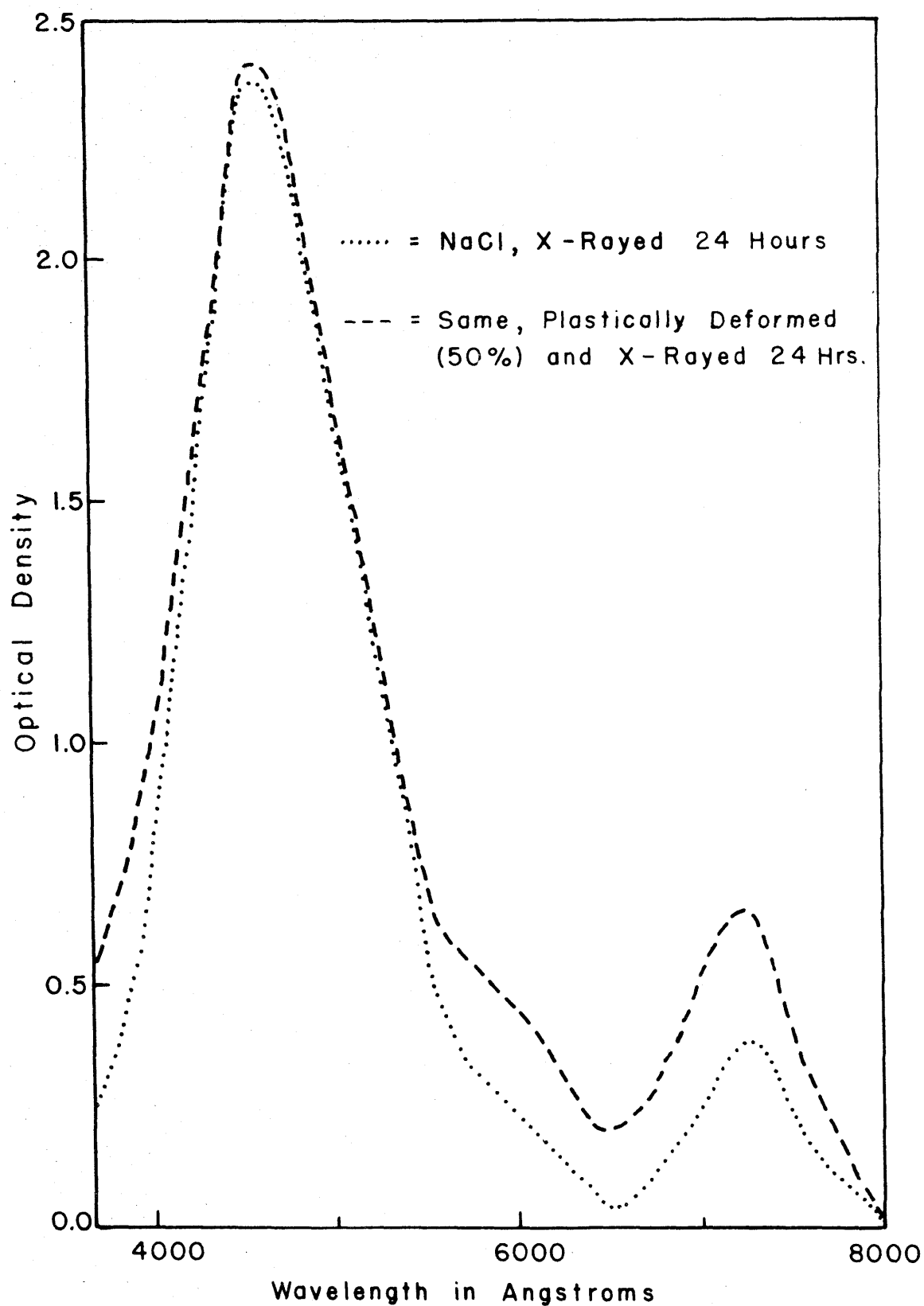


Figure 6. Effect of Plastic Deformation.

samples 2 mm thick. These could be rapidly bleached (completely within 15 minutes, as opposed to a day or more for undeformed heavily radiated samples), giving a deep blue color resulting from a rather peculiarly shaped absorption band at approximately 5900 \AA^* with several complex shoulders (see Fig. 7). Several bands in the ultraviolet were also observed.

The effect has long been known but has received no detailed study⁽¹²⁾. Some recent workers have noted an increase in the M, R, and N bands at strains of 5-10% but have reported no new bands as above.

The processes of radiation and deformation can be reversed with no change in effect. A sample x-rayed for 24 hours was subjected to plastic strain of 50% with no appreciable change in color. However, the sample was now highly sensitive to optical bleaching, and rapidly developed a deep blue color corresponding in intensity and depth gradient to the original F color. The absorption spectra indicated an RX-type band (see Fig. 7) and had a notable resemblance to the spectrum of natural blue rocksalt.

In some samples a structure in the color was observed, there being bands of color along the (110) plane. This was not always the case however, the blue being frequently quite uniform except for occasional yellow spots which apparently indicated zones of undeformed material.

Upon storage in the dark these samples tended to bleach spontaneously and irregularly, small zones perhaps a millimeter in diameter bleaching at various intervals, while other areas of color, or even whole specimens, remained deeply colored after a year. The writer has found this phenomenon described in detail elsewhere, under the name of "recrystallization"⁽¹⁴⁾. It is there noted that x-ray diffraction of the blue and the

* For want of a better designation, we will refer to this as the RX band.

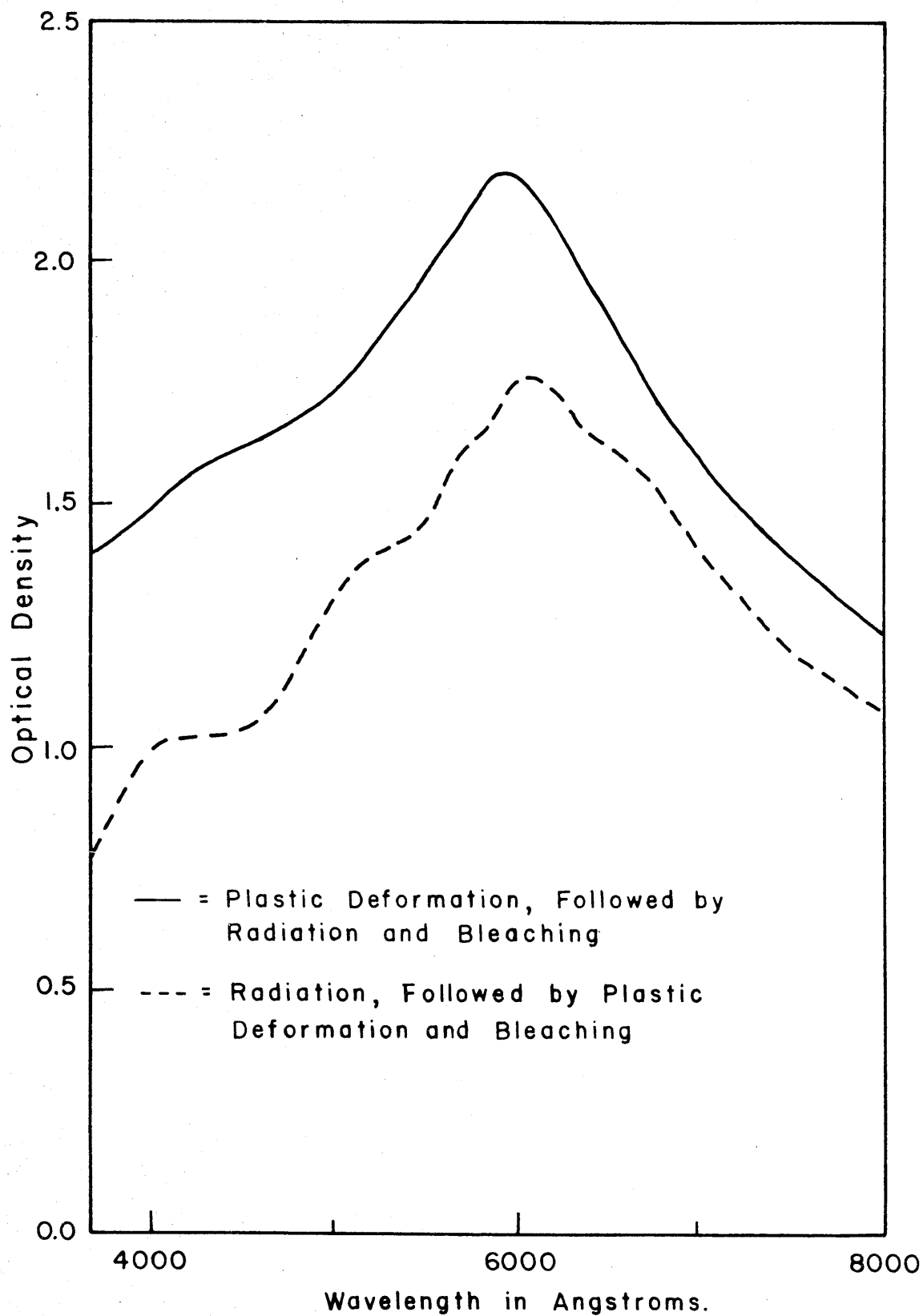


Figure 7. The RX Band.

white zones shows the former to have diffuse Debye-Scherrer rings characteristic of a highly imperfect crystal structure, while the clear areas show the usual Laue spots.

When there is an interval between deformation and subsequent x-radiation the Blaumschlag* sensitivity decreases rapidly, diminishing by about one-half in the course of a week and being almost imperceptible after a month. However, the effect persists qualitatively. Even a month after deformation, a brief exposure to x-rays, followed by rapid bleaching, produces a pale blue color throughout the crystal, rather than the thin skin of violet coloration characteristic of undeformed specimens.

Thermal Bleaching: When x-irradiated NaCl is heated to about 150° C. a gradual change from brown to violet takes place. This coloration is stable up to 200°; above this all color disappears within 5 minutes. If the crystal is cooled before bleaching occurs, the violet color reddens to a heliotrope or magenta, distinguishable from the bluer color of optically bleached F centers, although occupying precisely the same position in the crystal (i.e., the "skin" area). Absorption spectra show a single peak at 5700 Å. (see Fig. 8) rather than the complex of M, R, and F bands which result from optical bleaching. This has been occasionally called the R' band in the old literature, but since this symbol is now widely used to describe other phenomena we shall refer to the color developed by heat treatment as the RT band.**

The purple colored samples, produced by optical bleaching, containing the M and R centers seem to change over to the RT center upon heating

* The literal translation from the German is "sudden change to blue", in contrast to the gradual darkening of unsensitized material⁽¹⁵⁾.

** Rates of thermal bleaching and development of the RT band have been studied elsewhere, showing a distinction between "soft" and "hard" centers resulting in a complex decay and growth curve⁽¹⁶⁾. Other writers claim that no simple mechanism or rate equation can describe this reaction⁽¹³⁾.

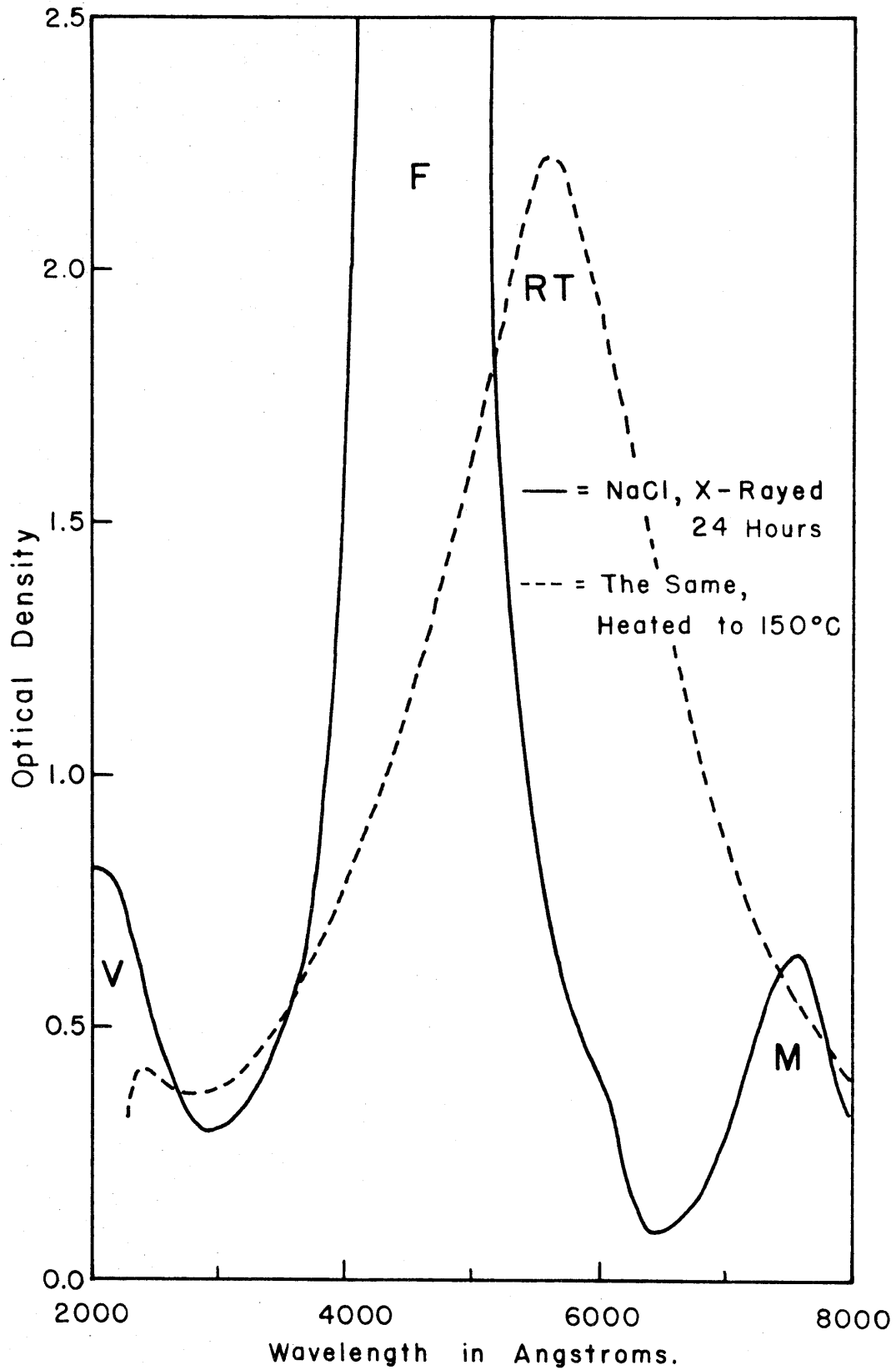


Figure 8. The RT Band.

to 150° C. as shown by a slightly redder color. This has not yet been checked by a spectrophotometric study.

The RX band of plastically deformed material is of similar temperature stability; at 150° C. the band tends to become purple without a loss of intensity. At 200° it is almost violet, resembling the RT band, and when held at this temperature begins to bleach. After 10 minutes at 210° it is about half bleached and ultimately fades completely. There seems to be a continuous range from 150° C. to 220° C. where the RT band, or the RX reverting to the RT band, bleaches continuously, but with a highly temperature dependent rate.

INTERPRETATION OF DATA

Tentative conclusions, drawn from the experimental results reported above, are as follows:

1) That unfiltered x-radiation produced two separate effects; an intense "skin" coloring less than 1.5 mm deep and a lighter, more diffuse, "background" coloration extending 5.0 mm further. It was at first assumed that the former involved the generation of new vacancies from dislocations in the crystal, while the latter represented merely the formation of F centers from existing vacancies. These effects were ascribed to the direct action of x-rays in the "skin" area and to secondary soft x-rays or exciton propagation through the background area.

2) That the secondary color centers - M, R, RX, RT, etc. - develop only in the "skin" area.

3) A .020" aluminum filter completely eliminated the skin coloration while permitting all of the background color to develop.

4) Plastically deformed crystals do not color appreciably more than undeformed ones; there is however a deeper skin area and less background

coloring. A slightly higher proportion of M coloration is developed, but no other bands are found prior to bleaching; there is not even a broadening of the F band.

A recent paper by R. B. Gordon and A. S. Nowick reports similar but more extensive findings⁽¹⁷⁾. Their abstract reads as follows:

Room temperature measurements of the rate of coloring of NaCl crystals by x-rays at different depths below the irradiated surface and for different states of deformation and heat treatment are reported. From the results it is concluded that two mechanisms of coloring operate in these crystals. The first, or "rapid-type" coloring, approaches a saturation density of F-centers of the order of $10^{17}/\text{cm}^3$, and appears to result from the generation of color centers from vacancies already present in the unirradiated crystal. The second, or "slow-type" coloring, takes place at a constant rate until F-centers in excess of $10^{18}/\text{cm}^3$ are formed. This type of coloring, which is usually observed only near the irradiated surface, is due to the generation of F-centers at dislocations, and is responsible for the hardness and density changes produced by the X-rays. Rapid-type coloring is found to occur at essentially the same rate in deformed crystals and in carefully annealed crystals; recovery at low temperatures after deformation, however, decreases the colorability. These results indicate that the principal effects of deformation and heat treatment on colorability may be related to the state of dispersion of impurities.

Radiation was from a commercial copper tube operated at 40 kvp. The two rate effects were separated by use of thin NaCl filters. It is inferred, but not explicitly stated in the article, that the two types of coloration result from the soft and hard x-rays respectively, the former being strongly absorbed near the surface; however no explanation is given as to why soft x-rays should generate F centers from dislocations, while more energetic x-rays do not.

Last year, Professor V. Schomaker of this department expressed the opinion that the separation of "skin" from "background" effect by the aluminum filter indicated that the former was due to the longer wavelength radiation. A brief qualitative check was made by taking powder photographs of CsCl using copper radiation with and without the various

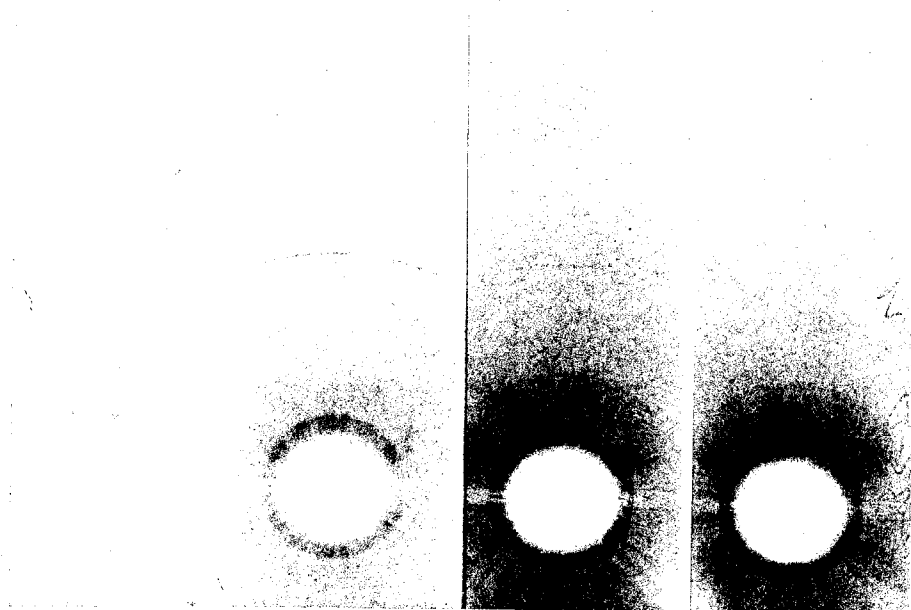
filters in question (see Fig. 9). The .001" nickel filter, aside from screening out the $K\beta$ lines, absorbs the soft x-rays only slightly more than the short wave component. The .020" aluminum filter is far more effective in favoring the shorter wavelengths, while the .015" NaCl filter completely obliterates the long wave, and even the $K\alpha$ lines leaving only the short wave component.

Therefore the two coloration types seem definitely to result from a wavelength effect. However no explanation of the resulting qualitative differences - formation of M centers, bleaching to secondary centers, etc. - can be given. Experiments with monochromatic radiation should be carried out.

It is difficult to account for the apparent limitation of all primary x-ray coloration, even in plastically deformed crystals, to only F centers, V centers, and a few M centers. If the more stable electron traps of the secondary color centers already exist, they might be expected to trap the electrons immediately. It is especially notable that upon comparison of an undeformed sodium chloride crystal x-rayed 24 hours and a plastically deformed crystal x-rayed for the same length of time, the ratio of M centers to F centers increases in the latter case only by 70%.

An obvious explanation is that the capture cross sections of all electron traps in the crystal are about equal. This has been used successfully to explain the optical bleaching of color⁽¹³⁾. Even in heavily deformed material the single vacancies probably outnumber all vacancy aggregates; thus only F centers would be observable. Excitation of electrons by bleaching would favor the most stable traps and give rise to secondary colors.

A more refined approach might involve the concept of recombination centers. The immediate cause of coloration is most likely excitons -



No
Filter

.001"
Nickel

.020"
Aluminum

.015"
NaCl

Figure 9. Effect of Filters on Copper X-Radiation

electron-hole pairs travelling through the crystal together. An isolated anion vacancy would probably capture the electron, forming an F center, and free the hole to wander further, but a more complicated vacancy group, having energy levels available for both electrons and holes, might permit the electron-hole pair to annihilate itself. Secondary coloration would involve independent electrons and holes no longer subject to this restriction.

A third mechanism may be inferred from a recent paper on low frequency dielectric loss in alkali halide crystals⁽¹⁸⁾. A small peak in dielectric loss was noted in alkali halide crystals which had been plastically deformed or quenched (a process which considerably increases this x-ray colorability). These peaks vanished if the crystals were x-rayed to form color centers, but reappeared as soon as the coloration was bleached. The authors suggested that dielectric loss was due to clusters of vacancies forming around kinks in dislocations; that the x-radiation destroyed or scattered these clusters and the bleaching restored them.

Let us assume therefore that these vacancy clusters are present to some extent in all crystals, or possibly are generated by the interaction of a soft x-ray with a dislocation. Such a high energy process might well be imagined to produce and scatter a large number of vacancies; in addition the same process produces electron-hole pairs, the result being a cluster of F centers scattered about a dislocation. Presumably the V centers - holes in positive vacancies - are also scattered about in some different manner. One might expect the scattering to produce an occasional cluster of 2 or 3 ions; therefore the presence of M centers. Bleaching would constitute a migration of F centers into the range of the cluster. We might expect that F centers would be distributed in various degrees of proximity from each other and from hole centers, hence the phenomenon of

"soft" and "hard" color centers⁽¹⁶⁾. This coagulation would lead to annihilation of some color centers and to the formation of secondary color centers by others. Optical bleaching would probably result in very limited migration of vacancies, or perhaps only migration of electrons to nearby vacancy clusters, hence only the simpler multiple color centers would be formed. Thermal bleaching might result in more coagulation, giving either a variety of aggregates or larger aggregates.

The plastically deformed material might, because of the high density of lattice irregularities, cause very large aggregates related to the colloidal band (q.v.). Indeed it has been observed that intense radiation and bleaching can produce the colloidal band or its color center precursors.

B. COLOR CENTER AGGREGATES IN SODIUM CHLORIDE

ADDITIVE COLORATION - THE COLLOIDAL BAND

INTRODUCTION

F centers may also be formed by heating the alkali halide crystal in alkali metal vapor. The spectra and electron spin resonance properties are the same as those of crystals colored by radiation. There are, however, no holes to recombine with the electrons, and exposure to light produces a broad band in the long wavelength region called the F' center, which has been explained as two electrons trapped in a negative ion vacancy⁽⁵⁾. Moreover, when additively colored crystals are annealed at high temperature, another band forms in the long wavelength region, which has received extensive investigation⁽¹⁹⁾.

The early German workers ascribed this band to colloidal particles of sodium metal trapped in the crystal lattice. Siedentopf, using an ultramicroscope, observed colloidal particles in blue, additively colored NaCl⁽²⁰⁾. Gyulai examined the photoconductivity and concluded that it resulted from emission of electrons from metal particles into the salt⁽²⁰⁾. Savostianowa, applying the Mie theory of the scattering of light by metallic spheres, showed that the absorption frequency predicted from such a model roughly agrees with that observed for NaCl⁽²¹⁾. She concluded from measurements on crystals that colloidal band coloration involves particles of all sizes, up to perhaps 800 Å. Mollwo studied the shift of colloidal bands with temperature, and also showed that such crystals upon plastic deformation became dichroic, which could be accounted for by the compression of the metal spheres into ellipses⁽²²⁾.

In recent years, Scott and his associates have carefully examined the equilibrium between F centers, the colloidal band, and alkali metal

vapor at various temperatures and have shown that the model of a heterogeneous phase (i.e., aggregate color centers involving at least 10 electrons and ions) is necessary to account for the equilibrium data⁽²³⁾. Westervelt has extended this further⁽²⁴⁾.

The failure of several attempts to find these colloidal particles with the electron microscope⁽²⁵⁾ has led these workers to assign a particle size range of 10 to 50 Å., smaller than the word "colloidal" usually implies. Moreover, although sodium metal in colloidal dispersion in paraffin has a distinctive electron spin resonance, attempts to find this resonance in additively colored sodium and potassium chloride have failed⁽²⁶⁾.

Several workers have observed colloidal particles in natural blue rocksalt and indeed the main absorption band in this substance is in the same wavelength region as the colloidal band of additively colored material. In view of the discrepancy between the large size colloidal metal spheres of the earlier workers and the sub-colloidal models of Scott and Westervelt, and since results obtained with this material vary from author to author, it seemed necessary to make at least a cursory examination of the colloidal band material before making any inferences about its natural counterpart. Moreover, the tentative failure of electron spin resonance and electron microscope observations seemed worthy of reappraisal.

EXPERIMENTAL

Treatment of NaCl with Alkali Vapor: Scott and his co-workers used sealed glass tubes (or copper tubes crimped at both ends) partially crimped in the middle to provide a lower compartment for the alkali metal and an upper compartment for the alkali halide crystals. Alger, in his

earlier work, used a stainless steel bomb sealed with a copper gasket. It is interesting to note that despite the general reliability and reproducibility of their results, both Scott and Alger complain about the erratic nature of the process and occasional complete failures.

In the present work, a copper gasketed, stainless steel bomb with a stainless steel needle valve was used so that the process could be carried out in a vacuum or inert atmosphere. The alkali metal was placed in a small metal capsule at the bottom of the bomb. The alkali halide crystals, wrapped in stainless steel gauze, were placed on a wire platform in the middle of the chamber (see Fig. 10). The bomb was sealed, evacuated, and heated in a furnace to the desired temperature for 4 hours or more. It was then either quenched in oil or allowed to cool slowly in the furnace.

For the first few runs the bomb successfully held a vacuum. Subsequent runs were made in a helium atmosphere.

Three sets of conditions for NaCl in alkali vapor have been tried. In the first case, the samples were heated for 8 hours at slightly over 700° C. and then quenched in oil. Many samples were still hot when the bomb was opened; they were quenched in oil. The samples were of a deep blue, with some yellow and purple spots through them, as well as halos of darker blue around irregularities in the crystals. Cleavages of these pieces gave a fairly uniform blue, or blue and purple, by transmitted light, but showed central zones or irregular areas of pink scattered light which did not correspond with any pattern of the color in transmitted light. All specimens showed a 1 mm thick surface layer of lighter coloration. Specimens from later runs, made at the same temperature, but with a helium atmosphere and cooled two minutes in air before quenching, were more uniform in appearance. The absorption spectra, however, varied

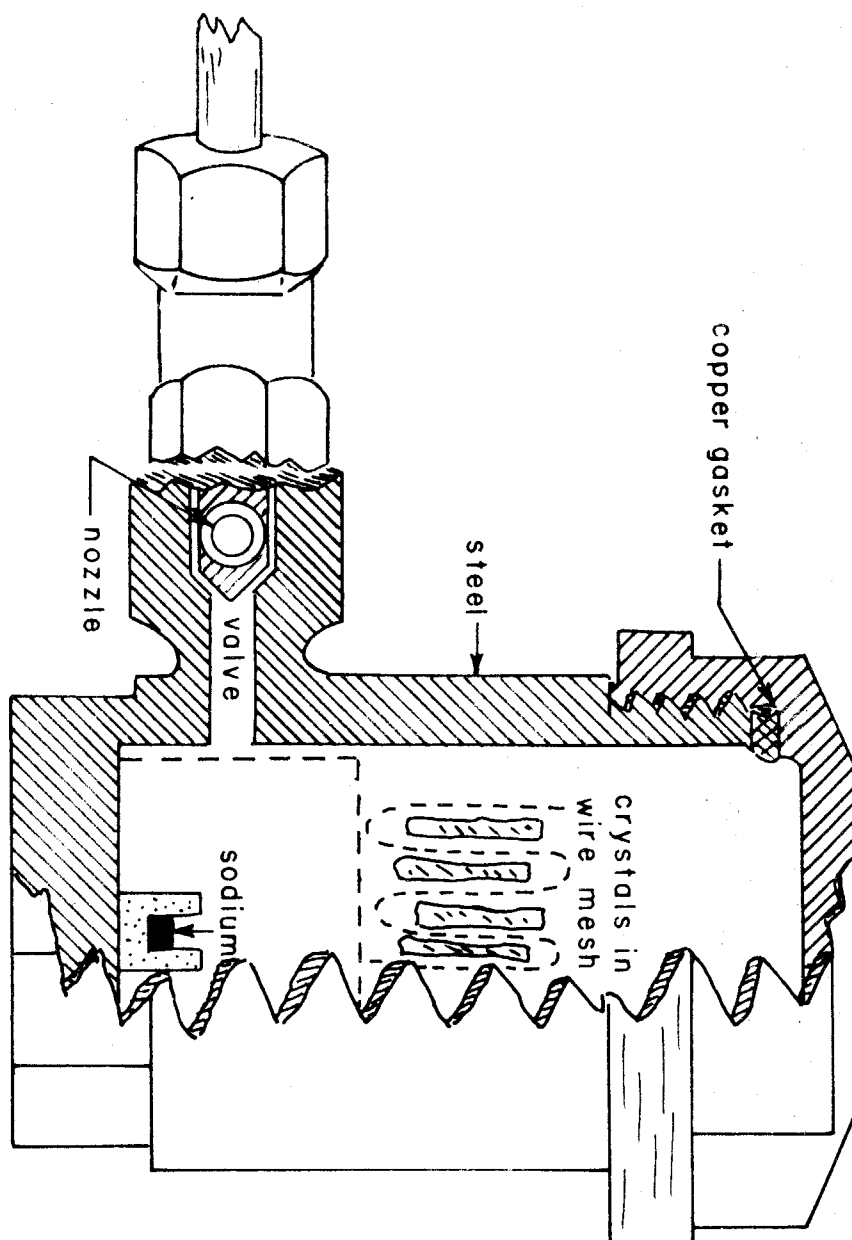


Figure 10. Bomb for Additive Coloration (actual size).

from one experiment to another (see Fig. 11).

Another group of crystals was heated for 20 hours at 650° in sodium vapor, and cooled slowly at the rate of 4° per minute. These were much paler, individual crystals being on the whole uniformly colored, but differing one from another in shades of blue or purple (the purple color being presumably a combination of the colloidal and the F bands). Here again the samples exhibited a 1 mm skin of a paler and less purple tint. The pink scattered-light effect was slight and very uniform.

Potassium chloride crystals, colored at the same temperature, but quenched in oil, showed a very uniform purple color, with a lighter 1 mm skin. Absorption spectra showed a pure F band with a very small colloidal band (see Fig. 12).

Another group of sodium chloride crystals were treated with sodium vapor at 550° for 8 hours and cooled at 4° per minute. These crystals were a pale, uniform blue. No light scattering effect was noticeable. Here again a lighter colored skin of about 0.2 mm was observable in cross section.

One striking irregularity was encountered in this run. Some of the crystals, "random pieces" from the Harshaw Chemical Company, had curved edges, indicating that they had grown next to the crucible wall. These edges were colored a clear bright yellow to a depth of 1.5 mm, in striking contrast to the rest of the crystal. Spectrophotometric examination, after a storage of one year, showed an F band of striking purity, together with a small well-defined peak at 4000 \AA . and an intense edge at 2100 \AA . (see Fig. 13), but no colloidal or M band. As a rule, the F band in additively colored NaCl must be prepared by heating the sample to about 750° C. and quenching as rapidly as possible. Some colloidal band is always present and the samples are relatively unstable, turning pink in the

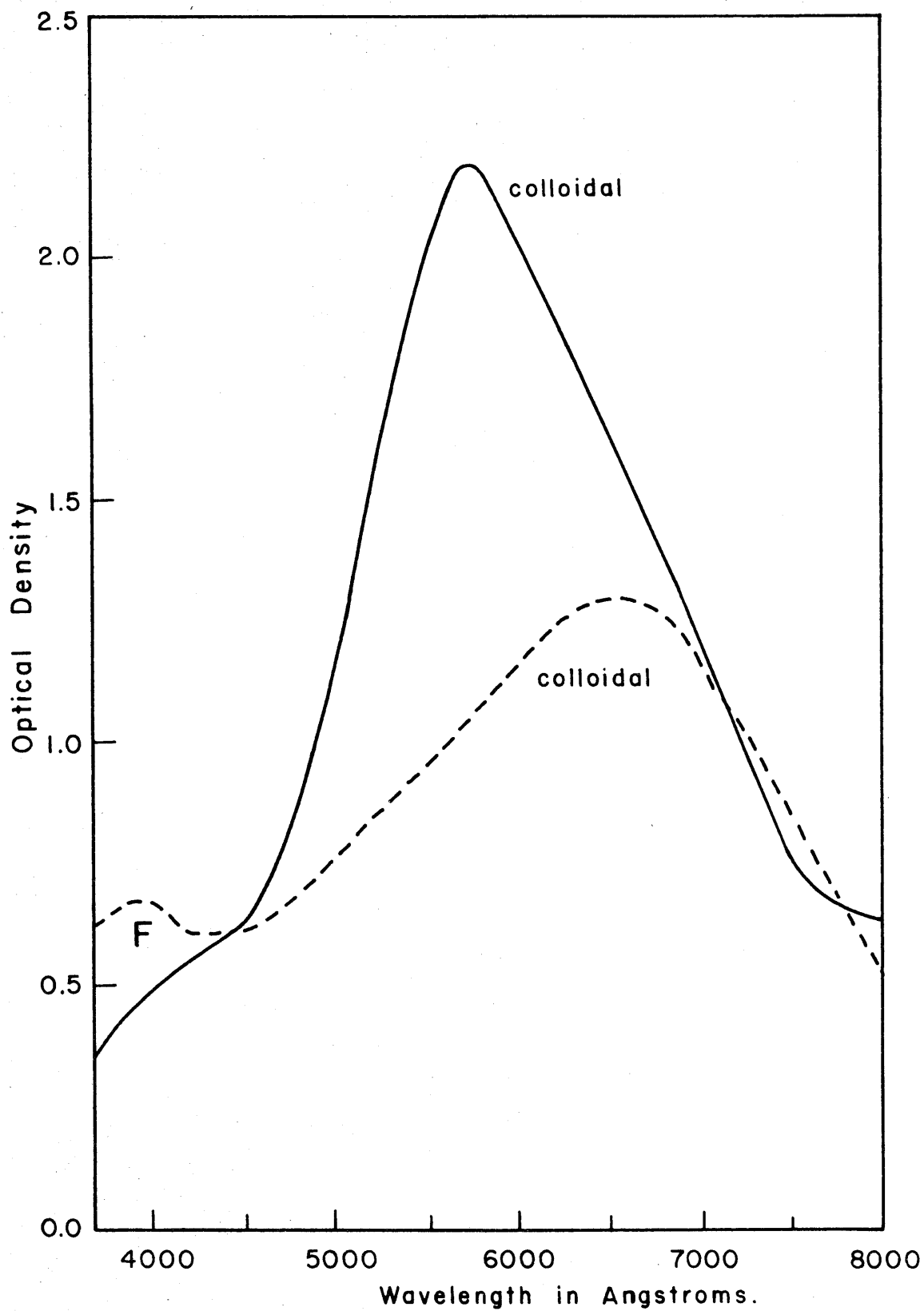


Figure 11. Additive Coloration of NaCl.

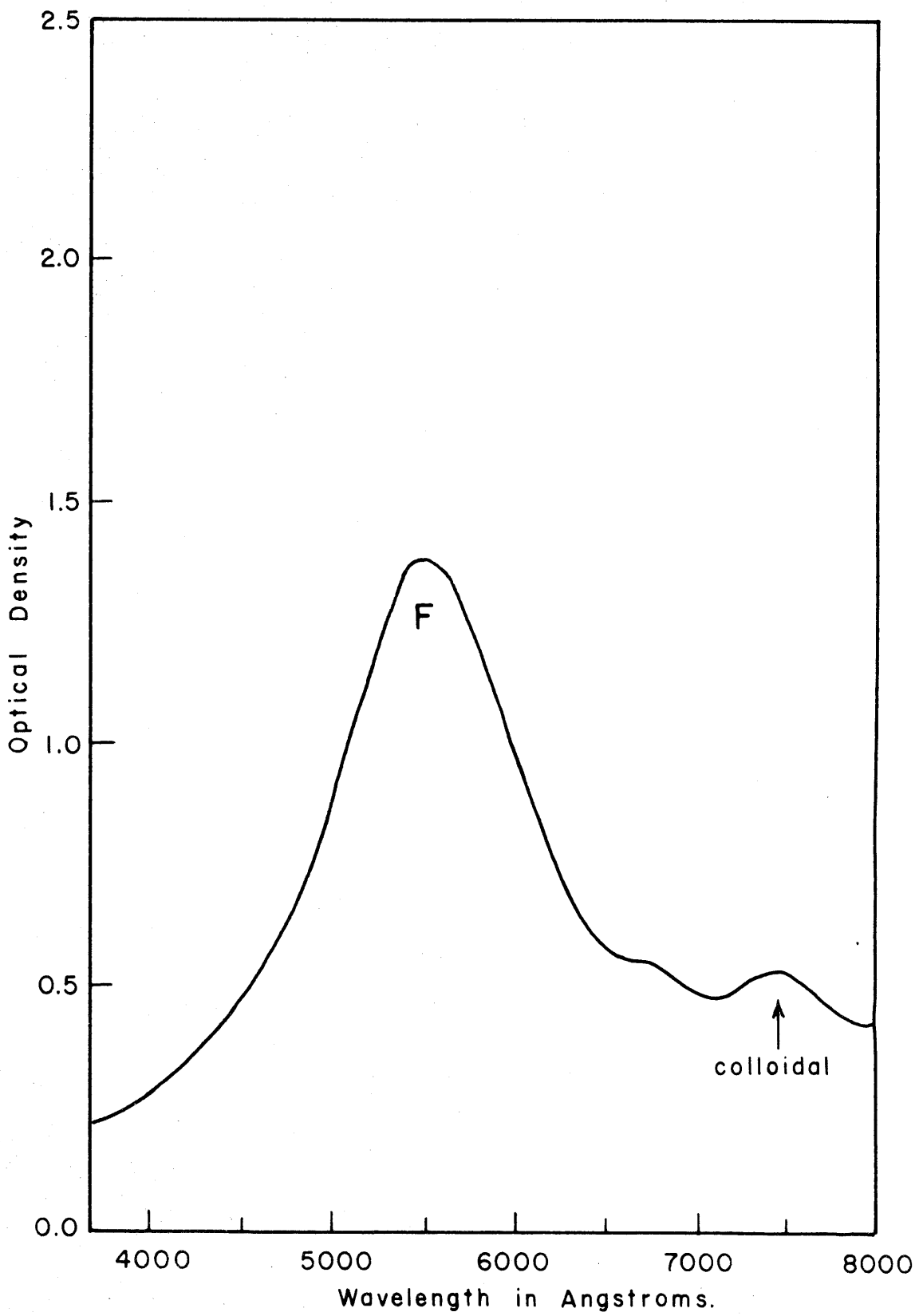


Figure 11. Additive Coloration of KCl.

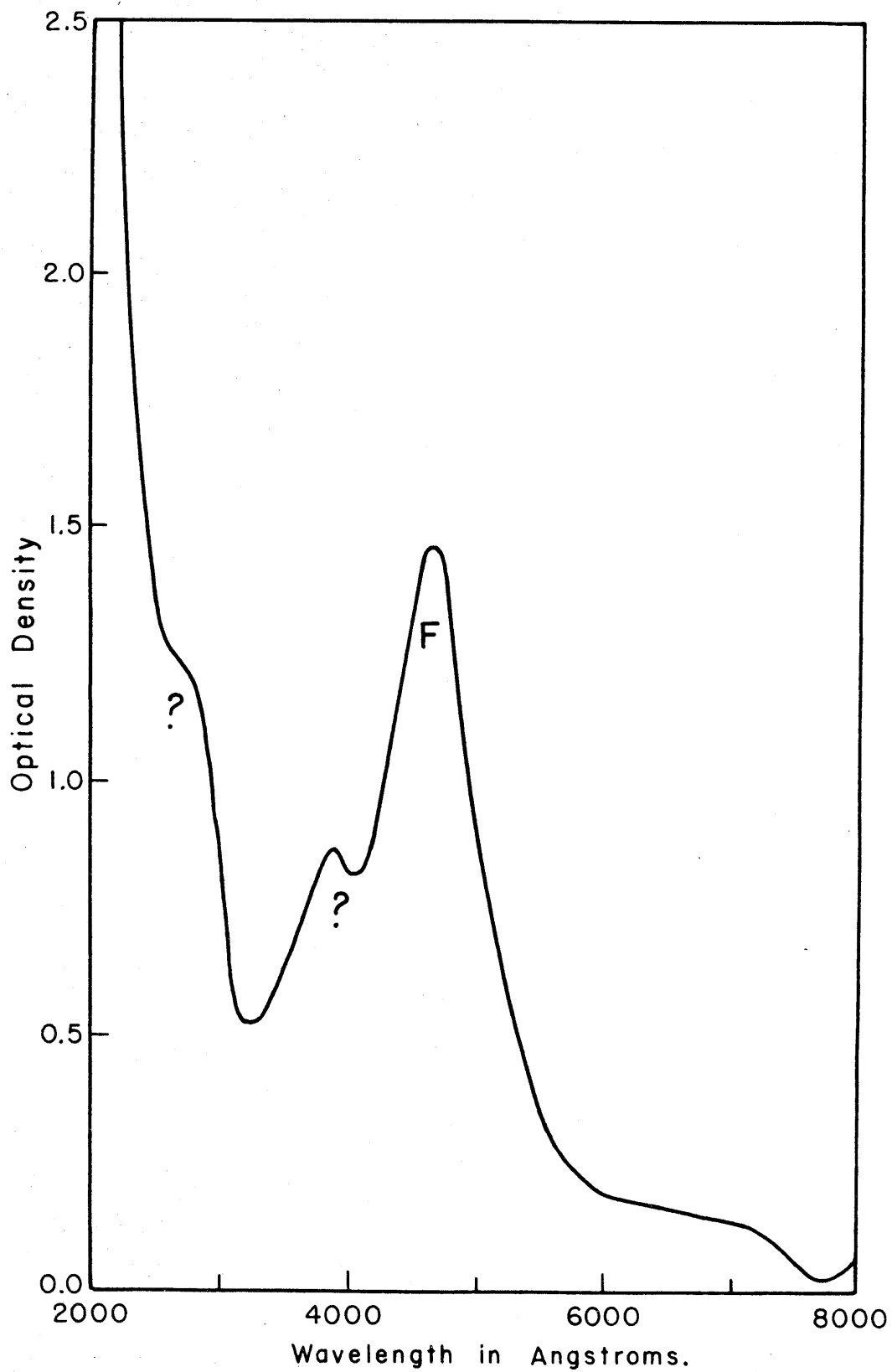


Figure 13. Yellow Zones in Additively Colored NaCl.

course of time as the colloidal band grows.

A re-examination of the specimens colored at 650° disclosed another specimen with a curved edge, which had a far more purple color (i.e., concentration of F centers) than the rest of the crystal.

Only one experiment was made with alkali halide crystals heated in the vapor of other metals. Sodium chloride heated to 700° C. for 4 hours with strontium metal showed a 0.2 mm skin of color with a rather unusual spectrum (see Fig. 14).

Heat Treatment of Additively Colored Crystals: The earliest work involved coloring crystals additively, reheating, and quenching them to produce the yellow F centers, and then heating them slowly in the furnace described in the preceding section, carefully noting the color changes.

Samples of a mixed yellow and blue color were heated at an approximate rate of 5° per minute. Up to a temperature of 300° C. the yellow phase gradually changed to reddish brown, then purple, and finally to a bluish purple, while the blue phase gradually became bluish purple. At 300° C. the crystals were of one color, indicating the conversion of F center zones and colloidal band zones to an equilibrium mixture of the two. From 300° to 400° the color gradually changed to a clear cyan blue, which remained after quenching. Upon further heating, however, to 450 - 500° C., the blue gradually changed to pink. Rapid quenching from 500° C. or higher resulted in the yellow color of the F center. At 600° C., the pink color gradually withdrew from the edges of the crystal into central zones and increased in intensity, and only upon prolonged heating at temperatures well above 600° did the color fade completely (see Fig. 15).

One crystal, cooled from 600° to room temperature at a rate of less than 25° per hour, was almost colorless, exhibiting a very faint pink scattering effect with no color by transmitted light. However, reheating

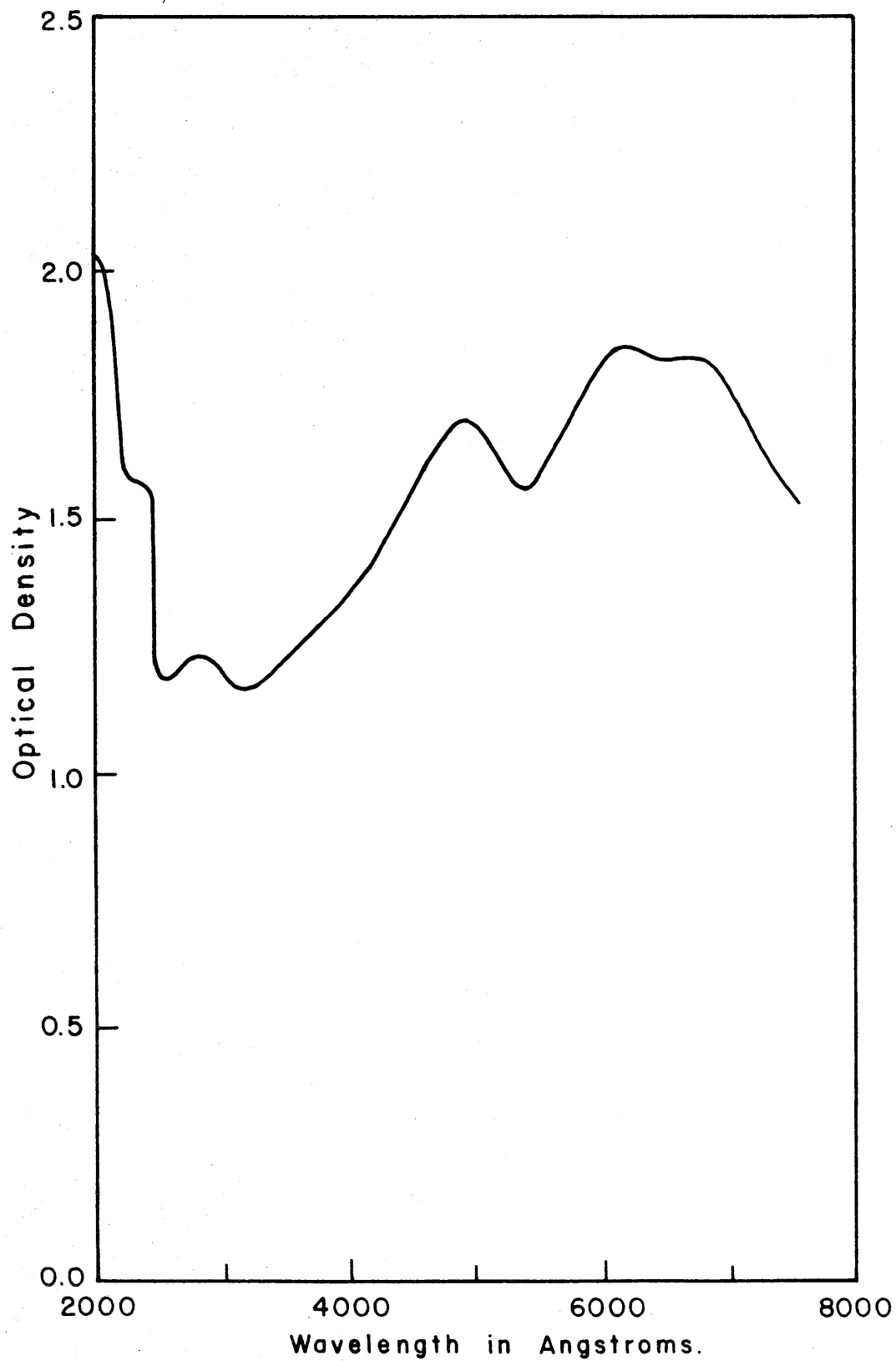


Figure 14. NaCl Treated with Strontium Vapor.

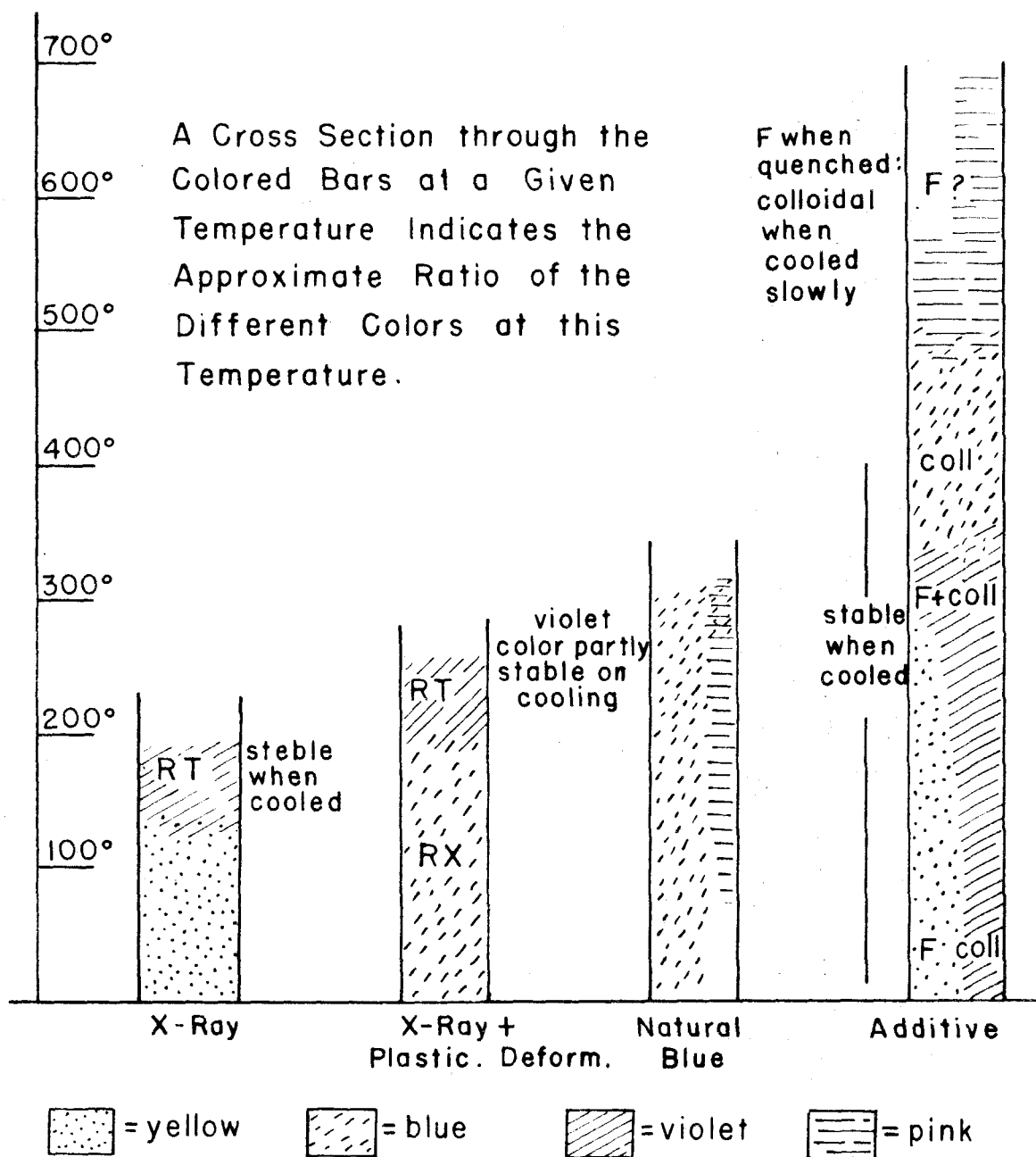


Figure 15. Effect of Heat Treatment on Color Centers.

and quenching gave an intense F band color. This may represent a true colloidal dispersion.

Electron Spin Resonance of the intense blue "colloidal band" of sodium chloride was searched for by Mr. Floyd Humphrey of this department, and by Mr. Robert Levy, with the paramagnetic resonance spectrograph at Berkeley. In both cases, no absorption could be detected. Since our apparatus also failed to give absorption band for F centers in KCl, and since Mr. Levy's apparatus failed to detect the resonance of V centers, later reported elsewhere, further experiments may reveal a colloidal sodium resonance.

Electron Microscope: An examination of potassium and sodium chloride crystals exhibiting the colloidal band was made with an electron microscope by Scott and by a group at Cornell⁽²⁵⁾, in both cases with no success. Attempts on sodium chloride crystals with an intense blue color and showing a strong pink Tyndall effect were made here by Mr. Edward Henderson, also with no success, thus presumably ruling out the presence of particles greater than 30 Å. in size. Etching of the samples with alcohol and alcohol-water mixtures did not change the results. However, other sodium chloride crystals known to contain colloidal copper (see next section) also showed nothing in the electron microscope. According to Mr. Henderson, such experiments are sensitive to the manner of preparation of the sample, and negative results are not conclusive.

BLUE ROCKSALT

INTRODUCTION

Deposits of rocksalt in Stassfurt and Herringen, Germany, show an intense blue coloration frequently occurring in irregular streaks or layers. This color is not caused by any obvious impurity, since adjacent

colorless areas give the same analysis⁽¹⁵⁾. Therefore we might expect the color to result from color centers.

These deposits originated as precipitates from sea water, as is evident from the associated minerals. They were then buried under other sediments and subjected to fairly intense heat and pressure, which apparently caused the microcrystalline deposit to recrystallize into large single crystals. Throughout this process the sodium chloride was subject to emanations from radioactive impurities, the nature of which have long been the subject of discussion. The most recent work seems to establish the source of radioactivity as radium D, a lead isotope⁽²⁷⁾.

The accepted theory is that the coloration is due to colloidal, RT, or RX bands⁽¹²⁾, but the spectra of the natural rocksalt have qualitative characteristics different from those of the synthetic color centers. It seemed worth while to compare them with the color centers produced artificially.

EXPERIMENTAL

Specimens: In the general classification of blue, violet and yellow rocksalt, there are numerous specific types, distinguished by their color and reaction to heat treatment. All samples used in this work came from two locations. A series of specimens from Herringen, Germany, obtained from various dealers, showed the same reaction to heat treatment and the same qualitative spectral features. The color occurs in fairly large solid zones alternating with colorless areas. Frequently there is layering along various crystallographic planes. These features are described in detail by Przibram⁽¹⁵⁾. Another specimen from Stassfurt, Saxony, having blue and violet mixed together in irregular zones, has somewhat different thermal properties.

Heating: Cleavages of blue rocksalt were placed in the furnace described in preceding sections and observed while being slowly heated. The Herringen material was apparently stable in intensity up to 250-300° C., but showed a slow qualitative color change. Areas originally white would become pale pink and the crystal as a whole deepened from a cyan blue to a more violet tint. In the range around 300° this effect was accompanied by slow bleaching, the last traces of color being usually violet. Upon sudden cooling during the violet phase, the sample was partially restored to its original blue state although some of the violet tint remained. The Stassfurt material distinguished itself by showing a greater tendency to become violet and even pink at high temperatures; this color could largely be retained on cooling. For a comparison with x-ray and additively colored crystals see Figure 15.

The spectra (see Fig. 16) of the Herringen and Stassfurt material are quite similar, showing only slight quantitative differences in the peaks, but after heating they changed radically (see Fig. 17).

Plastic Deformation: As has been reported previously, samples of blue rocksalt, when plastically deformed 50% or more, change to a pale pink⁽¹²⁾. These pink specimens were extremely photosensitive and rapidly regenerated a blue color in patterns roughly corresponding to the original coloration of the material. A spectrophotometric examination however (see Fig. 17) showed the bands to be very distorted and broad, with considerable frequency shift.

X-Radiation: Mixed blue and white specimens were bleached by annealing, x-rayed for 24 hours, and then subjected to optical or thermal bleaching. In no case could differences in the original blue and white zones be detected. This is contradictory to other reports⁽²⁸⁾. Samples of the blue material, x-rayed and inspected visually, seemed to show no

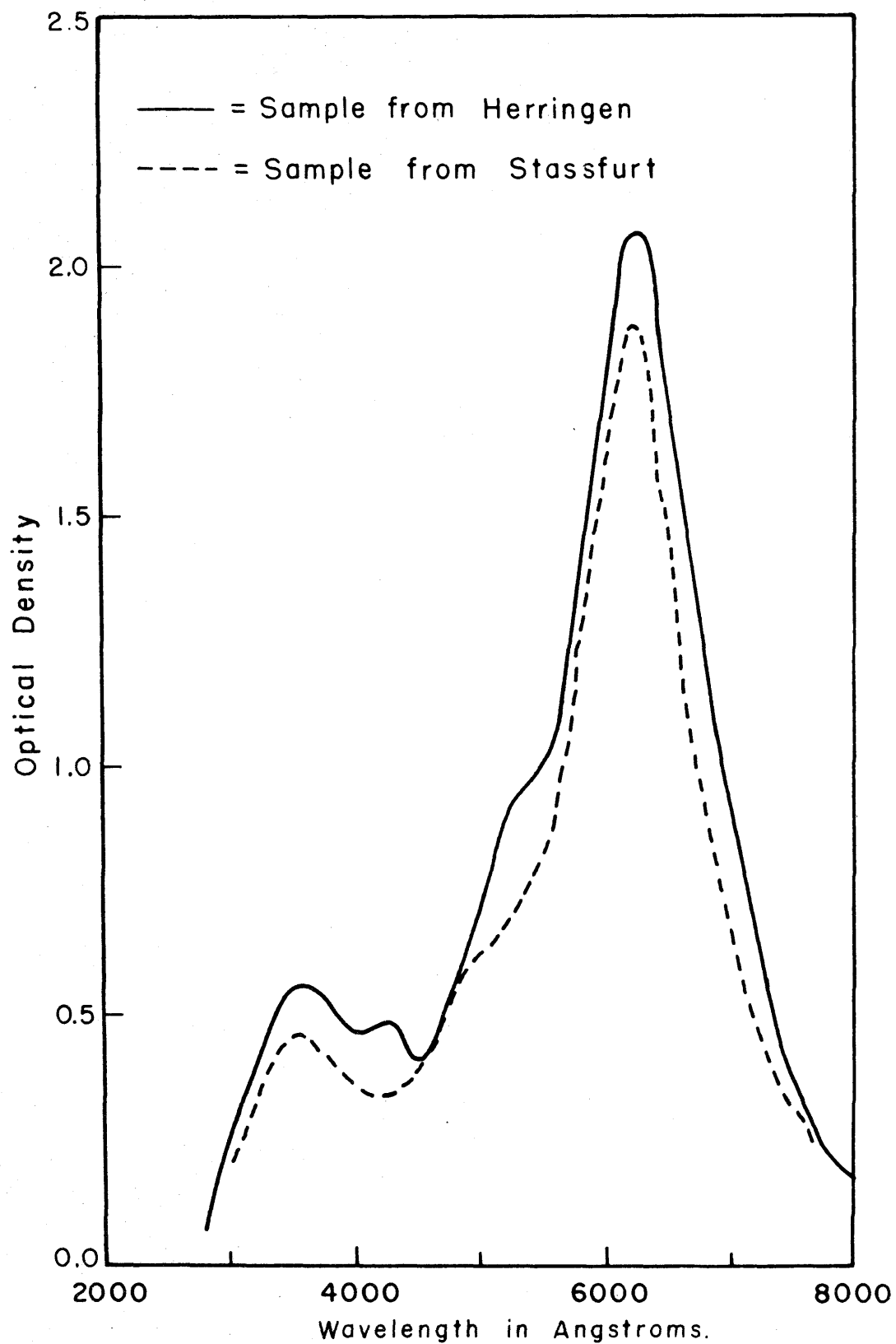


Figure 10. Rocksalt.

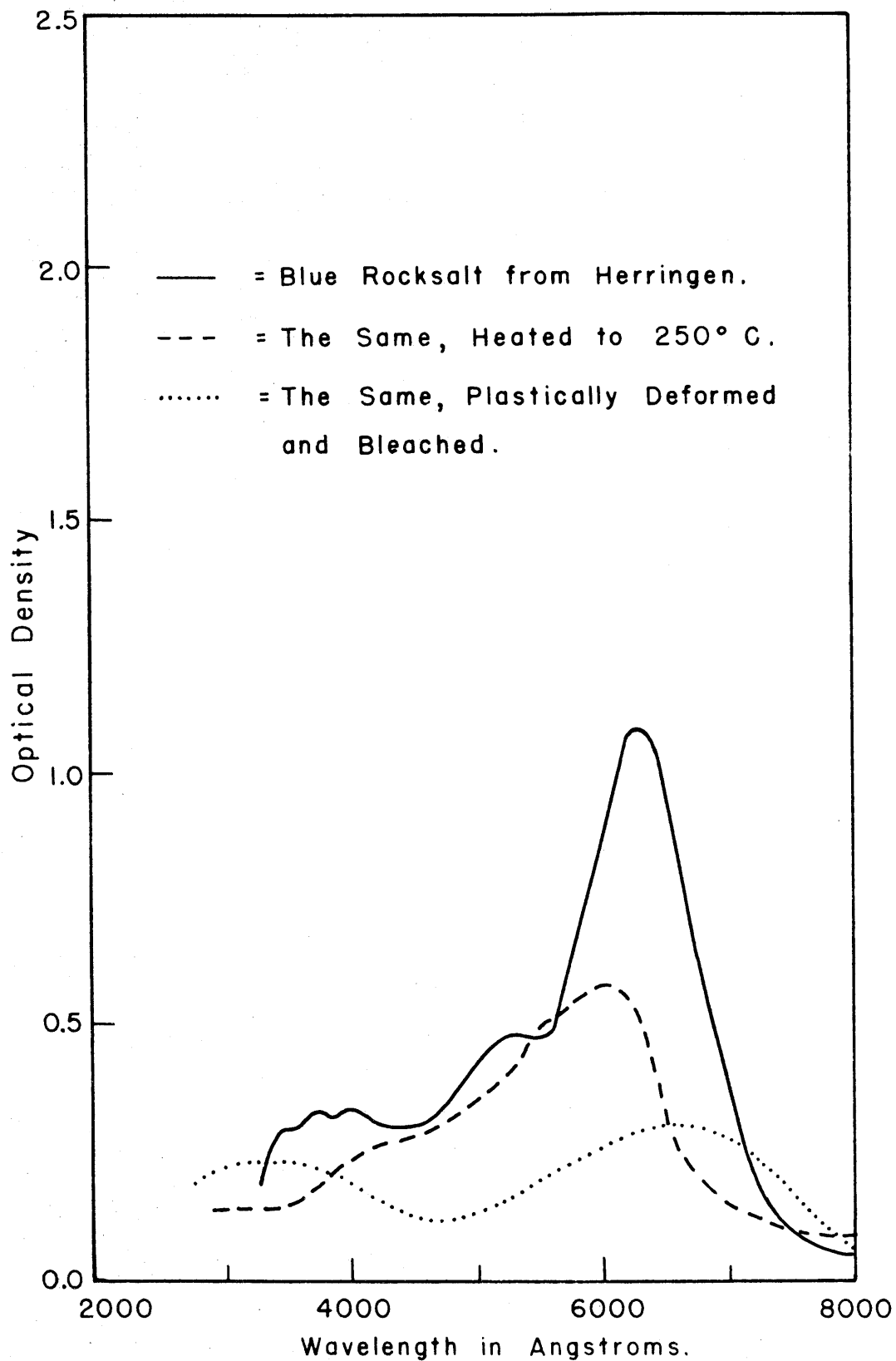


Figure 17. Heating and Deformation of Blue Rocksalt.

irregularities in either the degree of yellow x-ray coloration or in the background blue.

Natural Sodium Fluoride: The writer was especially fortunate in obtaining some samples of natural sodium fluoride, called Villaumite. These cleavages, far larger than the specks other workers have had to deal with, are deep red in color and give a very sharp spectrum (see Fig. 18). The coloration would seem to be due solely to F and M centers, principally the latter. The coloration is relatively stable to heat, remaining a pale pink after prolonged heating at 700° C. Specimens so heated seemed to regain their color after brief x-radiation.

INTERPRETATION OF DATA

The evidence for attributing the "colloidal" absorption band to a truly colloidal dispersion of alkali metal may be stated thus:

1) Early workers observed colloidal particles under the ultra-microscope. Similar particles have been more recently observed in uncolored crystals; these are ascribed to impurities.

2) There is approximate agreement between the absorption peaks predicted for such a dispersion by Mie and Pohl and the absorptions observed. However, in order to account for the observed variation in width and frequency of absorption, particles must be postulated as occurring in all sizes up to 500 Å⁽²¹⁾.

3) Studies of the equilibrium between "colloidal" and F centers in KCl⁽²³⁾, show that the former must be equivalent to aggregates of at least 10 F centers.

4) Westervelt has shown the reasonableness of the colloidal model from thermodynamic and energy considerations⁽²⁴⁾, albeit with rather extreme postulates about the physical state of the metal particle

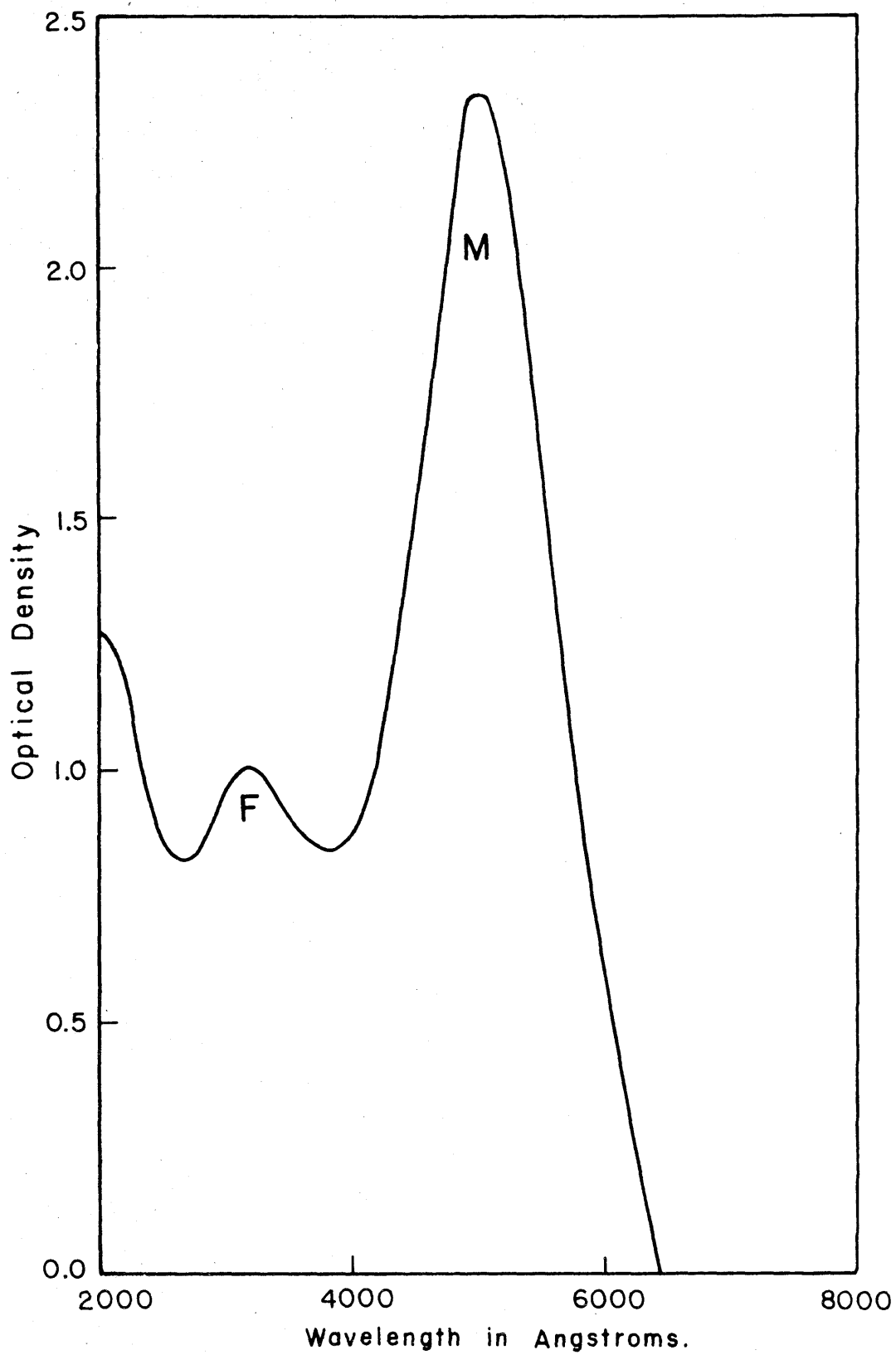


Figure 1. Villaurite.

(20 Å or less, liquid, and under 15% strain due to surface tension!). On the whole, this work seems to be evidence as much against as for a classical colloidal particle model.

There are only two pieces of evidence contrary to the colloidal theory.

5) The failure of the electron microscope to detect any colloidal particles has led Scott and others to assign 50 Å as a maximum size for the particles. This contradicts arguments 1 and 2 above. But the method has also failed in the case of sodium chloride crystals known to contain colloidal copper (this will be discussed in a later section).

6) Efforts to detect the electron spin resonance associated with sodium metal have failed. But both the apparatus used here and that at Berkeley failed to detect resonances known to occur (from F centers and V centers respectively).

An argument for a modification of the colloidal model arises from the close resemblance of the "colloidal" absorption band to the bands presumably caused by small aggregates of F centers: the RX, RT, and "blue rocksalt" bands. All occur between 5500 and 6500 Å, all vary erratically with slight changes in conditions of formation, and all are to some degree unstable to heating, the colloidal band disassociating into F centers.

The RX and RT bands are assumed to result from aggregates of F centers, formed by the diffusion of halide ions out of an area in the crystal and the trapping of electrons by the resultant vacancies. The extreme case of this, in which all of the anions are replaced by electrons, would result in a face-centered cubic lattice of neutral sodium atoms, in other words a face-centered modification of sodium metal. Such closest-packing phase modifications of alkali metals exist, and they seem to have physical

properties similar to those of the usual body-centered phase. Thus, the extreme case of F center aggregation would be equivalent to colloidal sodium metal.

It may therefore be suggested that the so-called colloidal band represents a highly aggregated state of F centers, with thermodynamic properties closely related to those of a sub-colloidal dispersion of metal.

A method for distinguishing between these two models would be a study of the variation of paramagnetic susceptibility with temperature. Alkali metals have temperature-independent paramagnetism⁽²⁹⁾. A temperature dependent susceptibility would indicate the F center aggregation proposed above.

The exact absorption frequency and peak shape would depend principally upon the "purity" of the aggregate zone, i.e., its freedom from halide ions and other forms of disorder. The thermal stability of the color would depend on the nearness and mobility of holes and electron traps.

The properties of the natural material may be explained by two additional assumptions:

First, by reason of the greater time for achieving thermodynamic equilibrium, the natural F center aggregates are expected to be in a more ordered condition than in any synthetic material. This would explain the more narrow and regular bands of the former, the smaller peaks at shorter wavelengths being ascribed to transitions to higher excited states. The purple colors resulting from heating or plastic deformation would represent disruption of these zones to form the more disordered RT and RX centers.

Second, as another consequence of this process of ordering and

attaining thermodynamic equilibrium, we might suppose that the holes and positive ion vacancies might also coagulate at other points in the crystal lattice. Therefore, since thermal bleaching involves a migration and recombination of electrons and holes, a process which places the holes further away from the free electrons - in more stable, less mobile aggregates and with fewer dislocations and intervening vacancies to facilitate electron or hole migration - would give an appreciably greater stability. This would account for the presence of both free sodium and free chlorine in natural blue rocksalt and in heavily irradiated synthetic material⁽³⁰⁾.

In the extreme case, the aggregates of "hole centers", being equivalent to free chlorine, might have a chance to migrate through the crystal and evaporate, according to the particular conditions of formation. This would explain the great variation in thermal stability of blue rocksalt, some species maintaining their color almost to the melting point⁽³¹⁾.

C. COLOR CENTERS IN CRYSTALS CONTAINING IMPURITIES

INTRODUCTION

The purest alkali halide crystals now obtainable contain impurities in higher concentration than any color centers that can be formed in them. But, as will be shown below, impurities frequently have a profound effect upon color center formation. Therefore it has not yet been disproved that color centers are exclusively an impurity phenomenon; this fact has been pointed out by eminent workers in this field, but with the expressed opinion that dislocations would provide a minimum color effect⁽³²⁾.

Research on the relation of color centers to impurities has received little attention. Color center studies have been made on crystals containing alkaline earth ions, the hydride ions, and those heavy metal ions which act as phosphor activators. A few mixed alkali halide crystals have also been studied.

The ions that activate alkali halides as phosphors, namely copper, lead, thallium, and silver, were observed to have absorption peaks in the ultraviolet region, apparently due to the impurity in itself or considered as a complex ion⁽³³⁾. Jahoda, and later Smakula, observed that these and other metal ions increased the colorability of these alkali halide crystals by radiation and that the dependence of this effect upon concentration in impurity showed an optimum similar to that observed for the luminescence effect⁽³⁴⁾. These colors also bleached more readily. It has long been known that many other salts and minerals have their radiation colors caused, enhanced, or altered by the presence of impurities⁽³⁵⁾.

Pohl and Rupp, and later Arsenjewa, studied the influence of

x-radiation on the absorption spectrum of alkali halide phosphors. In addition to F band formation the original absorption bands of the phosphor are elevated or depressed, depending upon the specific impurity⁽³⁶⁾. Also the formation of a broad and intense shoulder plateau in the ultraviolet region has been observed. Slight shifts in absorption band frequency were also noted. Later workers on phosphors have occasionally studied the F band as an intermediary or energy reservoir for the luminescence effect.

Various measurements have been made on the changes in electrical conductivity of alkali halide crystals containing impurities, notably the alkaline earth ions. Increases are chiefly ascribed to the existence of extra vacancies, compensating for the higher charge of the impurity ion. Recent studies, contrasting the effects of calcium and cadmium, show that the latter has a non-linear increase of conductivity with concentration, which suggests an association of cadmium ion with the adjacent vacancy⁽³⁷⁾.

Investigation of a new color center, the U band, formed by the addition of hydride ion, is described in a paper by R. Alger⁽³⁸⁾.

Coloration of mixed alkali halide crystals, notably RbCl-KCl and KCl-KBr, has produced broad absorption peaks of frequencies intermediate to those of their end members. This effect can be satisfactorily explained as arising from a distribution of hybrid color centers bounded by various combinations of the component ions⁽³⁹⁾.

Additive coloration of crystals containing alkaline earth ions as impurities, notably strontium, produces new absorption bands, called Z centers. These were discovered by Pick and his associates and are now receiving extensive study by a group of Italian investigators⁽⁴⁰⁾.

EXPERIMENTAL TECHNIQUES

Growth of Crystals from Solution: It is difficult to grow clear alkali halide crystals from aqueous solution, dendritic crusts being the

usual results. Buckley reports, as a unique case of enhancement of crystallization by impurities, that clear single crystals of sodium chloride result from the addition of about 0.1% lead ion to a saturated solution of NaCl from which CO₂ has been removed by slight acidification and boiling, the crystals being grown at 90 to 100° C. (41).

This method was tried out with a seed crystal of NaCl suspended in a 1 litre beaker of the solution described above, covered by a watch glass and placed in an oven set at 95° C. This attempt yielded several crystals, 1 cm on edge, clear but with a pronounced mosaic structure. The technique was improved by using a modification of the Soxhlet extractor apparatus, as suggested by Mr. Dale Rice of this department, and as shown in Figure 19. The solution in the flask was maintained at a temperature of 95° by a heating mantle. The vapor evolved was condensed, passed through a paper thimble containing more powdered salt, and returned to the flask. Thus the solution was maintained at a slight supersaturation, favorable to the growth of large crystals. The crystals so grown gave several cleavages 1/4-1/2" square and 2 to 4 mm thick, the central zone of which was the rod of the original seed crystal. A slight mosaic structure was observed, but not enough to render the specimens unsuitable for spectrophotometric work. The uncolored crystals showed twin absorption peaks, very narrow and intense, in the ultraviolet region at about 2800 Å. and 2300 Å. It has been reported that traces of lead in sodium chloride give absorption peaks at 1930 Å. and 2740 Å. and since lead is an impurity in crystals so grown, it is the probable cause of the peaks observed here.

The cleavages showed a great capacity for coloration. Upon exposure to x-rays for an hour followed by a few minutes bleaching they were not only darker than the central seed crystal but of a different tint. The

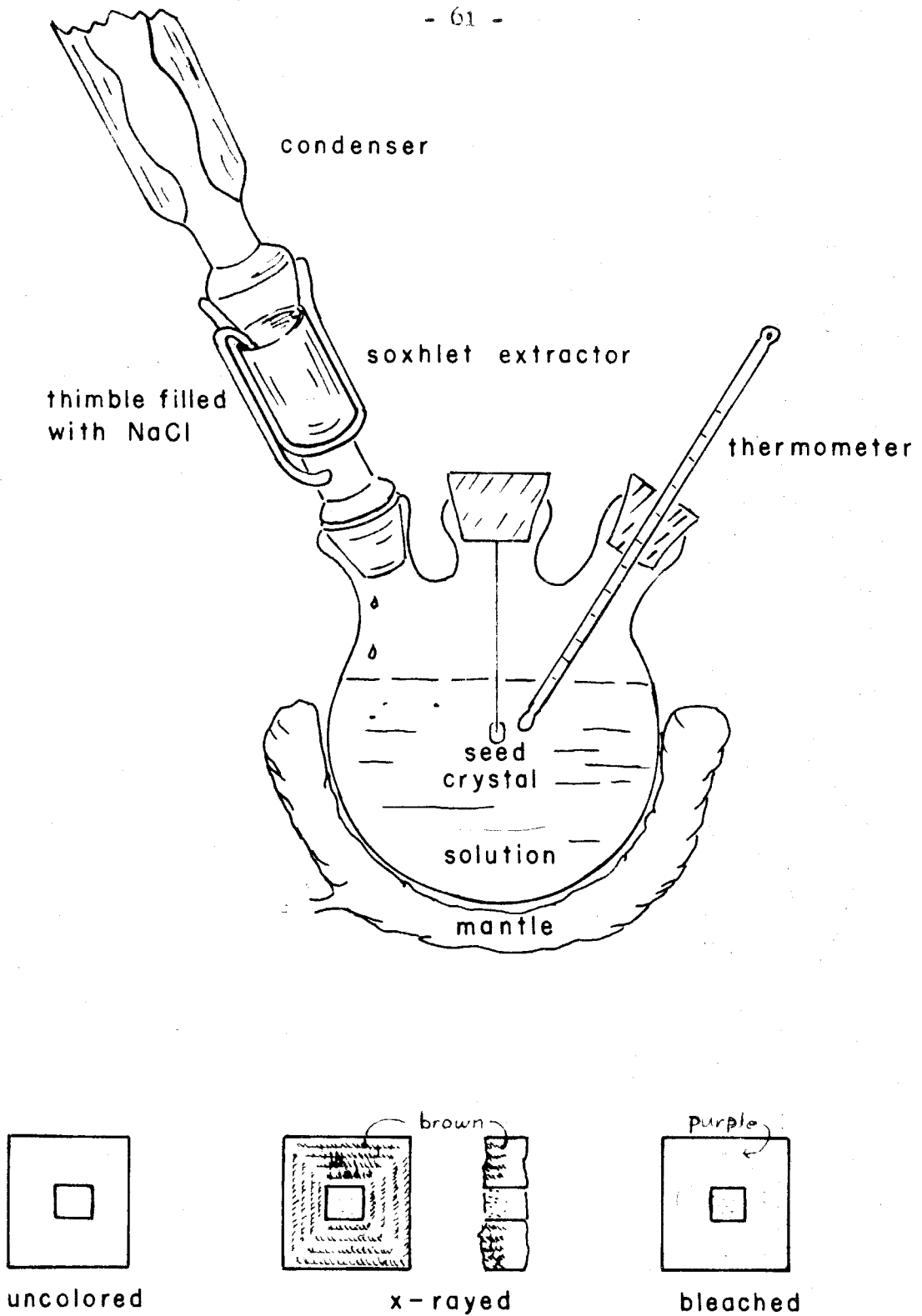


Figure 19. NaCl Grown From Solution.

spectra showed a small, somewhat broad F band and another band at 7000 \AA .; the peak at 2800 \AA . had all but disappeared while the one at 2300 \AA . remained. Upon further bleaching the crystal decolorized completely, but the ultraviolet peaks were still quite small and distorted (see Fig. 20). Another sample, grown by the earlier method, x-rayed, and about $3/4$ bleached, showed a single intense band at about 2000 \AA .

Examination of the solution-grown part of the cleavage showed an interesting structure in coloration and bleaching. The coloration occurred in distinct layers at (100), very pale around the seed crystal but in alternate light and dark layers further out. Uncolored diagonal lines were evident, giving the crystal a sort of "hour glass" appearance (see Fig. 19). The depth of coloration varied; 2 mm or more in some of the dark layers, and of greater intensity than that of the seed crystal. At one or two of the lighter layers near the seed crystal a pale bluish-green tint could be observed.

Upon nearly complete bleaching, fine lines of pale violet color remained where the pale layers had been and also a few small spots of pale blue-green coloration. The central, seed crystal zone was still a pale brown. A few crystals were subjected to several weeks of irradiation and were then bleached; no stable violet color could be developed.

Growth of crystals from melt: The method developed by Professor Kyropoulos was used, which consists of immersing, into a crucible of the molten salt, a seed crystal attached to a cooling apparatus. As the seed crystal grows, the apparatus is gradually raised until a large crystal is slowly drawn from the melt. In the first method reported, the seed crystal was attached mechanically to the cooling device. In a later method (preferred by Professor Kyropoulos himself) the cooling device, a platinum tube closed at one end and cooled by means of an air

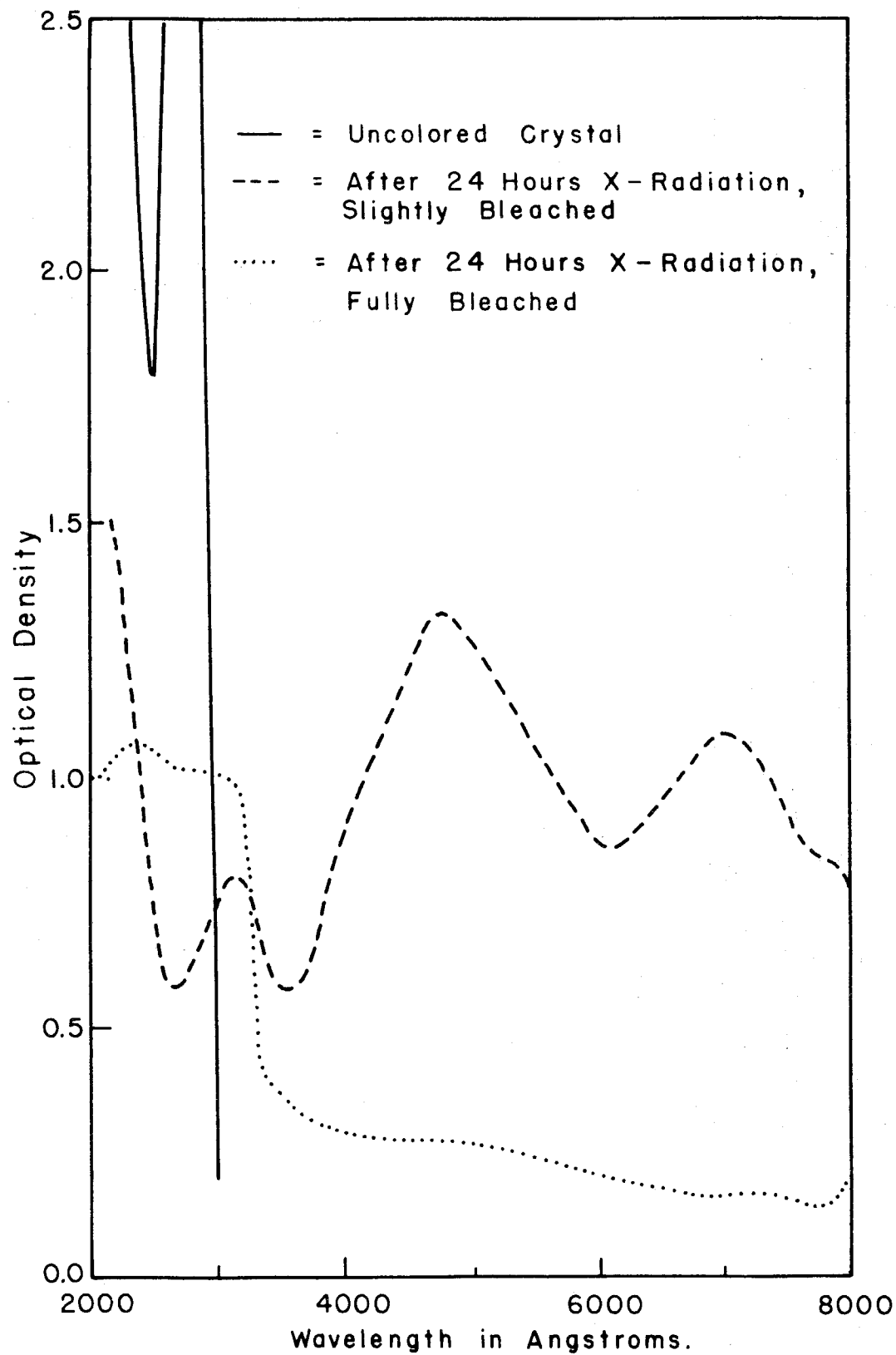


Figure 20. NaCl Crystals Grown from Solution.

blast, was first immersed in the melt until a hemisphere of radiating crystals had grown on the tip of the tube. This was then raised until only the bottom tip of the hemisphere was in contact with the melt. This area served as the seed for growth of the main crystal⁽⁴²⁾.

Construction of apparatus was started in the fall of 1954. The furnaces consisted of heating wire wrapped around a threaded alundum core, insulated with several layers of asbestos paper, and fitted into a length of transite pipe. Temperature was regulated by a Wheelco Capacitrol, which is essentially a thermocouple operated relay switch. The temperature fluctuation was about $\pm 10^{\circ}$.

A screw-driven platform was constructed for slowly raising the crystal (see Fig. 21). At first it had to be operated manually and required constant attention; later a clock motor drive was added for automatic operation. Following the suggestion of Mr. Richard Carrouche' of the Physics Department, another lift was constructed utilizing a hydraulic piston. This is as satisfactory as the other device and of greater strength and versatility.

In addition to the platinum tube, several cooling devices were constructed for use with seed crystals. The first, consisting of a copper tube attached to a group of copper fins cooled by air blast, grew satisfactory crystals but tended to corrode and contaminate the melt with copper oxide. A silver rod, insulated by an alundum tube and attached to a water-cooled copper block, was more satisfactory. Another device, a small quartz cold finger condenser (see Fig. 22), was used either with a platinum adapter for growing crystals by the seed method, or by itself to grow chloride and bromide crystals by the second Kyropoulos method.

The pure alkali halide powder and the contaminating salt were weighed into a large crucible (preferably of quartz, though porcelain

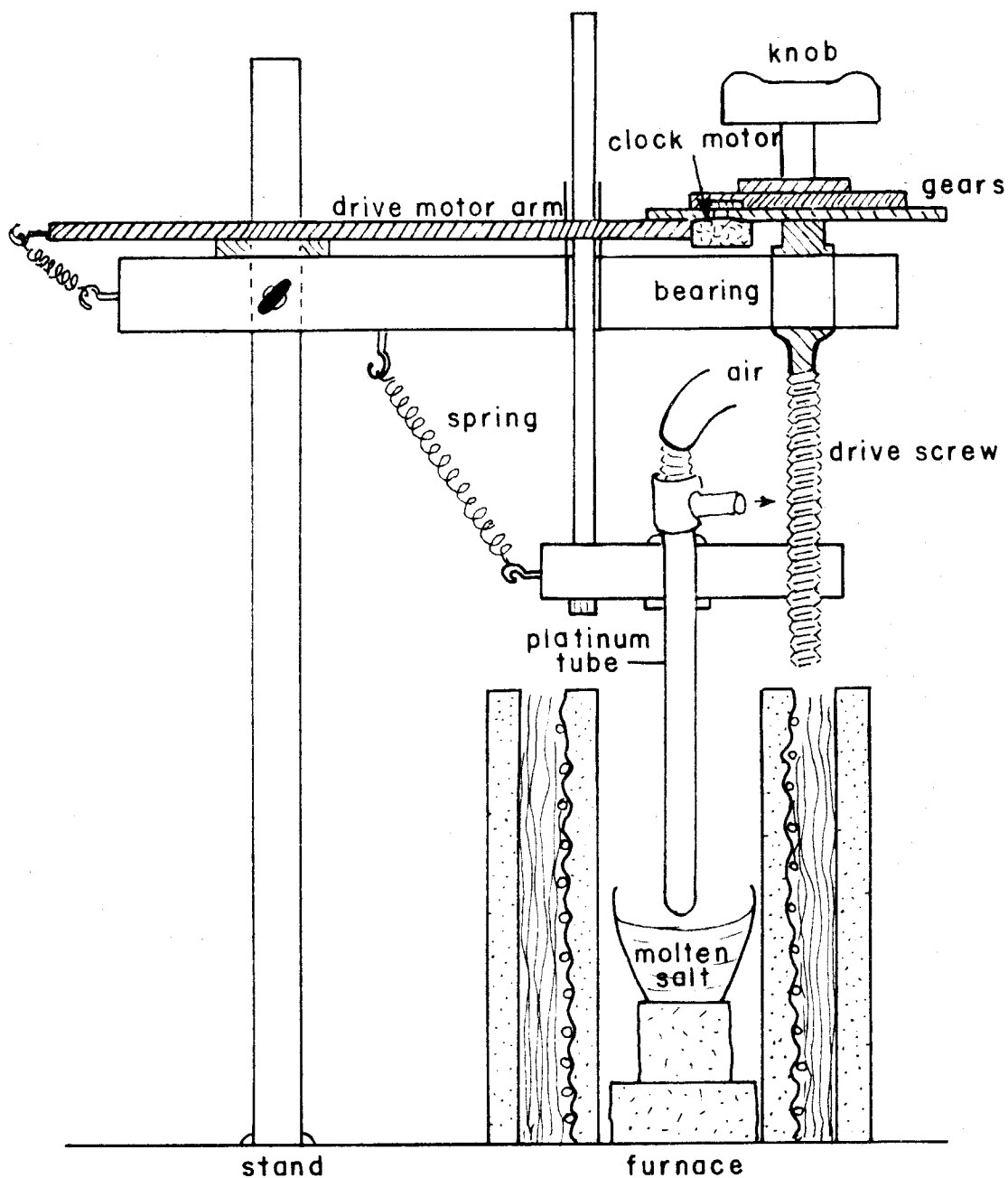


Figure 21. Crystal Grower.

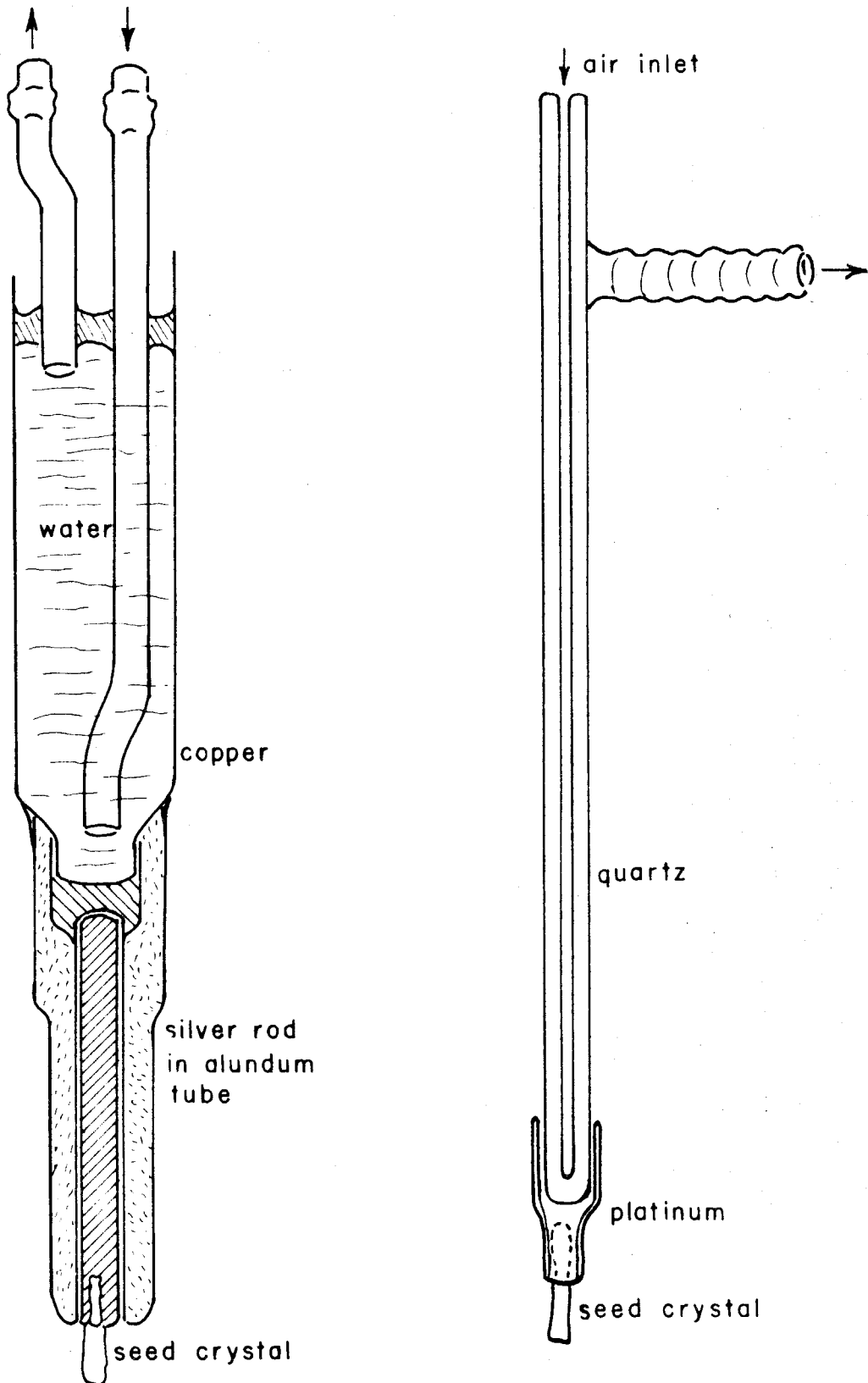


Figure 22. Cooling Heads (actual size).

was adequate for most purposes), placed in the furnace, and heated for at least 1/2 hour at one or two hundred degrees above the melting point. If the seed method was to be used, the melt was then cooled to a very few degrees above the melting point. The seed crystal, attached to the cooler, was lowered cautiously until the tip just touched the melt. It was often necessary to readjust the temperature. The proper regulation of furnace temperature resulted in a transparent hemisphere of crystal, gradually growing out from the small seed. When the hemisphere was of desired size, the raising mechanism was started and the crystal was drawn out from the melt; this process took 1 to 2 hours to grow a crystal of 20 to 30 grams. The apparatus had been inspected from time to time during this process to make sure that the crystal did not grow so wide as to stick to the sides of the crucible, nor diminish to a thin rod.

Most contemporary researchers prefer the above method to the second Kyropoulos method, which involves the growth of the seed crystal from the melt itself. Professor Kyropoulos himself thought that the poor results with the second method resulted from a failure to follow directions, as set forth in his original paper⁽⁴²⁾, such as the directions to grow the seed crystal and to start to grow the main crystal at 50° or more above the melting point, also to allow the seed hemisphere to grow to 3 or 4 times the diameter of the platinum tube, and very carefully and quickly to raise it so that just the tip touches the melt. Following these directions carefully, I was able to grow fine sodium chloride crystals, but because of the greater attention required, the other method was used almost exclusively in the work.

Crystals so grown varied widely in size and shape, averaging 1" to 1.5" in diameter and height. More than half the attempts resulted in excellent single crystals, and almost all were good enough to yield a

requisite number of cleavages. There was usually a small zone of mosaic crystals at the very top. After growing, the crystals were allowed to cool slowly in the furnace, and examination under polarized light showed no more strain than is usually encountered in natural or synthetic crystals.

Treatment with Sodium Vapor: Because of the large number of samples which had to be treated with alkali metal vapor, preliminary tests were made using small metal pill boxes as bombs. As a rule the "gettering" of the oxygen in the box caused it to contract enough to insure an air-tight fit. A sample of pure alkali halide always accompanied the doped crystal as a check upon the reliability of the coloring process.

At the termination of research, one series of runs had been made upon most of the crystals grown, using these pill boxes. Although most of the crystals containing impurities developed various colors, many of the control crystals were colorless.

Radiation Colors: The techniques used in x-radiation, optical, and thermal bleaching, are the same as described previously.

EXPERIMENTAL RESULTS

About a dozen impurities were incorporated into sodium chloride, most of these being ions of transition metals.

NaCl:Ca The melt consisted of 50 g. of NaCl to which was added approximately 1 g. of CaCl_2 . The crystal weighed 30 g., was clear, without any color or turbidity, and provided excellent large cleavages. There were no visible or ultraviolet absorption peaks. Upon being heated in sodium vapor, the crystal developed a pale yellow color, which resulted from weak, broad band around 4150 \AA ., in all probability an incipient F band.

NaCl:Rare Earths The anhydrous chlorides of the rare earths metals are difficult to prepare and decompose in air at high temperatures to form oxychlorides. This decomposition, plus the high valence state of the rare earths, made them a very unpromising impurity for incorporation in sodium chloride. However, a few attempts to grow such crystals were made so as to provide Mr. Floyd Humphrey with samples for electron spin resonance. The melt consisted of pure sodium chloride to which 0.2 g. of a mixture of anhydrous rare earth chlorides was added just before crystallization started. After a few minutes a white scum of oxychloride formed on the surface of the melt, therefore addition of the anhydrous chloride was repeated frequently during the crystallization. Crystals so grown weighed about 25 g. and were slightly greenish, cloudy, and polycrystalline, yielding a very few imperfect cleavages. The electron spin resonance results were negative, implying that the rare earth nuclei were in an unsymmetric environment, probably as oxychloride mechanically incorporated into the crystal. There were no significant absorption spectra.

NaCl:Cd Approximately 0.5 g. CdCl_2 was added to 35 g. of NaCl to form the melt. A crystal was grown weighing 20 g., showing no color or cloudiness and yielding several clean cleavages greater than $1/2$ " square. The remaining melt showed no residues or precipitates. Absorption spectra showed a weak, broad band at 4250 \AA . and a gradual absorption edge starting at 2300 \AA .

Treatment with sodium vapor for 4 hours at 750°C . yielded a brown coloration (by transmitted light), the spectra of which has not been examined. A zone 1 mm wide around the edge of the crystal was of deeper color. By reflected light (i.e. as a result of light scattering), the crystal has zones of white, blue gray, and black, resembling an agate. Microscopic examination reveals numerous irregular inclusions. These

facts suggest the existence of colloidal cadmium metal, but an electron microscope examination showed nothing. The control sample of pure sodium chloride was almost colorless.

NaCl:Ag A crystal was grown from a melt of initially pure sodium chloride in a silver crucible. At the onset of crystallization the melt had a slight brownish cast and during growth the lower half of the crystal was a distinct pale brown. The crystal weighed 30 g., was somewhat polycrystalline but yielded several good cleavages. The upper half of the crystal was almost colorless and showed no light scattering. The lower half, upon cooling, was a pale brown, and somewhat turbid. The remaining melt was cryptocrystalline, an opaque pale brown, and obviously contained silver oxide. When briefly x-rayed, the sample developed an intense long-lived phosphorescence, giving off a violet glow reminiscent of F band light. X-ray colorability was greatly increased over that of pure NaCl, the crystal being deeply colored after only a few minutes exposure.

The uncolored crystals had no significant spectra in the visual region but a very intense peak around 2100 \AA ., in agreement with the literature (see Fig. 23). Treatment with sodium vapor at 750° developed a deep brown color whose spectra showed a gradual rise in absorbence towards shorter wavelength; the sharp ultraviolet absorption was replaced by a very broad weak band at 2600 \AA .

NaCl:Mn From a melt consisting of 0.60 g. MgCl_2 in 60 G. of NaCl, a crystal was grown weighing 23.5 g. The melt grew dark in the course of crystallization and the crystal itself was a pale violet color during crystallization and the first hour of cooling. The cold crystal was colorless. It showed, especially on the bottom, a faint turbidity which microscopic examination showed to be due to the presence of tiny brown particles, probably of MnO_2 , since the melt was heavily contaminated with

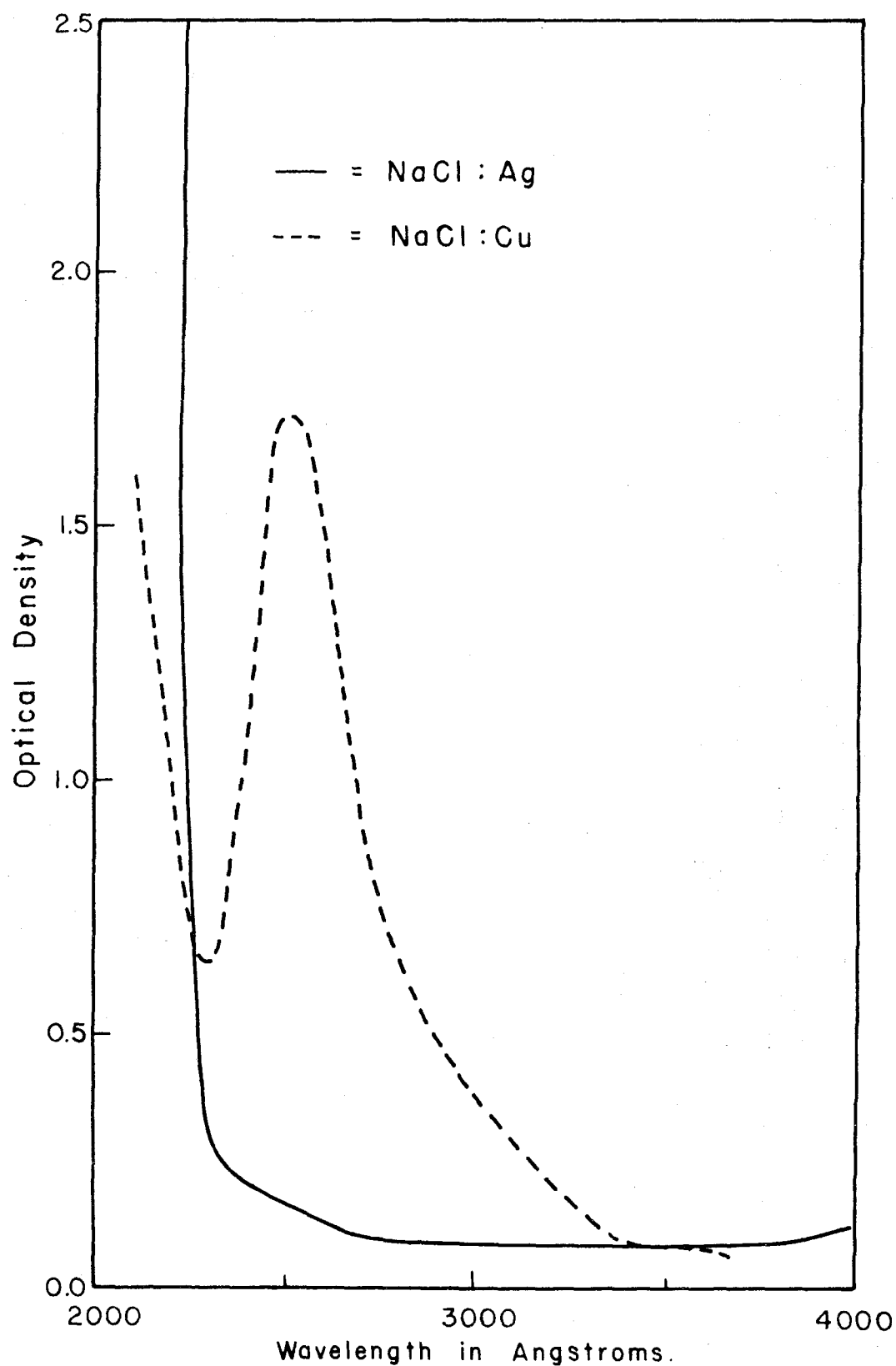


Figure 23. NaCl:Ag and NaCl:Cu.

this material. The upper part of the crystal was polycrystalline but the bottom 10 g. gave excellent cleavages 1" in diameter.

The crystal showed a strong blue phosphorescence, as is the case for all alkali halides containing manganese. The crystal showed no absorption bands either in the visible or ultraviolet, aside from a very weak band at 2750 \AA . in specimens from the bottom of the crystal 1 cm thick. Treatment with sodium vapor at 750° C . gave a deep brown color which was not examined spectroscopically.

Another crystal grown from a melt consisting of 0.05 g. MnCl_2 in 50 g. of NaCl showed no dark precipitate in the melt and gave a clear crystal, colorless when hot or cold, which has not received further study.

$\text{NaCl}:\text{Cu}$ The melt, consisting of 0.6 g. of CuCl_2 in 60 g. of NaCl , gradually developed a greenish color during crystallization, but the crystal showed no color while hot. The crystal weighed 20.5 g., was a single crystal with a very slight mosaic structure, and gave many good cleavages. The bottom 0.1" of the crystal had a yellow turbid tint. The residue of the melt was microcrystalline and opaque, and light brown in color, the edges being translucent turbid yellow.

The crystal gave a distinct blue luminescence, and very narrow, intense absorption peaks at 2550 \AA . and 2000 \AA . Only the former peak has been reported elsewhere (See Fig. 23).

Treatment with sodium vapor for 8 hours at 750° developed an intense and beautiful ruby-red color. In cross-section, this specimen showed a transparent layer 0.5 mm thick on the surface next an opaque colloidal-like layer 0.5 mm thick, with the inside a clear deep red. The color strikingly resembled that of ruby-red glass, ascribed to colloidal gold or copper.

A crystal of $\text{KCl}:\text{Cu}$, grown from a melt containing 1% CuCl_2 , was initially yellow and faintly turbid. Treatment with sodium vapor resulted

in a clear deep red. Absorption spectra were taken of these red crystals, of a borax glass bead containing traces of copper and tin and heated in a reducing flame, and of a brown copper sol formed by reducing a copper sulfate solution with sodium hyposulfite. All showed the same peculiar peak and inflection near 6000 \AA . A thin film of copper metal, evaporated on glass by Mr. Carrouche', showed an inverse absorption peak at this frequency (see Fig. 24).

NaCl:Cr The melt contained 1% CrCl_3 . A crystal was grown only part way (15 g.) when a power failure interrupted the process, so that the crystal became stuck to the congealed melt. The salvaged crystal was clear, gave good cleavages, and had a faint purple color while hot but was colorless upon cooling. The congealed melt was dirty, with a light green precipitate.

The crystal showed no obvious luminescence when exposed to x-rays. The absorption spectrum had an intense sharp band at 2480 \AA . (see Fig. 25). Treatment with sodium vapor at 700°C . gave a pale brown color (the control being colorless), which has received no further study.

NaCl:Fe The melt, containing originally 1% FeCl_3 , developed a thick brown precipitate during crystallization and gave off a faint smell of chlorine. The crystal, weighing 20 g., was for the most part transparent and gave good clear cleavages. In the bottom $1/8$ ", where it had stuck to the melt, there were translucent brown areas. The crystal showed no luminescence or absorption spectra. Treatment with sodium vapor at 700°C . gave a very faint yellow (the control being colorless) which has not been studied further.

NaCl:Ni The melt consisted of 0.5 g. NiCl_2 in 50 g. of NaCl and showed no sign of decomposition during or after crystallization. The crystal, weighing 35 g., was clear and colorless, somewhat polycrystalline,

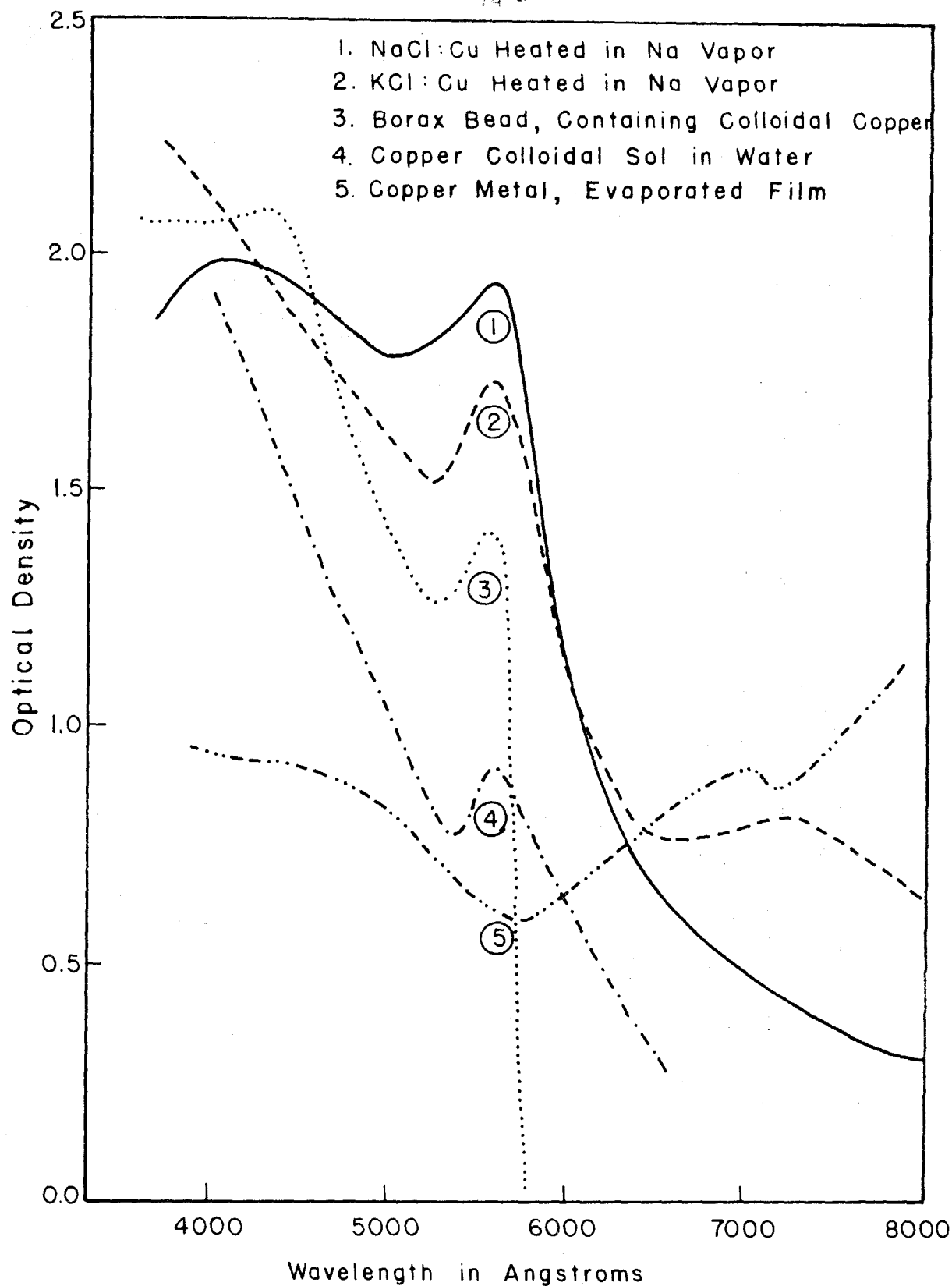


Figure 24. Colloidal Copper in NaCl:Cu.

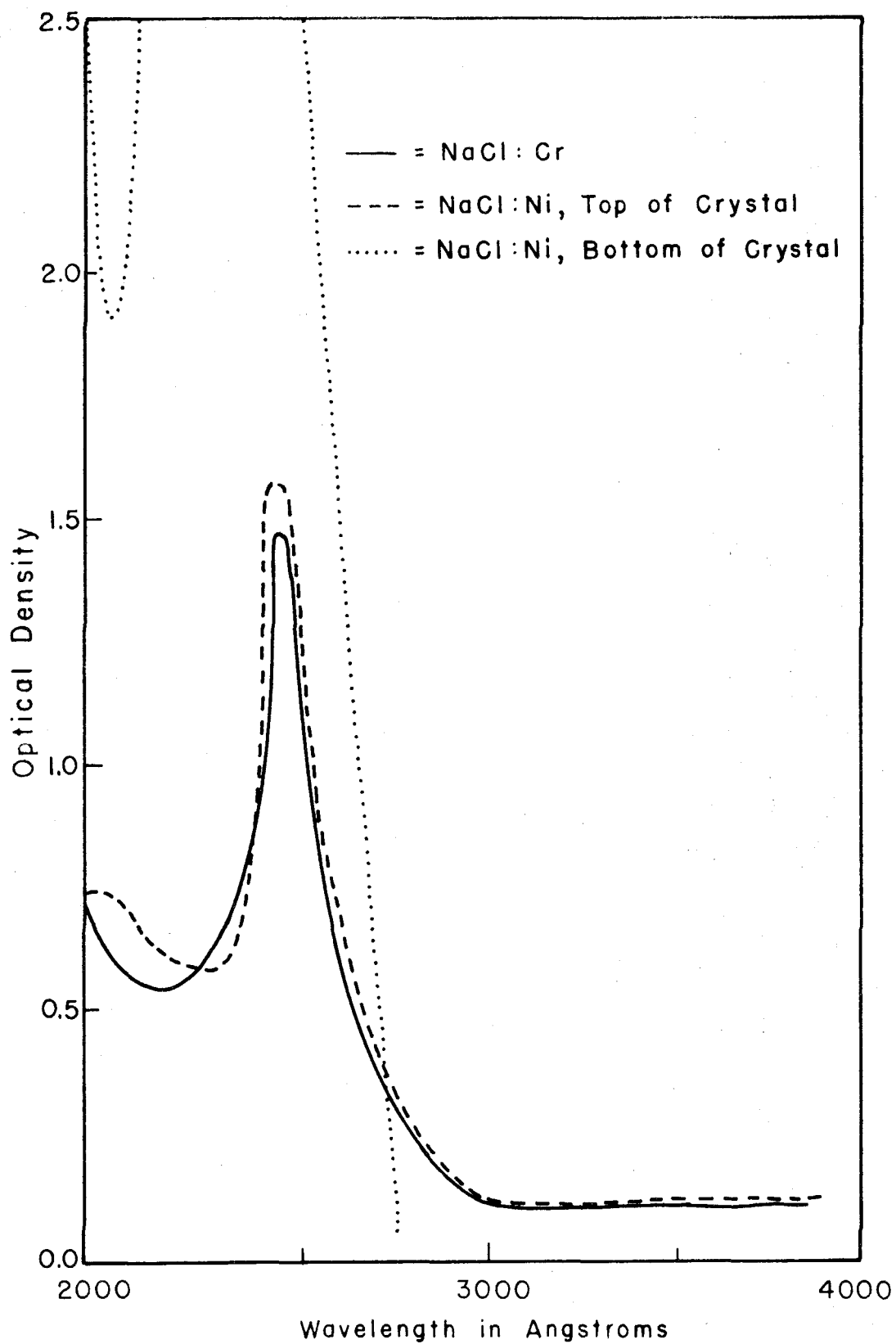


Figure 25. NaCl:Cr and NaCl:Ni.

but gave large, flat cleavages. The bottom had a faint yellow turbidity. The crystal gave a narrow intense absorption band at 2450 \AA . almost identical to that of NaCl:Cr . A sample from the bottom of the crystal gave the same band with much greater intensity than a sample of corresponding thickness from the top of the crystal (see Fig. 25). Upon treatment with sodium vapor at 700°C ., a faint yellow color developed, which has received no further study.

NaCl:Pt Since PtCl_2 decomposes at high temperature, small quantities of the salt were added during crystallization. The crystal was grown by the second Kyropoulos method, utilizing the platinum tube. It was colorless, although slightly turbid, and gave good cleavages. There were no absorption peaks, either in the visible or ultraviolet. Upon treatment with sodium vapor at 700° , the crystal developed a slight gray tint, which has not been examined further.

NaCl:Au The melt consisted of 50 g. of pure NaCl to which 0.5 g. of AuCl_3 was added just before crystallization. The crystal itself weighed 20 g., was quite clear and free of turbidity, and gave excellent cleavages. During crystallization bright flakes of gold were observed moving about rapidly through the melt. Upon cooling the residue at the sides of the crucible was a bright pink, reminiscent of colloidal gold. The residue at the bottom of the crucible was a single crystal with fine flakes of gold metal disseminated throughout.

The crystal showed no absorption spectra whatever. The pink pieces showed a band at 5500 \AA . followed by a steady rise towards shorter wavelength (see Fig. 26). The piece at the bottom of the crucible showed a very faint band at 5750 \AA . Samples of the crystal gave a negative benzi-dine test and it was feared that no Au^+ ion had been incorporated in the crystal, but treatment with sodium vapor for 4 hours at 750° rendered

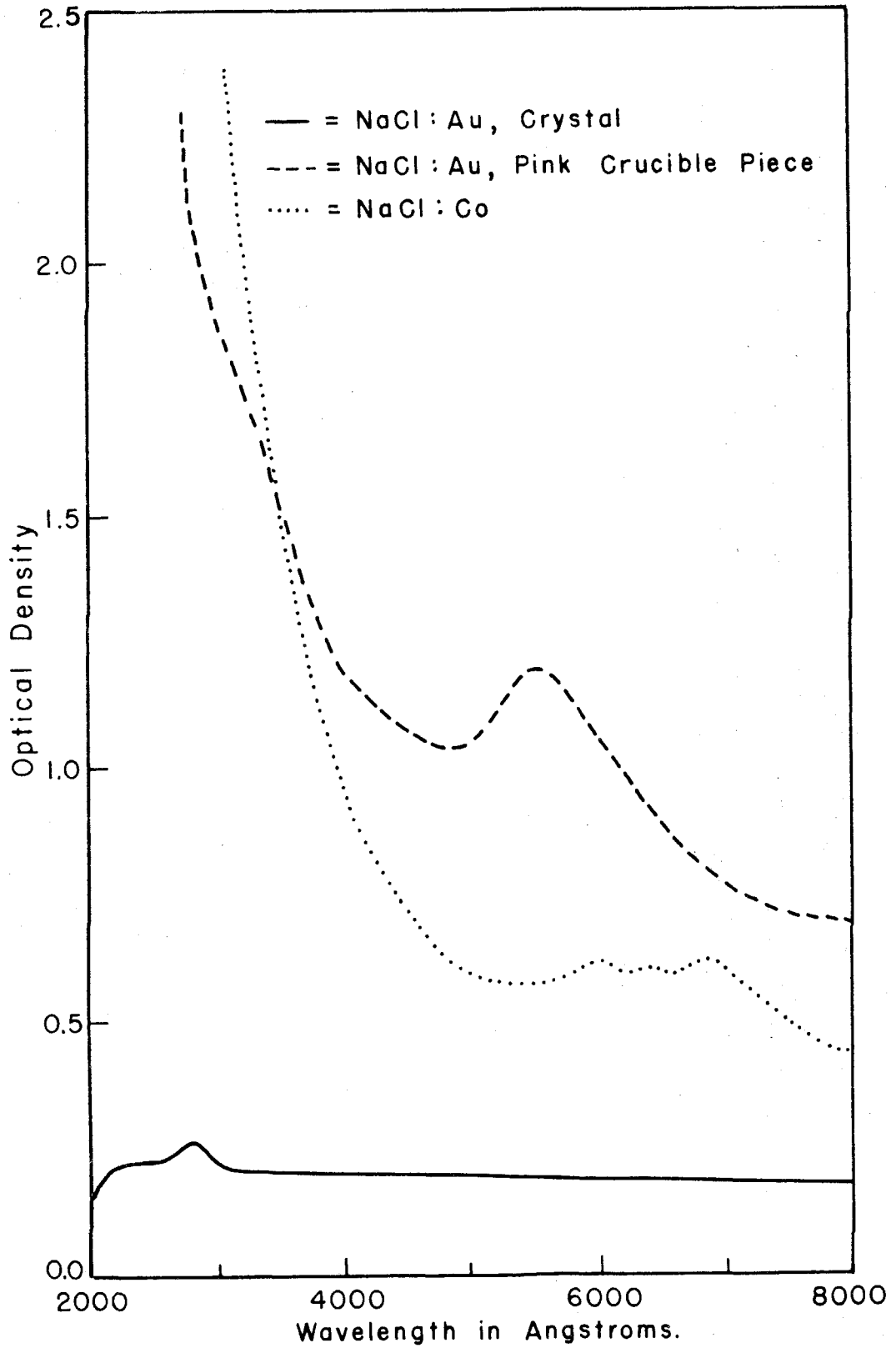


Figure 26. NaCl: Au and NaCl: Co.

the crystal an opaque brass color. This was due to a layer 0.5 mm deep on the surface of the crystal, apparently quite thick with fine particles of gold, the interior of the crystal being perfectly colorless. The control also was colorless. Another sample, treated the same way but cut from the top of the crystal and presumably with a lower impurity concentration, had streaks of dull blue mixed with the brass color. This may indicate colloidal gold. Time did not permit the growth of new crystals with a lower concentration of gold ion, in further attempts to develop a colloidal blue color.

NaCl:Co The melt consisted of 0.5 g. of CoCl_2 in 50 g. of NaCl. A large single crystal was grown, weighing 35 g., with excellent cleavages throughout. At the time of formation, and during the first 15 minutes of cooling, the crystal was a beautifully intense transparent blue. This color remained down to 600° , but when the crystal was later inspected at room temperature, it had become pale sky-blue and was opaque. Thin sections showed a few transparent pale blue zones, but were a turbid yellow, suggestive of colloids, in the more deeply contaminated zones. Reheating caused the transparent blue color to return, and cooling brought back the pale blue and turbidity.

A 12 g. sample was taken from the bottom of the crystal and added to three times its weight of pure NaCl to provide the melt for a second, more dilute, crystal. This gave a transparent blue of medium intensity at high temperatures, which cooled to pale blue showing zones of yellow turbidity, much like the upper parts of the previous crystal. This showed a weak broad band at about 6900 \AA , and a steady rise in absorption towards shorter wavelengths (see Fig. 26). Treatment with sodium vapor at 750° rendered the crystal somewhat less turbid and of a more greenish tint. The absorption spectra were not studied.

NaCl:Pd Approximately 0.5 g. of PdCl_2 were added to 50 g. of molten NaCl. The crystal grown from this weighed about 25 g., was somewhat polycrystalline, but gave good cleavages. The crystal had irregular brown spots, as if from colloidal metal. The uncolored parts showed a small peak at 2600 \AA . and a sharp absorption plateau starting from 2400 \AA . (see Fig. 27). Treatment with sodium vapor did not appear to change the coloration.

NaCl:Ba The crystal, grown from a melt containing 1% BaCl_2 , had a white and turbid appearance, although giving excellent cleavages. The remaining melt was diluted with three times its volume of pure NaCl and a second crystal grown. This was clear and free of turbidity but had a faint brownish cast. A specimen 4 mm thick gave 2 weak absorption lines at 2700 and 2200 \AA . (see Fig. 28).

NaCl:O The crystal was grown from melt consisting of 50 g. of NaCl to which had been added 0.5 g. of Na_2O_2 . A cleavage 3 mm thick showed a fairly intense absorption edge starting at 2100 \AA . (see Fig. 28).

X-ray Coloration: The project was terminated just as this work got under way, so that only a few qualitative facts can be noted here:

NaCl:Ag has remarkably strong coloring powers, becoming a deep brown after a few minutes of radiation. It is also difficult to bleach as compared with pure NaCl. A sample x-rayed for 24 hours and bleached for several days still showed a faint yellow tint, although the spectra were substantially the same as for the unirradiated material, the chief difference being an increase in the ultraviolet edge and a new band at 2550 \AA . (see Fig. 29).

NaCl:Cd, after 17 hours radiation, developed F and M bands of the same wavelength and intensity as the pure salt, but had in addition a

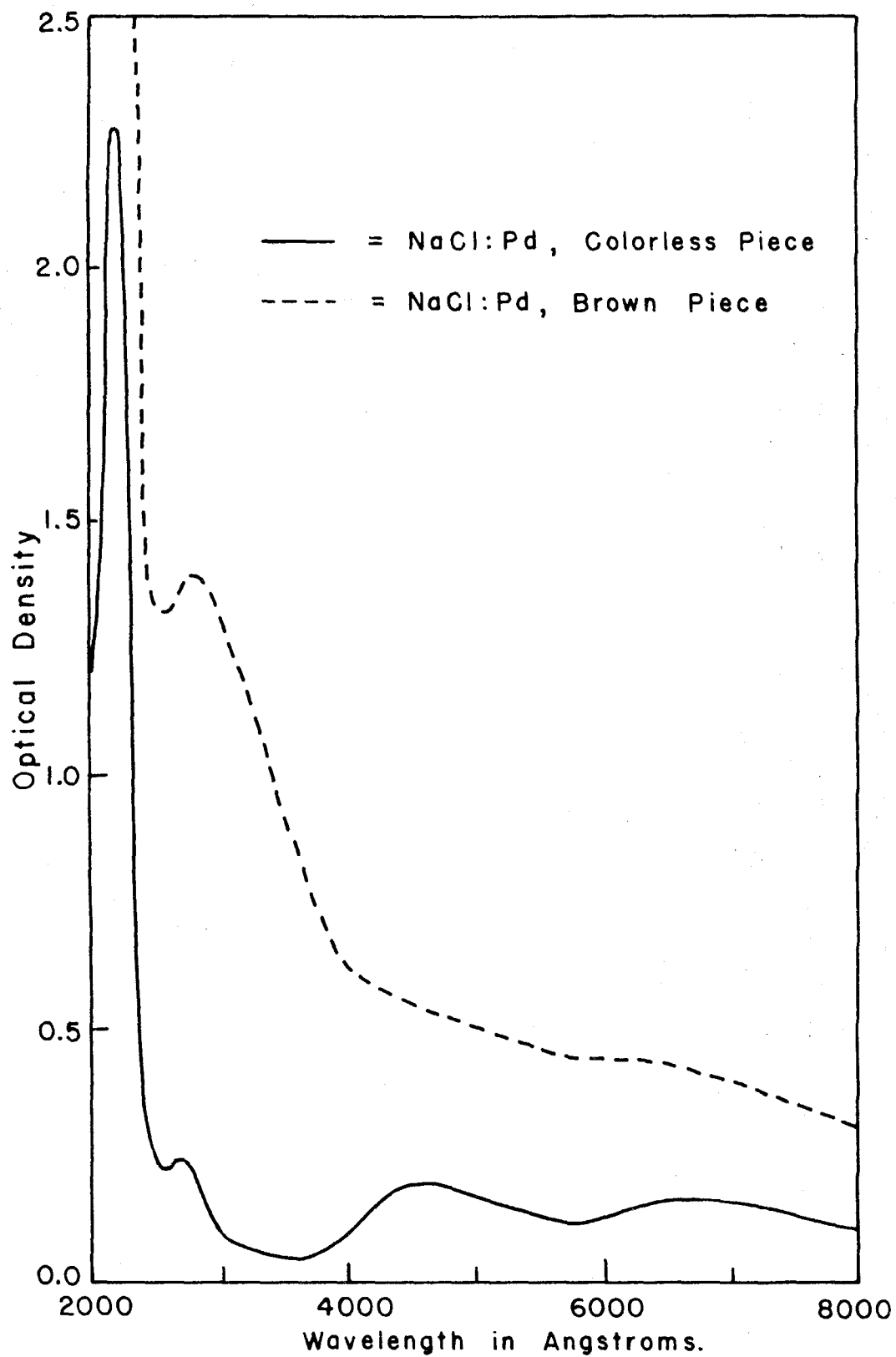


Figure 27. NaCl:Pd.

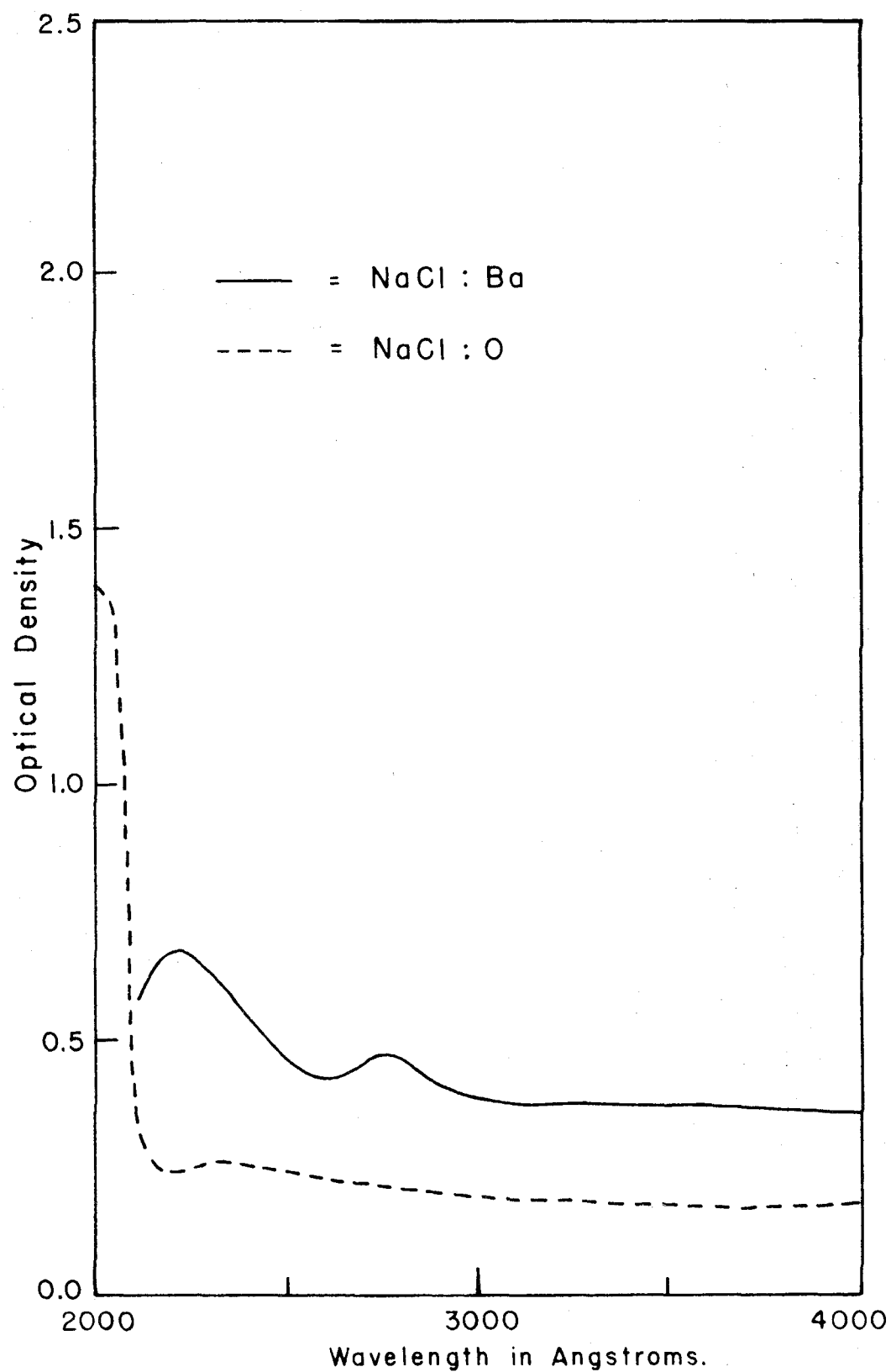


Figure 28. NaCl:Ba and NaCl:O.

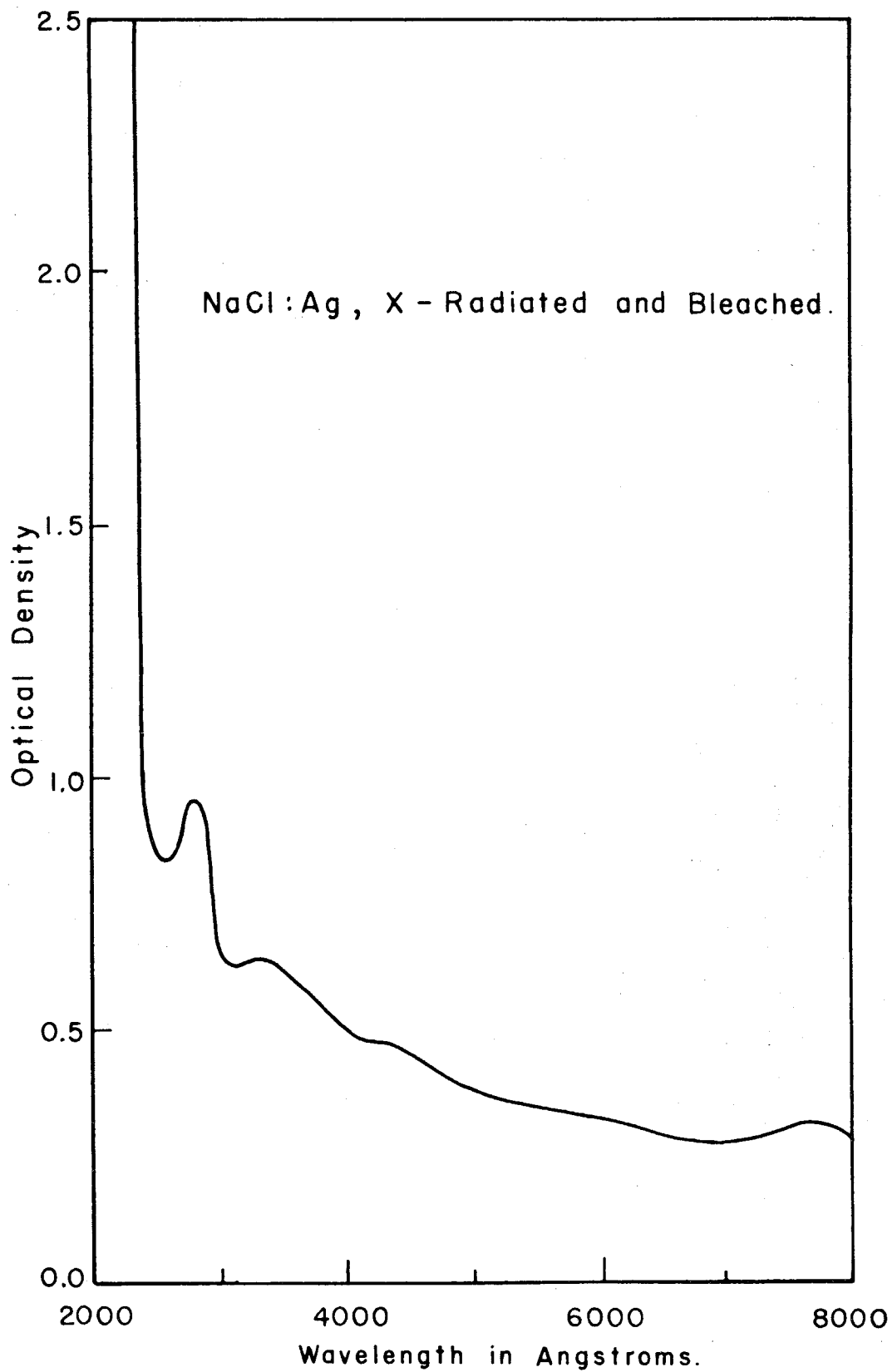


Figure 29. Radiation Coloring of NaCl:Ag.

very strong band in the ultraviolet. The sample bleaches with extraordinary rapidity, having after 20 minutes only an ultraviolet peak of such intensity as to be unmeasurable. A thin section cut from the original sample showed this band to have a rather complicated peak at about 2500 Å. (see Fig. 30).

A quantitative comparison was made of the colorability of NaCl:Cu and NaCl:Mn as compared with the pure salt (see Fig. 31). The following table gives the optical densities of the F band for these samples, after a 3 minute exposure to copper radiation at 25 kv and 15 ma and after 24 hours of radiation at 49 kv and 15 ma:

	OPTICAL DENSITY		
	NaCl	NaCl:Cu	NaCl:Mn
3 minute exposure	0.19	0.28	0.48
24 hour exposure	4.85	5.6	8.3

Thus, for short periods of radiation copper increases colorability by 47% and manganese by 150%. But for long exposures to x-rays copper gives an increase of only 15% and manganese of 70%. Therefore enhancement of coloration is at least partially a rate rather than an equilibrium phenomenon.

Other qualitative features are notable for the copper activated material. The F band seems to shift slightly towards longer wavelengths. The ultraviolet absorption peaks, observed in the uncolored material, diminish upon 3 minutes of x-radiation, and after 24 hours exposure are completely altered (see Fig. 32). Salt containing manganese shows no unusual features.

Secondary Coloration: Heavily irradiated samples of NaCl:Cd develop no secondary R centers upon optical or thermal bleaching. In the former case an intense ultraviolet absorption arises instead. The same effect

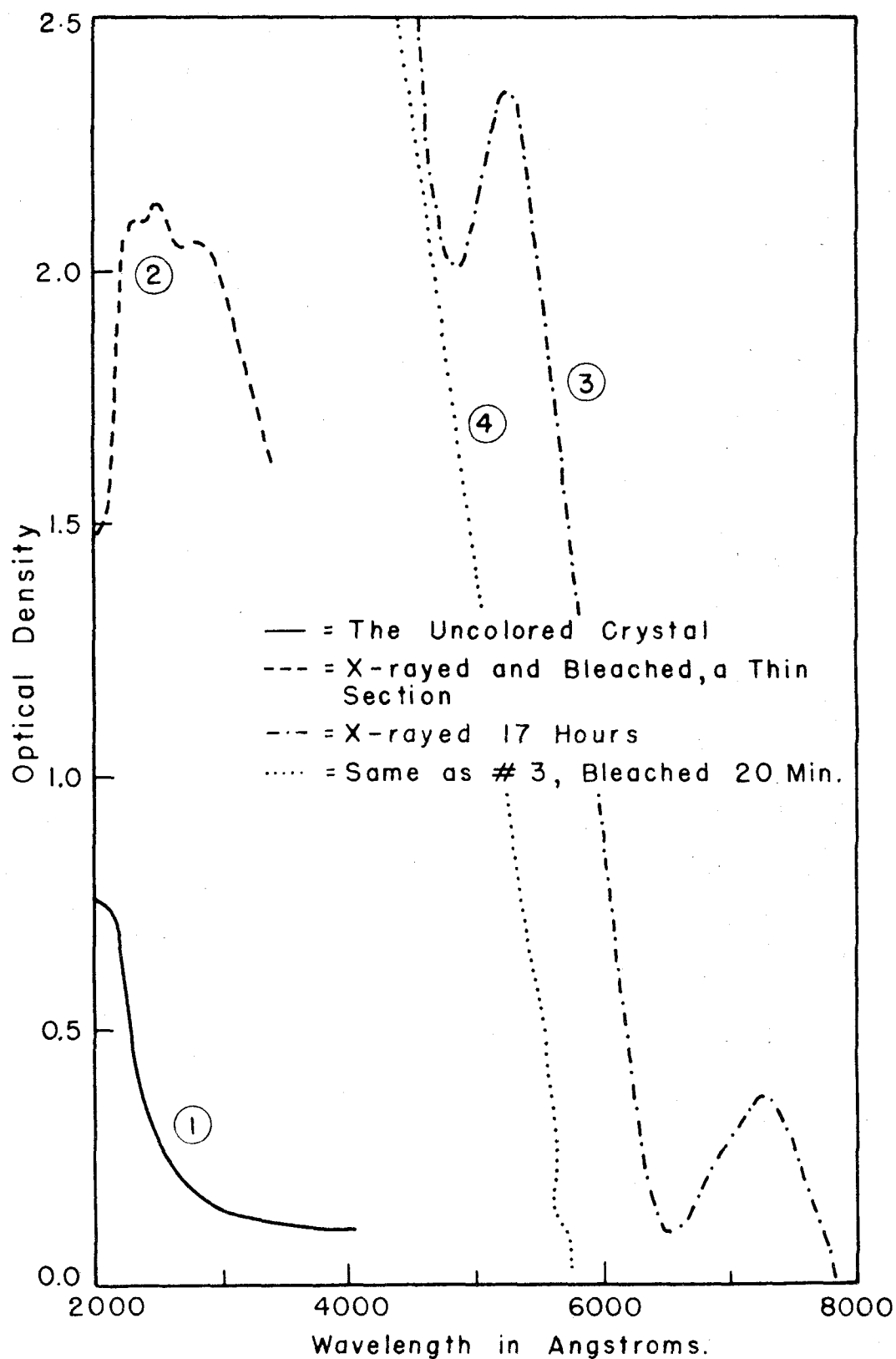


Figure 30. Coloration and Bleaching of NaCl: Cd.

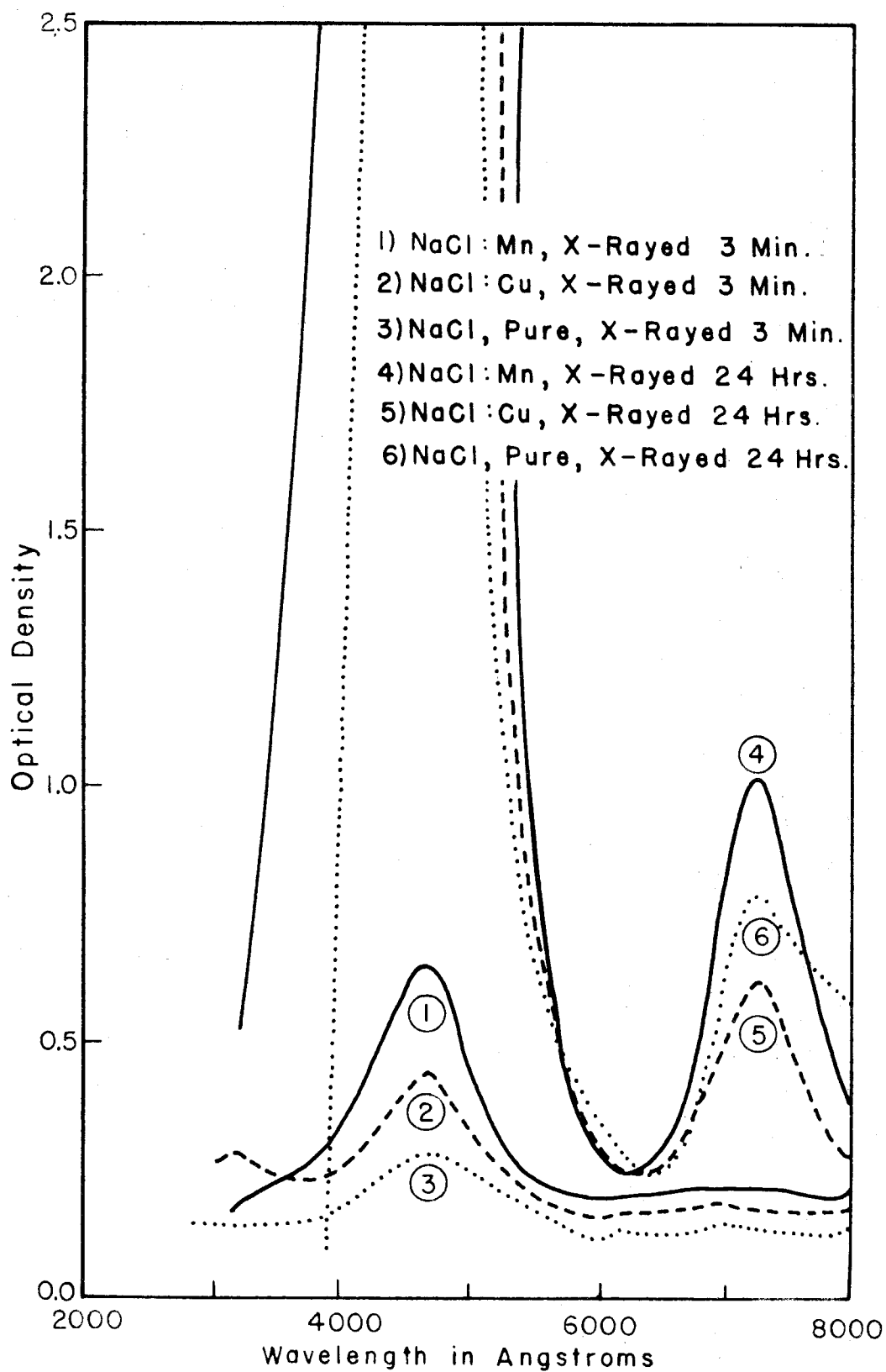


Figure 31. Effect of Impurities on Coloration of NaCl.

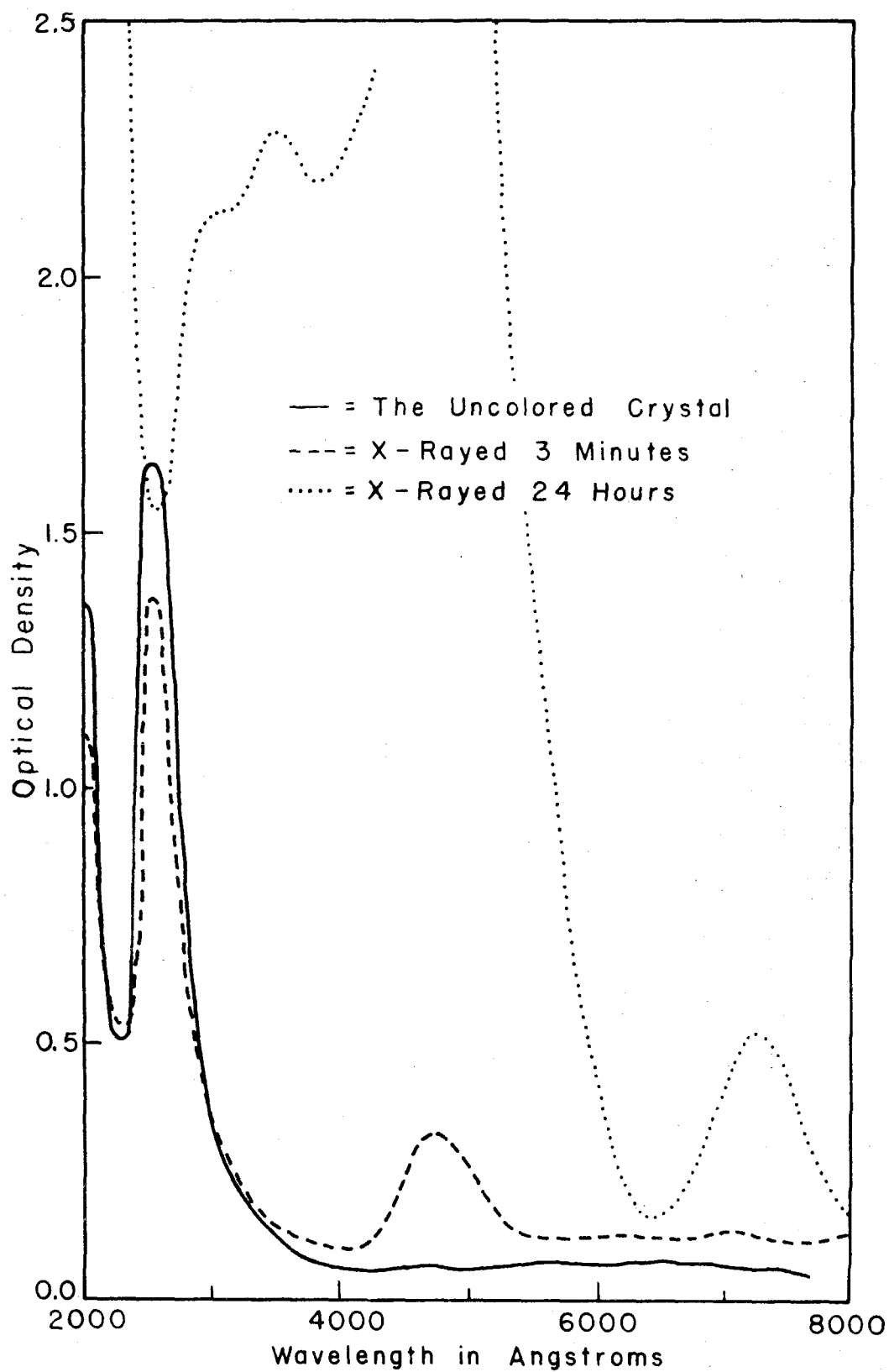


Figure 32. Coloration and Bleaching of NaCl:Cu.

was observed upon plastic deformation and radiation; instead of forming a blue color, the sample merely bleached clear.

INTERPRETATION OF DATA

The State of the Impurity Ion in the Crystal: Presumably the impurity ion is always admitted to the crystal as a single ion, probably replacing a sodium or chloride ion. It may not necessarily be true that the ion remains in this position or in an isolated state in the cooled crystal. A striking example of such a transition was the thermochromism observed for NaCl:Co. The intense blue color was presumably the cobaltous ion in sodium ion lattice positions. The sudden transition to a pale blue colloidal state indicates that with changing temperature the ion became less stable, presumably because of a tendency to change its configuration of coordination to the chloride ions. Presumably this instability occurred in temperatures high enough so that cobalt ions could migrate together and coalesce into a separate phase.

We have assumed that the impurity ion could not occur as a Frenkel defect, due to the close packing of the sodium chloride structure at room temperature; however, the crystal may be more capable of such disorder near its melting point, and the change of phase may result from the instability of Frenkel defects at lower temperatures. A spectrographic study at high temperature may settle this point. The high-temperature violet tints in sodium chloride containing chromium or manganese and the turbidity observed in NaCl:Ba and the bottom yellow portions of NaCl:Cu should be considered in a similar manner.

Another difficulty arises from ions whose chlorides are unstable at high temperatures, such as gold, palladium and platinum. The brown spots observed in NaCl:Pd might be colloidal metal. Such impurities might be more easily incorporated as ions in crystals grown from

solution. The valence state of the impurity for these and other metals may be determinable by suitable chemical spot tests.

Identification of valence states of impurity ions might be possible in certain cases by electron spin paramagnetic resonance, but the best tool seems to be absorption spectra. The peaks observed in the ultra-violet region for Cu, Cr, Ni, etc. are destroyed upon treatment with sodium vapor and must therefore be functions of specific ionic valence states.

Treatment with Sodium Vapor: Several of the impurities, such as manganese, cadmium, and silver, seem to have resulted in colloidal metal precipitation, since they give the dirty brown colors associated with colloids of these metals in solutions and give a diffuse absorption spectra.

The red crystals of NaCl:Cu and KCl:Cu, heated in sodium vapor, are probably the first proved case of a metal colloid in an alkali halide crystal. The comparison with a colloidal copper sol, with respect to absorption spectra (see Fig. 24) is impressive, and a theoretical argument can also be adduced. The predicted absorption coefficient for particles of colloidal metal in a transparent dielectric is essentially a function of the ratio of the refractive indices of the metal and dielectric⁽⁴³⁾. According to the Kramers-Kronig Formula, the refractive index varies as the derivative of the absorption coefficient with respect to wavelength. Therefore, since copper metal shows an inverse absorption peak at 6000 Å, we should expect a derivative of this, i.e., a sharp peak and dip, to occur in all the spectra of copper colloids, which is indeed the case.

* The shape and location of the absorption band for small spheres of metal, of diameter much less than the wavelength of the incident radiation and imbedded in a medium of refractive index n_u , can be calculated from the equation

The failure of electron microscopy to detect these particles of copper in NaCl:Cu may be due to unsatisfactory preparation of the surfaces examined. Mr. E. Henderson, who studied these specimens under the electron microscope, states that such cases are common in this work, and that a wide variety of preparative techniques might have to be tried to attain positive results.

Since a metal colloid of such fine dispersion is hard to obtain, the samples seem ideal for conduction electron spin resonance. Professor E. Purcell of Harvard has requested that samples of the copper colloid be sent him for that purpose.

Ultraviolet Absorption Peaks and X-ray Coloration: Hitherto, the intense narrow absorption peaks in the ultraviolet have been observed only for impurities which serve as phosphor activators and have been vaguely connected with this property. The writer has also found them for other impurities, notably chromium and nickel, and has noted their absence in such phosphors as NaCl:Mn. The absorption peaks have usually been ascribed to the impurity ion alone or to the "complex molecule", i.e., $PbCl_4$, etc. We have noted that these peaks occur only at two general wavelengths; at about 2500 Å. and 2000 Å., which suggested they may be due to some other phenomenon only indirectly connected with the

$$K = \frac{36 \pi N_v V \frac{n^2 k}{n_u}}{\lambda \left[\left(\frac{n}{n_u} \right)^2 + \left(\frac{nk}{n_u} \right)^2 \right]^2 + 4 \left[\left(\frac{n}{n_u} \right)^2 - \left(\frac{nk}{n_u} \right)^2 + 1 \right]}$$

where K is the extinction coefficient defined by: (path length) $K = 2.303$ (optical density); N_v is the number of particles per unit volume; V is the volume of a single particle, λ is the wavelength in the air for which K is sought; n is the refractive index of the metal; and nk is the "absorption coefficient" defined by $nk = K \lambda / 4\pi$ (23).

impurity ion. These peaks happen to occur only for those ions whose salts had a tendency to decompose at high temperatures, forming the oxide. Therefore, to eliminate the possibility that these peaks were caused by the oxide ion, a crystal was grown with sodium peroxide as an impurity. This showed only an absorption edge at 2000 \AA .; moreover, the peaks in the vicinity of 2500 \AA . were destroyed by reduction with sodium vapor, which probably would not be the case for the oxide ion. It will be noted that the V_2 band, which consists of a hole resonating between two adjacent cation vacancies, lies at 2230 \AA . We may therefore suggest the following model. The impurity ion, if divalent, might well have a cation vacancy adjacent, to balance the charge⁽⁴⁴⁾. These ions, having a strong electron affinity, could capture an electron from the halide ions adjacent to the vacancy, thus causing a hole to resonate between the vacancy and the impurity ion. This would be equivalent to a V_2 center. Upon radiation, free electrons might be captured, thus diminishing this effect; treatment with sodium vapor would naturally destroy it.

Such a model might also explain the increase in coloring and bleaching rate. It has long been known that in semiconductors a special process involving an impurity ion is usually necessary to account for the creation or destruction of an electron-hole pair. This is known as the "deathnium" mechanism. A divalent ion, associated with the vacancy, is at once an electron trap and a hole trap. We might expect both electrons and holes to be attracted to this point and thereto annihilate each other. It is interesting to note that a vacancy pair - a cation vacancy adjacent to anion vacancy - is probably present in appreciable concentration in pure crystals. This complex might well serve the same purpose, which would account for the fact that no color center associated

with this vacancy pair has been found⁽⁴⁵⁾.

The vacancy need not be adjacent to the divalent impurity. If it is near enough to have any interaction at all, the electrons and holes might tunnel from one site to the other. The critical factor would then be the average distance between the two. These mechanisms could account for the phenomenon of optimum concentration in the enhancement of coloration and bleaching.* We might for example assume that there are two separate effects. The first is the increase in colorability due to the presence of extra vacancies balancing the divalent ions; this is the usual mechanism proposed. Such an effect would increase linearly with concentration. The effect of recombination centers, enhancing bleaching, would depend upon the average distance between color center sites and the recombination center, and would increase drastically with concentration as this distance approached tunneling range.

It would be interesting to grow crystals containing equal amounts of divalent positive and negative impurities, and to study the effect upon coloration. There would be no tendency for excess vacancies of

* Recently, an ingenious mechanism was suggested for the phenomenon of optimum concentration in phosphors⁽⁴⁶⁾. The decay in luminescence with excessive activator, has been ascribed to there being sufficient activators throughout the crystal to allow the electron to pass rapidly from one activator site to another, until it finally hits a trap or recombination center.

This theory might well be examined in the light of some experimental results obtained recently by Mr. Floyd Humphrey. The well known paramagnetic resonance of manganese ions in calcite (0.1% M_{II}) shows an elaborate hyperfine structure. The writer suggested that runs be made at far higher concentrations, namely on samples with sufficient manganese to give a bright red fluorescence (3-4% M_{II}). The results indicated a powerful electron-electron interaction, completely destroying the resonance hyperfine structure. This would seem to contradict the decay-by-interaction theory.

either charge in such a crystal, demonstrated in the case of $\text{NiO}:\text{Li}^{(47)}$. If coloration enhancement were less than the combined effect of the impurities, it would suggest vacancy mechanisms; if exactly additive, it would suggest that both ions acted as isolated recombination centers; if the effect were greater than additive, it would suggest that the divalent positive and negative ions formed adjacent pairs, which served as strong recombination centers.

The inhibition of secondary color formation, even with plastically deformed crystals, has received little study so far and aside from the possibility that the impurity ions compete with the secondary color center traps, no explanation can be given at this time.

III A STRUCTURAL INVESTIGATION OF THE
STRONTIUM-ZINC SYSTEM

III

A STRUCTURAL INVESTIGATION OF THE STRONTIUM-ZINC SYSTEM

The work reported below was done under the immediate supervision of Professor B. Gunnar Bergman, in connection with a long-term program of structural determinations of intermetallic compounds.

The strontium-zinc system is of special interest in that it involves atoms of considerably different size. Ketelaar⁽⁴⁹⁾ has reported the existence of the compound SrZn_{13} , having the same structure as NaZn_{13} , the structure of which has been worked out in detail^(50,51). Ketelaar's investigation was, however, not at all exhaustive, and it was considered desirable to study the system further to establish whether other Sr-Zn intermetallic compounds exist. It was considered likely that the corresponding crystal structures would be of new types.

The system was first explored by means of x-ray powder photographs of Sr-Zn alloys. The number of phases and their compositions were then verified by x-ray investigations, density determinations, and chemical analyses of the pure phases. Finally the crystal structure of one of these phases was determined.

A. PHASES OF THE Sr-Zn SYSTEM

X-RAY POWDER PHOTOGRAPHS

Preparation of the melts: The zinc used in these experiments consisted of 1/8"-1/4" pellets of reagent grade (99.9% pure). The strontium consisted of "purified" lumps obtained from the Matheson Company. No analyses were given.

The metals were weighed out to a precision of better than 1%, the strontium being kept under hexane except during the weighing and sealing

in bombs. For most melts, bombs of Shelby steel tubing were used. The tubing was welded shut at one end; the metals were placed inside and argon gas passed through for several minutes. The top of the tube was then crimped shut and welded. Quartz bombs were used for a few melts of high zinc content. These were filled, evacuated and sealed off in vacuo. Melts were made varying in composition from pure zinc to pure strontium at intervals of 10 wt. % Zn.

The bombs were heated to 900° C. and held at this temperature for 10 minutes. Several times they were taken out of the furnace and shaken thoroughly. The bombs were then cooled at an average rate of about 50° per hour, broken open, and the melts removed as quickly as possible and placed under hexane to prevent corrosion.

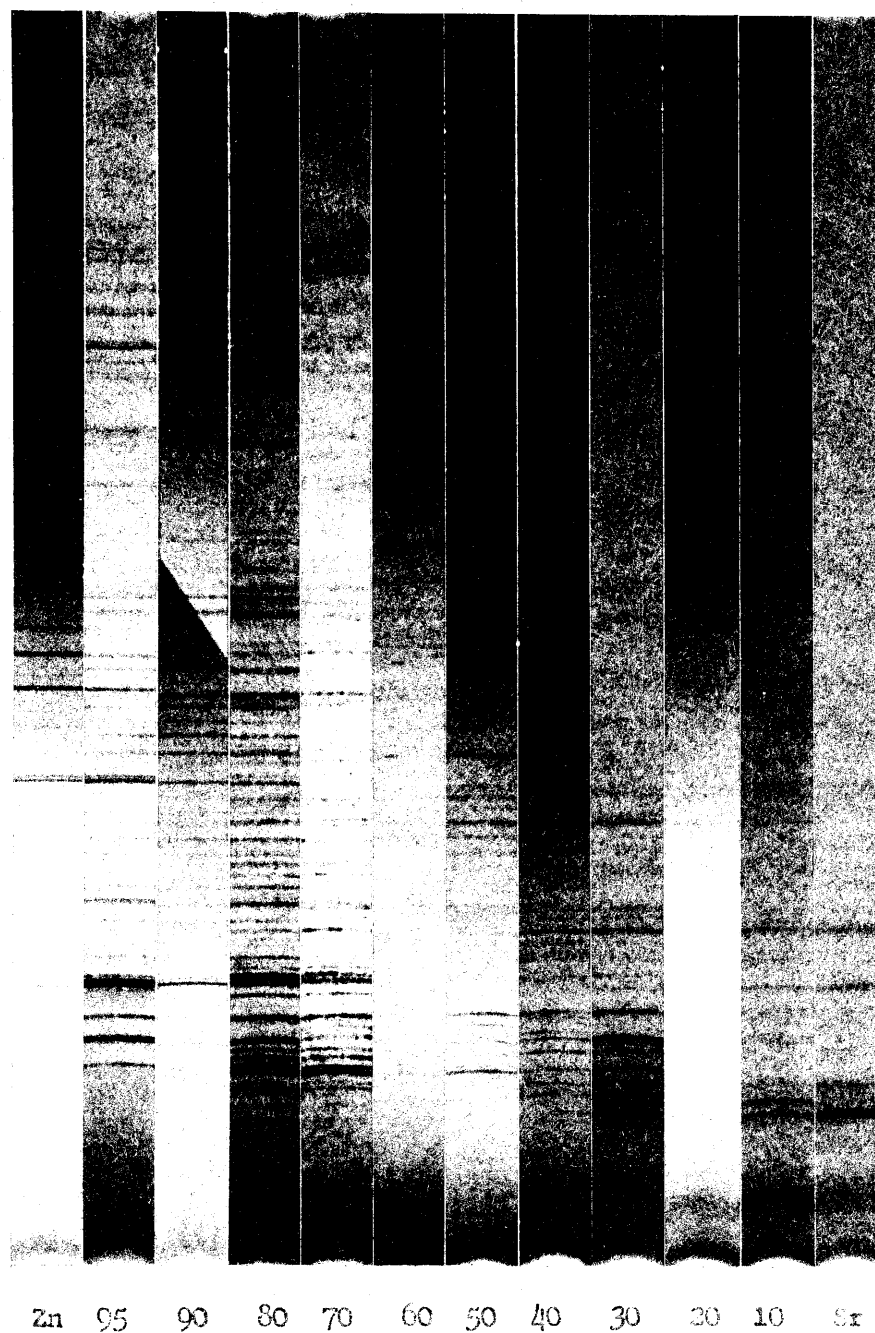
Most of the quartz bombs shattered during cooling. An examination of the fragments showed that the inner surfaces had developed a dark brown film as a result of reduction by strontium. Although no large amounts of silicon were formed, the reaction presumably weakened the quartz enough to cause shattering. The melts from iron bombs were tested with potassium thiocyanate for contamination with iron. A melt of pure zinc gave a strong positive test for iron. A powder photograph showed many lines in addition to those of zinc, indicating alloying with the iron of the bomb. The 90 wt. % Zn melt gave a slight positive test for iron, but produced a x-ray powder pattern which could be explained entirely on the basis of SrZn_{13} . All melts of higher strontium content gave a negligible or negative test for iron. Therefore all melts of higher strontium content than SrZn_{13} (91 wt. % Zn) were made in iron bombs; all of higher zinc content in quartz bombs.

Preparation of the x-ray powder photographs: Powder samples were prepared by grinding half a dozen small pieces, selected from various parts of the melt, under hexane in an agate mortar. The samples were

loaded into 1.0 mm glass capillaries. To prevent oxidation, a paste consisting of the sample and some hexane was introduced into a glass Y tube, with the capillary mounted on one end, and through which argon gas was passed. When the hexane evaporated, the capillary could be loaded with powder in an inert atmosphere.

Photographs were taken with a Philips powder camera of 360 mm circumference, using copper K α radiation at 40 kvp. Fluorescence from the strontium was prevented from blackening the film by placing a nickel filter strip immediately in front of the film. The resultant photographs are shown in Figure 33. Some of them show a graininess due to large crystallites, even after long grinding of the samples. Photographs of the more strontium-rich alloys showed broad lines, probably due to imperfections in the crystallites as a result of the grinding. Attempts to remove the imperfections by annealing failed. The darkening in the region of high angle reflections was later reduced by the use of 0.3 mm capillaries.

Interpretation of Powder Photographs: An inspection of the entire series of powder patterns shown in Figure 33 indicated that at least four intermetallic phases exist. The 90 wt. % Zn photograph was apparently of a single pure phase belonging to the cubic system. A photograph of a 95 wt. % Zn melt, prepared in the manner described above, showed only these lines and lines from zinc; therefore no phases of higher zinc content than SrZn_{13} exist, if thermodynamic equilibrium is assumed. The lines from the 90 wt. % Zn phase (Phase I) are present in the 80 wt. % Zn photograph and absent for all alloys of higher strontium content. The remaining lines of the 80 wt. % Zn photograph and the lines of the 70 and 60 wt. % Zn photographs all formed very similar patterns, which were consequently assumed to be due to Phase II. Another pattern, observable on the 40 and 50 wt. % Zn photographs, was assigned to Phase III. All photographs of



Composition in Weight Percent Zinc

Figure 33. X-Ray Powder Patterns of Strontium-Zinc Alloys.

lower zinc content than 30 wt. % Zn possessed another pattern of lines (Phase IV) superimposed upon the strontium lines. The four intermetallic phases can be assigned the following limiting compositions.

Phase I	91 wt. % Zn*
Phase II	75 to 60 wt. % Zn
Phase III	60 to 40 wt. % Zn
Phase IV	40 to 20 wt. % Zn

These preliminary results were checked by a quantitative comparison. The lines were measured with a photocomparator and the corresponding Q values were calculated. The quantity Q is as usual, defined by the equation:

$$Q = \frac{1}{d^2} = \frac{4\sin^2 \theta}{\lambda^2}$$

A set of Q values could in this way be assigned to each phase.

No assignment could be made which would account for all of the major lines, although there still seemed to be a general indication of the four phases mentioned above. A satisfactory assignment of the majority of the lines was achieved only after powder photographs of the pure phases were available. This assignment is tabulated in the appendix.

ISOLATION OF THE INDIVIDUAL PHASES

EXPERIMENTAL

Examination of the melts: A microscopic examination of the alloys described in the preceding section showed four distinct crystalline species. The 90 wt. % Zn melt seemed to consist of a single, brittle, silvery phase. Several well-developed crystals of cubic form were observed. The 80 wt. % Zn melt was similar in appearance but yielded no

* Calculated for SrZn_{13} .

distinct crystals. The 95 wt. % Zn melt consisted of well-developed small cubes, disseminated in parallel orientation in a soft matrix.

The 70 wt. % Zn and 60 wt. % Zn melts contained only a few small, well-developed, lath-shaped crystals and crystal groups.

The 40 wt. % Zn melt contained many prismatic crystals, up to 0.2 mm in size, embedded in a dark matrix. The crystals had a habit similar to that of the mineral stibnite (Sb_2S_3) and usually had a dull gray or bronze tarnish. The 50 wt. % Zn melt also yielded a few of these crystals.

Another preparation of 40 wt. % Zn melt was made by cooling at a rate of 30° per hour in a furnace with a temperature gradient of 3.3° per cm of bomb length. From 20 grams of this melt, 100 mg of crystals a millimeter or more in length were isolated.

The 30 wt. % Zn and the 20 wt. % Zn melts contained small sheaf-like clusters of flat crystals, but these crystals were so soft that isolation of undeformed single crystals was not possible. The great reactivity of these melts frustrated all attempts to separate a sufficient amount of pure phase for a powder photograph.

The presence of these four crystalline types is in agreement with the results of the x-ray powder photographs. The results of the microscopic examination may be summarized as follows:

- | | |
|-----------|--|
| Phase I | Cubes, occurring in 95, 90 and 80 wt. % Zn melts. |
| Phase II | Lath-shaped crystals, occurring in 70 and 60 wt. % Zn melts. |
| Phase III | Prisms " " 50 " 40 " " " " |
| Phase IV | Sheaves of flat crystals " " 30 " 20 " " " " |

X-ray photographs of the pure phases: A small cluster of crystals of phase II, which appeared to contain little or no adhering material, was selected from the 60 wt. % Zn melt and pulverized. A powder photograph obtained with this sample was quite complex and contained most of the lines

observed in the 60 and 70 wt. % Zn photographs, including many lines assigned to phase III.

One of the crystals of phase II, 0.1 mm long, was mounted with its largest dimension parallel to the axis of the goniometer. After alignment two Laue photographs were taken with the azimuth angle 90° apart. The patterns were different but each had two perpendicular, non-equivalent mirror planes (see Fig. 34).

From the layer line spacings on a rotation photograph the unit cell dimension a , parallel to the rotation axis was calculated to be 5.3 \AA . This same photograph was superimposed upon a powder photograph of the 70 wt. % Zn melt taken with the same camera. Several of the strong spots coincided exactly with the lines of the powder photographs, but the matching of spots and lines was in general very difficult because of the large number of powder lines. Moreover, the rotation photograph obviously contained only a small proportion of all of the possible reflections. The attempt to identify the phase II powder lines was consequently only partially successful.

Weissenberg photographs were taken from the layers $h = 1, 2, 3, 4$ and 5. These were easily indexed by inspection. The remaining two cell constants were calculated on the basis of $(0k0)$ and $(00\)$ data. The results were:

$$b = 6.72 \text{ \AA}$$

$$c = 13.15 \text{ \AA}$$

Systematic extinctions were noted. Only the following type reflections were observed:

$$(hk0) \text{ present only when } h + k = 2n$$

$$(h0l) \text{ present only when } l = 2n$$

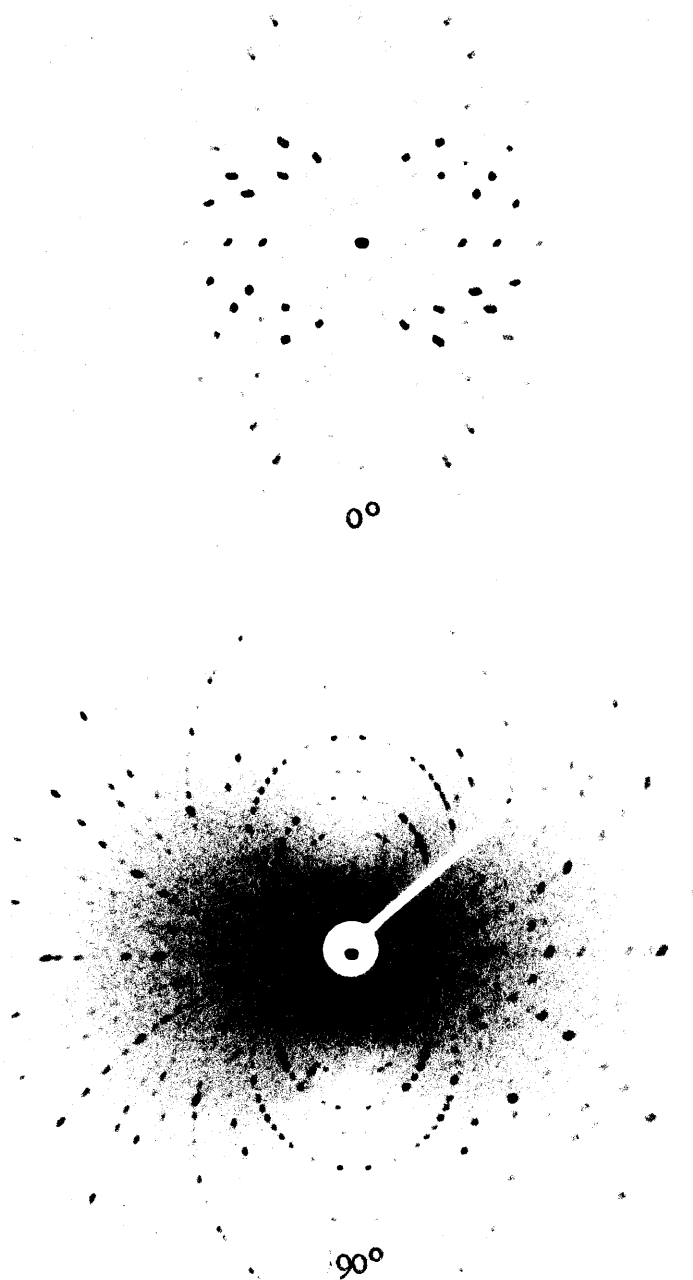


Figure 34. Laue Photographs of Phase II.

Attempts to prepare large amounts of the pure phase by gradient cooling (Bridgeman technique) failed. Since no appreciable amounts of the pure phase could be obtained, chemical analysis and a reliable density determination were not possible. The densities of the 65 wt. % Zn and the 70 wt. % Zn melts were determined by pycnometry and found to be 5.48 and 5.55 respectively.

The single crystals of phase III obtained from the 40 wt. % Zn melts were used for chemical analysis and density measurements. The structure of this phase was worked out in detail and is reported in the next section. It may be mentioned here however that a powder photograph of the pure phase was made by grinding up some of the single crystals. Every reflection of a single crystal rotation photograph coincided with one of these powder lines. It is possible, however, that a few of the weaker lines were due to small amounts of adhering matrix or to compounds formed by corrosion. A powder photograph of the 55 wt. % Zn melts gave a pattern almost identical to that of powdered phase III crystals, except for a few additional weak lines.

Since no single crystals of phase IV could be isolated, an attempt was made to determine the composition of this phase by additional powder photography. A 35 wt. % Zn melt gave a powder pattern similar to that of the 30 wt. % Zn melt, but with several of the weaker lines missing. None of the lines assigned previously to phase III were visible. Therefore the composition of phase IV was tentatively set at 35 ± 3 wt. % Zn.

INTERPRETATION OF DATA

Phase I: The observed Q values for the powder lines of the 90 wt. % Zn photographs were compared with those calculated for the SrZn_{13} phase⁽⁴⁹⁾. Calculated and observed Q values are shown in Table IV.

TABLE IV - COMPARISON OF PHASE I AND SrZn_{13}

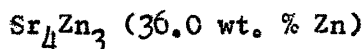
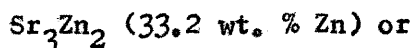
$Q = \frac{1}{d^2}$			$Q = \frac{1}{d^2}$		
Indices	$Q_{\text{calc.}}$	$Q_{\text{obs.}}$	Indices	$Q_{\text{calc.}}$	$Q_{\text{obs.}}$
420	13393	13754	10,00, etc.	66965	67404
422	16072	16463	10,02 "	69643	69983
333	18081	-	"	71653	-
440	21429	-	10,22 "	72322	-
531	23438	23891	"	-	74122
442, 600	24107	24567	935 "	77010	77259
620	26786	27255	804 "	77679	-
533	28795	-	10,42 "	80358	80532
622	29465	-	775 "	82367	-
444	32143	32577	880 "	85715	-
711, 551	34152	-	955 "	87224	87934
640	34822	35266	882 "	88394	88520
624	37500	37982	866 "	90172	-
713, 553	39509	-	973 "	93081	93142
444, 800	42857	43348	10,62 "	93751	-
733	44867	-	884 "	96430	96605
802	45536	46000			
660	48215	48704			
555, 751	50224	50568			
662	50893	-			
840	53572	53866			
735	55580	56012			
842	56250	-			
664	58929	59372			
931	60938	61388			
	-	62976			
844	64286	64708			
755, 771	66295	66052			

Only one weak line cannot be accounted for and the overall agreement is satisfactory. Therefore phase I is identifiable with the SrZn_{13} phase (91 wt. % Zn).

Phase II: The Laue photographs show a Laue symmetry of D_{2h} assigning this phase to the orthorhombic system. The extinctions show that the unit cell is primitive with two glide planes, the probable space group symmetry being $Pmn2_1$. The range of unit cell molecular weight as determined from the unit cell dimensions and density of 65 wt. % Zn and 70 wt. % Zn melts is from 1550 to 1590. The glide planes, inferred from the x-ray extinctions, give a minimum multiplicity of four for the crystallographic positions. The composition inferred from the powder photographs, is probably well within the range of 60 to 80 wt. % Zn. The only unit cell composition which fits these requirements at all is $\text{Sr}_4\text{Zn}_{20}$ with a molecular weight of 1656 and a composition of 78.6 wt. % Zn.

This conclusion, however, must be accepted with reservations. The scarcity of phase II crystals and the inconsistencies in the powder photograph analysis suggest that phase II is either peritectic or metastable. In the latter event, the data on density and composition would probably be erroneous. Therefore the composition of the unit cell must be considered as tentative pending a detailed investigation of the phase diagram.

The estimated composition of phase IV suggests a formula of either



but no definite conclusion can be reached until single crystals are available for x-ray diffraction studies.

B. THE STRUCTURE OF PHASE III

EXPERIMENTAL

A single crystal of phase III, 0.2 mm long, was selected from the 40 wt. % Zn melt and was mounted so that the goniometer axis was parallel to the prism axis of the crystal. After alignment, two Laue photographs were taken with azimuth angles differing by 90° . The patterns were non-equivalent and both showed two perpendicular non-equivalent mirror planes (see Fig. 35). A rotation photograph was taken and from this the unit cell dimension along the rotation axis was calculated to be $a = 4.78 \pm .05 \text{ \AA}$.

A series of Weissenberg photographs was taken of the planes: $h = 0, 1, 2, 3$ and 4 , the first three of which are shown in Figure 36. The other two orthorhombic axes were chosen by noting the mirror planes and the photographs then indexed by inspection. The b and c axes were then calculated; both were equal to $7.8 \pm .1 \text{ \AA}$. On the basis of about 180 observed reflections the following extinction rules were noted:

(hkl) present only when $h + k + l = 2n$.

$(hk0)$ present only when $h = 2m, k = 2n$.

The intensity distribution was almost the same for layers with alternate values of h .

The chemical composition was determined by the analysis of a 50 mg. sample consisting of crystals picked out of a 40 wt. % Zn melt. The analysis (as reported by the Smith-Emery Company) was 55.57 wt. % zinc. No analysis was made for strontium. Prior to analysis the density of these crystals was determined by means of a quartz micropycnometer. The specific gravity so determined was 3.95; this value is too low as a result of small gas bubbles being formed in the pycnometer liquid

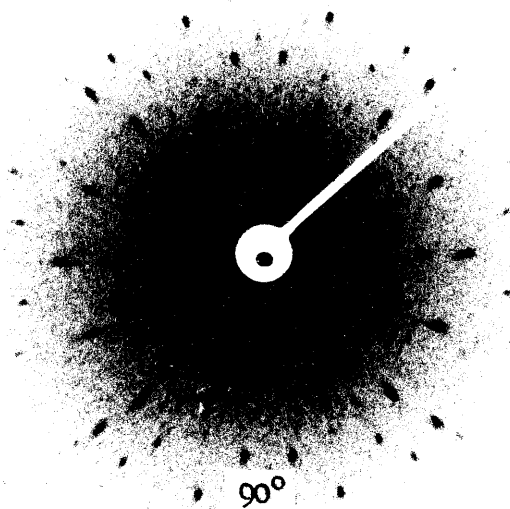
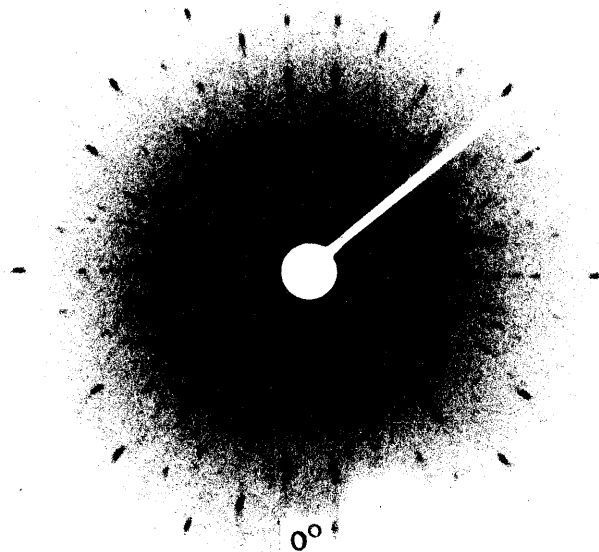
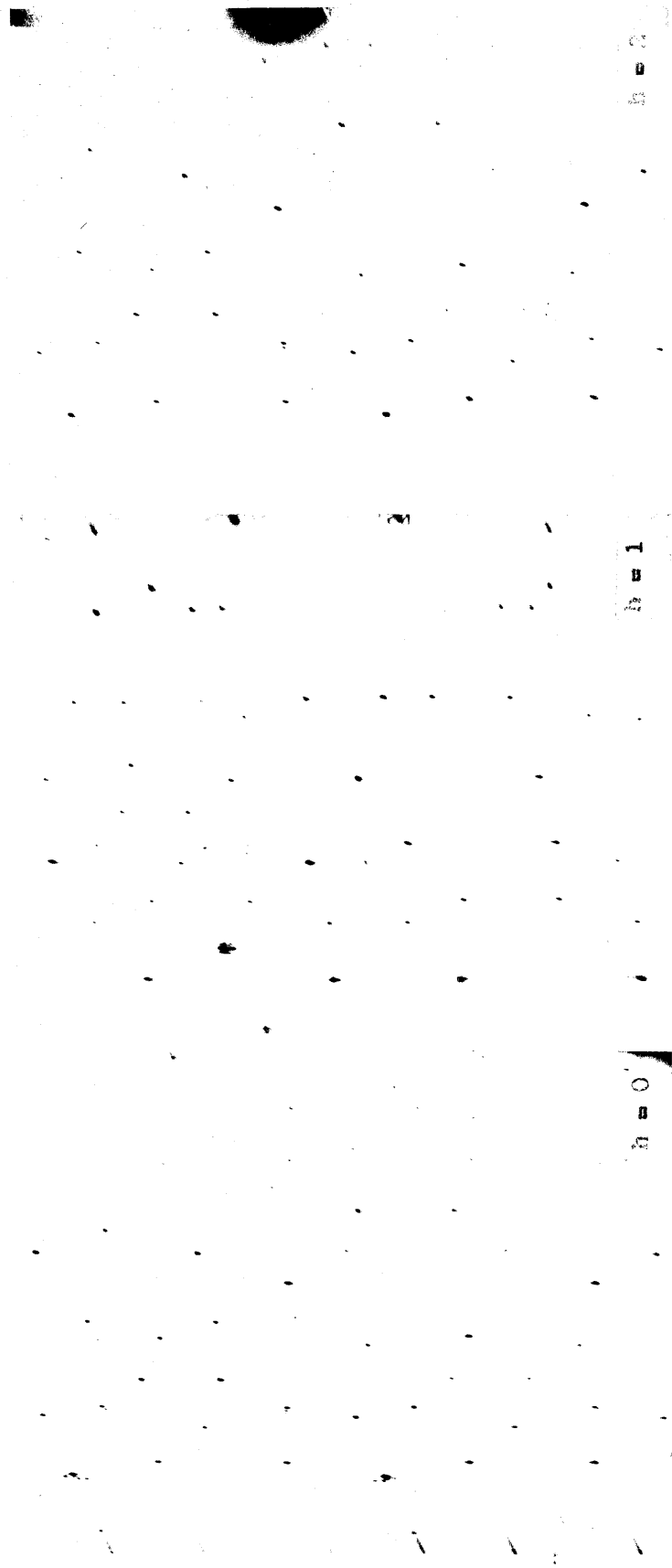


Figure 35. Laurie Photographs of Phase III.



$h = 0$

$k = 1$

Figure 36. Weissenberg Photographs of Phase III.

(toluene), probably as a result of reaction with the crystals.

Later on a density determination was made on a 55 wt. % Zn melt giving an x-ray powder photograph almost identical to that of pulverized phase III crystals. A density determination on a 5 g sample of this alloy gave a specific gravity of 4.71. This value is far more reliable than that obtained from the single crystals, due to the difficulties mentioned above.

DETERMINATION OF STRUCTURE

Space group: The Laue photographs indicate a Laue symmetry of D_{2h} assigning the structure to the orthorhombic system. The extinction rules indicate that the unit cell specified by the orthogonal axes assigned above, is body centered and also that there is a glide plane perpendicular to the c axis. In the notation of the International Crystallographic Tables⁽⁵⁴⁾, the probable space groups are:

$$D_{2h}(28) - Imma$$

$$C_{2v}(22\ a,b) - Ima$$

Layering: The periodicity of intensity distribution of reciprocal lattice nets perpendicular to the a axis indicates that the structure consists of atoms in or very nearly in planes perpendicular to the a axis and a distance $\frac{a}{2}$ apart. Physical justification for assuming slight non-planarity of these layers would be difficult to find, and it was consequently assumed that all atoms formed perfect layers. The structure therefore has a mirror plane perpendicular to the a axis.

Composition of the unit cell: On the basis of density measurements and chemical analysis, the unit cell was calculated to contain 4.14 atoms of strontium and 7.00 atoms of zinc. The body centering of the unit cell requires that there be an even number of atoms of each species per

unit cell. Therefore a choice must be made between the following compositions:

Composition	wt. % Zn	M.W.	density
Sr_4Zn_6	52.75	742.8	4.23
Sr_4Zn_8	59.8	873.6	4.98

The combination of body centering with a glide plane gives a minimum multiplicity of four. Therefore only the composition Sr_4Zn_8 is compatible with all of the observed extinction rules, and an Sr_4Zn_6 structure would have to have accidentally weak reflections to account for the apparent glide plane extinctions. However, the x-ray powder photograph data and the presence of phase II crystals in the 60 wt. % Zn alloy favor the Sr_4Zn_6 composition. Therefore, the first attempts at a trial structure were based on Sr_4Zn_6 , later attempts were based on Sr_4Zn_8 .

The Packing of the Strontium Atoms: The large size of the strontium atom (approx. 4.3 \AA in diameter for a twelve fold coordination⁽⁵²⁾) makes it possible to fix the approximate relative positions of the four Sr atoms in the unit cell. If one Sr atom is placed at 000 the body centering requires another at $\frac{1}{2}\frac{1}{2}\frac{1}{2}$. Then the only available space for the other two atoms is in the approximate position $0(\frac{1}{2} + y)$, 0 and $\frac{1}{2}, y, (\frac{1}{2} + z)^*$.

STRUCTURES BASED ON Sr_4Zn_6

Previously investigated A_2B_3 structures: A search of analogous structures in Wyckoff's Crystal Structures⁽⁵³⁾ reveals only one compound with any structural similarity. This was the mineral stibnite, Sb_2S_3 , which resembles phase III in general appearance, in having an orthorhombic unit cell with two axes almost equal, and in having its atoms arranged in

* or equivalently $0, y, (\frac{1}{2} + z)$ and $\frac{1}{2}, (\frac{1}{2} + y), z$.

layers perpendicular to the third, shorter axis. The unit cell composition, however, is Sb_8S_{12} and the space group $D_{2h}(16)\text{-Pbmn}$. No modification of the structure could be found which would give the smaller unit cell composition and body centering necessary for phase III.

A trial structure for Sr_4Zn_6 : An Sr_4Zn_6 structure, based on the assumption that the glide plane extinctions are accidental but that the body centering and layering are real, must have the space group $D_{2h}(25)\text{-Immm}$ or $C_{2v}(20)\text{-Imm}$. The arrangement of the strontium atoms, described above, corresponds to the special position $4_{(g)}$ of $D_{2h}(25)\text{-Immm}$; $(000; \frac{1}{2}\frac{1}{2}\frac{1}{2}) + 0y0; 0\bar{y}0$, with $.20 \leq y \leq .25$. The only possible position for the zinc atoms of multiplicity two is $2(b) - (0\frac{1}{2}\frac{1}{2})(\frac{1}{2}00)$ - if acceptable packing is to be attained.

The remaining four zinc atoms will best fit in the position $4(j); (000; \frac{1}{2}\frac{1}{2}\frac{1}{2}) + \frac{1}{2}0\bar{z}: \frac{1}{2}0z$. Reasonable inter-atomic distances are obtained for $.15 \leq z \leq .20$. The structure is shown in Figure 37.

The first rest of this trial structure utilized the $(0k0)$ reflections, the intensities of which depend only on the y parameter. The estimated intensities were:

(020)	weak
(040)	medium
(060)	very strong
(080)	very weak

The formula for the structure factor of the space group $D_{2h}(25)\text{-Immm}$ is:

$$A = 16 \cos^2 2\pi \frac{h+k+l}{4} \cos 2\pi hx \cos 2\pi ky \cos 2\pi lz$$

$$B = 0$$

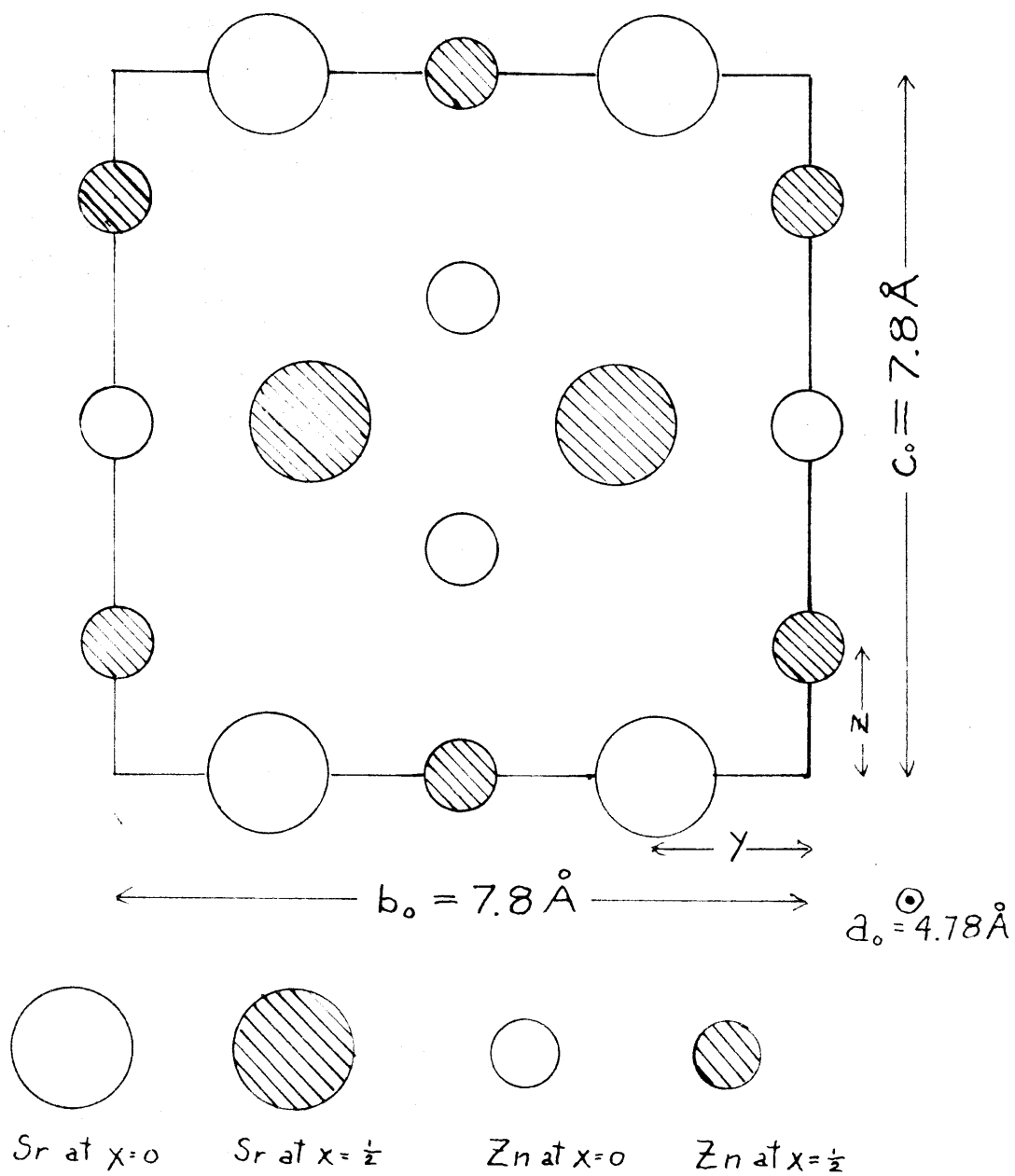


Figure 37. Trial Structure based on Sr_4Zn_6 .

For the (0k0) reflections of the trial structure, this simplifies to:

$$F_{Sr} = 4f_{Sr} \cos 2\pi ky$$

$$F_{ZnI} = 4f_{Zn}$$

$$F_{ZnII} = \begin{cases} 2f_{Zn} & \text{for odd values of } k \\ -2f_{Zn} & \text{for even values of } k \end{cases}$$

A plot of the calculated intensities* of these reflections for various values of y is shown in Figure 38. At the only place where the (080) reflection has a sufficiently small value, the (020), (040), and (060) reflections all have about the same intensity. Therefore the observed sequence $I_{060} > I_{040} > I_{020} \gg I_{080} \approx 0$ cannot be attained.

For the (hk0) reflections with k odd, $F = 4f_{Sr} \cos 2\pi ky + 2f_{Zn}$. $\cos 2\pi ky$ is constant for all odd values of k only when $y = .25$. This would make the structure factor of these spots equal to $4f_{Sr} - 2f_{Zn}$ corresponding to a moderately weak but observable intensity.

An interchange of the b and c axes of the trial structure would cause the intensities of the (0k0) reflections to depend on the interference of four zinc atoms with planar layers of four strontium and two zinc atoms. The minimum structure factor for an (0k0) reflection would therefore be $4f_{Sr} - 2f_{Zn}$, which is too large to account for the observed intensity of (080).

The trial structure therefore failed to give even the roughest agreement between observed and calculated intensities and had to be rejected. All other structures based on $D_{2h}(25)$ -Immm are unreasonable from a steric viewpoint. The only other space group compatible with the composition Sr_4Zn_6 is $C_{2v}(20)$ -Imm. The layering requirements cause all acceptable positions of this space group to be identical to those of $D_{2h}(25)$ -Immm. Therefore no reasonable structure could be found for Sr_4Zn_6 , and phase

* Corrected for Lorentz and polarization factors but not for absorption or temperature effect.

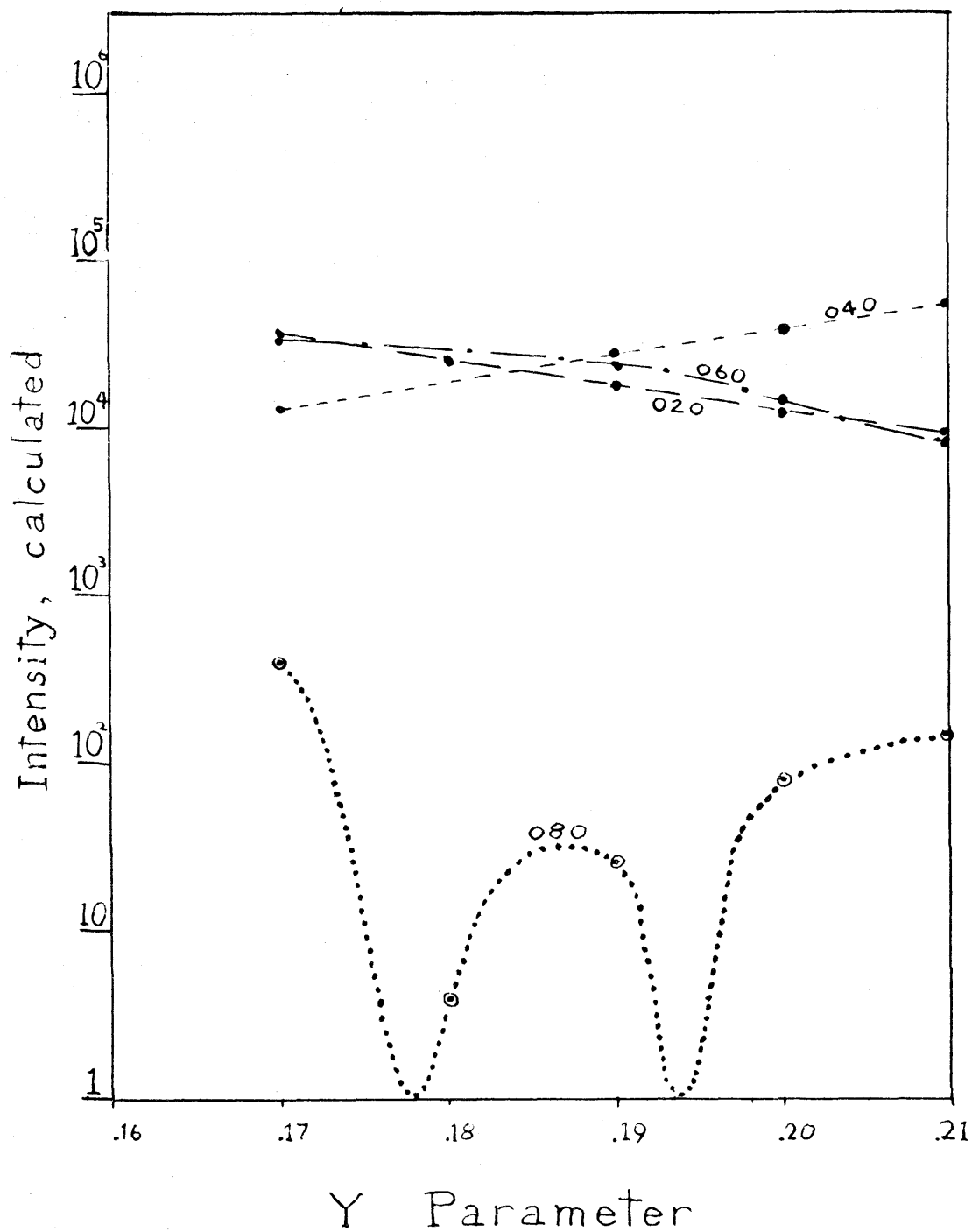


Figure 38. Test of Trial Structure based on Sr_4Zn_6

III must have an A_4B_8 structure.

TRIAL STRUCTURE BASED ON Sr_4Zn_8

Formulation of the trial structure: As has been mentioned above, the extinction rules for body centering and glide plane show the probable space groups to be $D_{2h}(28)$ -Imma and $C_{2v}(22)$ -Ima. The glide plane fixes the position of the strontium atoms at $(000; \frac{1}{2}\frac{1}{2}\frac{1}{2}) + 0\frac{1}{4}u; 0\frac{3}{4}\bar{u}$ which correspond to the special position $4(e)$ of $D_{2h}(28)$ -Imma. The only position of eightfold multiplicity in this space group which has x-coordinates compatible with the layering is $8(h); (000; \frac{1}{2}\frac{1}{2}\frac{1}{2}) + 0yz; 0\bar{y}\bar{z}; 0, (\frac{1}{2} + y), \bar{z}; 0, (\frac{1}{2} - y), z$. If y has a negative value the zinc atoms will fit nicely into the large holes of the strontium atom arrangement.

Estimate of parameters from inter-atomic distance: A consideration of the Sr-Sr distances alone suggests a value of .051 for u; this would make all nearest Sr-Sr distances equal to $3.97 \overset{0}{\text{\AA}}$. Assuming a normal contact distance of $2.7 \overset{0}{\text{\AA}}$ for adjacent zinc atoms, we get an appropriate value of .175 for the z parameter. If the distances are the same between a zinc atom and its four nearest neighboring strontium atoms, y will be approximately - 0.05. The structure is illustrated in Figure 39. This structure is closely related to the hexagonal magnesium boride structure, the chief spatial difference being the non-zero values of u and y.

Test of the trial structure: The general expression for the structure factor in the space group $D_{2h}(28)$ -Imma is:

$$A = 16 \cos^2 2\pi \frac{(h+k+\ell)}{4} \cos 2\pi hx \cos 2\pi(ky + \frac{k}{4}) \cos 2\pi(\ell z - \frac{k}{4})$$

$$B = 0$$

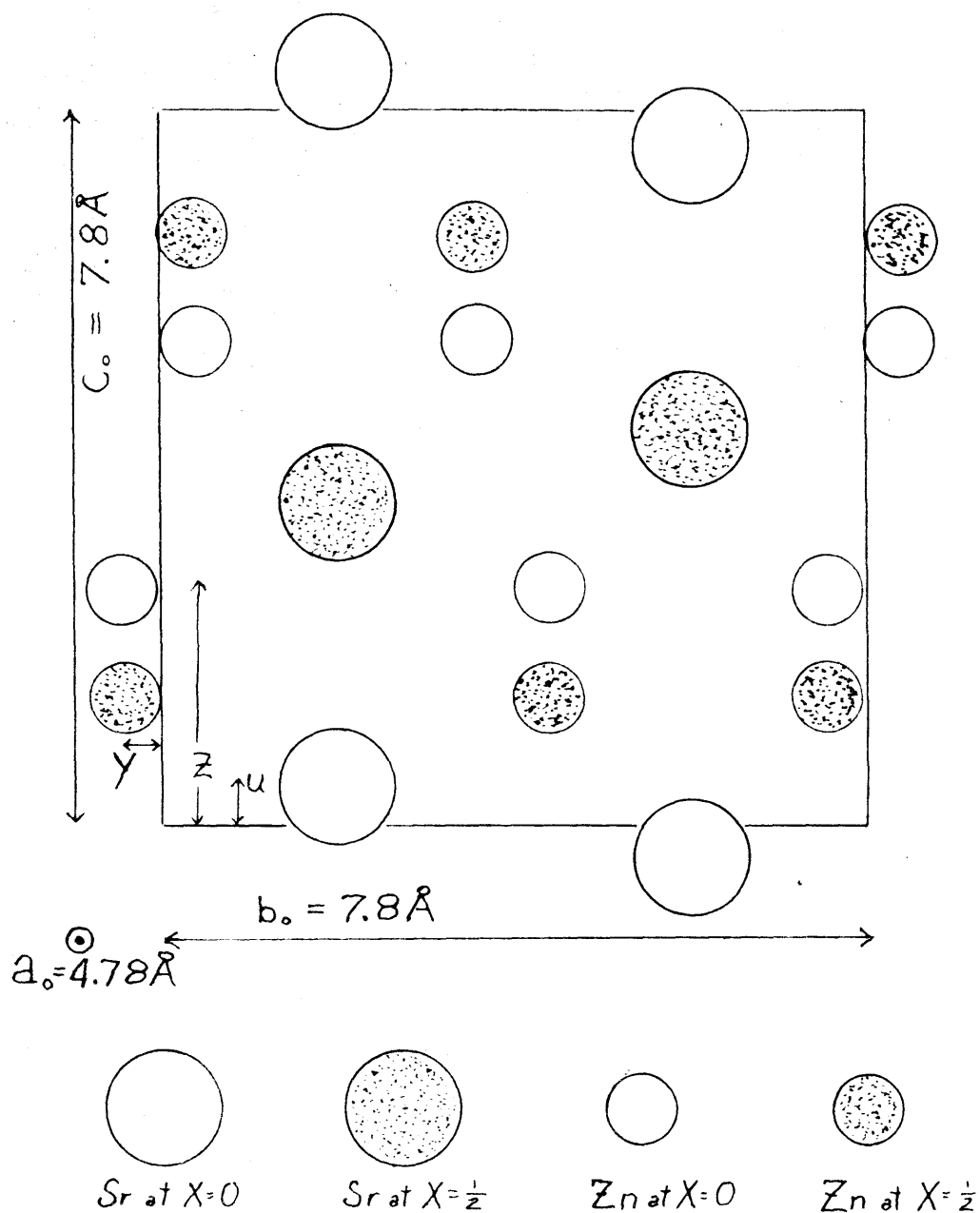


Figure 39. Trial Structure based on Sr_4Zn_8 .

For the (hk0) plane of the trial structure, the structure factor* becomes

$$F_{Sr} = 4f_{Sr} \cos 2\pi(lu - \frac{k}{4})$$

$$F_{Zn} = 8 P f_{Zn} \cos 2\pi(y + \frac{1}{4}) \cos 2\pi(lz - \frac{k}{4})$$

Where P represents the population factor for the zinc atoms.

The population factor was introduced because all evidence - x-ray powder patterns, thermal analysis and direct chemical analysis - indicated that the pure phase has a composition corresponding very nearly to Sr_4Zn_7 . This would give a non-stoichiometric structure in which about one zinc atom per unit cell is missing at random; such an effect is uncommon in intermetallic compounds. All of the x-ray data were obtained from single crystals picked out of the 40 wt. % Zn alloy, a composition highly zinc-deficient with respect to phase III. Under these conditions the existence of a non-stoichiometric phase is somewhat more plausible. Since the crystal from which x-ray photographs and intensity measurements were made came from this zinc deficient phase, preliminary calculations were made with a population factor $P = \frac{6.8}{8}$, corresponding to the chemical analysis. In the refinement of the structure, P will be varied to see which value gives the best fit with intensity measurements.

As for the previous trial structure, the test was made with reflections (0k0). For $y = -.07$, a good agreement between observed and calculated intensities is obtained;

* ignoring the first factor which merely gives the requisite extinction for body centering.

INTENSITIES

Reflection	Calculated*				Observed
	y = -.05	-.06	-.07	-.08	
(020)	1,840	121	576	3,840	weak
(040)	38,000	21,000	9,680	2,700	medium
(060)	16,300	28,500	28,500	45,000	v. strong
(080)	169	3	9	674	v. weak

A similar series of calculations was made with the (00) reflections which depend on the parameters u and z. A good fit was obtained by using the values $u = 0.05$ and $z = 0.33$. The results were as follows:

Reflection	Intensities	
	Calculated	Observed
(002)	144	v. weak
(004)	1,680	medium
(006)	8,000	medium
(008)	12,500	medium strong

Calculations were made for the entire (hk0) plane. The results are shown in Table V. Only five out of forty reflections were in poor agreement; all but one of these were at high values of θ and sensitive to slight variation of the positional parameters. The overall agreement was considered sufficiently good for the trial structure to be accepted as correct. The positional parameters appeared to be uncertain by about 0.01 of the corresponding cell edges.

* Corrected for Lorentz and polarization factors, but not for absorption or temperature effect.

TABLE V - COMPARISON OF PHASE III AND TRIAL STRUCTURE Sr_4Zn_8

Indices	Intensities		Indices	Intensities	
	I _{obs.}	I _{calc.}		I _{obs.}	I _{calc.}
002	W	144	060	VS	39,000
004	M	1,680	062	W	400
006	M	9,000	064	VW	64
008	MS	12,500	066	MW	2,020
011	M	4,100	071	W	900
013	MS	21,600	073	MW	3,700
015	S	23,700	075	MW	1,520
017	W	900	077	M	17,600
019	W	2,500	080	-	9
020	MW	576	082	VS	10,000
022	VS	65,600	084	MW	3,400
024	MS	17,700	091	M	6,160
026	M	11,200	093	MW	23,100
028	MW	1,520			
031	VS	67,500			
033	S	86,500			
035	W	0			
037	S	18,500			
039	W	130			
040	MS	9,680			
042	S	13,000			
044	W	1,600			
046	W	1,900			
048	MW	4,760			
051	M	4,900			
053	M	6,400			
055	VS	17,400			
057	-	20			

W = Weak
M = Medium
S = Strong

APPENDIX: ASSIGNMENT OF POWDER LINES OF
STRONTIUM-ZINC ALLOYS

80% Zn - 20% Sr (a)*

Observed Q Value	ASSIGNMENT:				Unassigned
	Phase I (b)	Phase II (c)	Phase III (d)		
02879 vw		02879 vw			
03034 vw				03034 vw	
08386 vw				08386 vw	
11345 m		11345 m			
11866 mw		11866 mw			
12915 vw			12836 vs		
13229 ms		13229 ms			
13414 ms			13401 m		
13788 m	13754 m				
14493 ms		14493 ms			
15413 mw		15413 mw			
16445 ms	16463 ms				
16795 vw			16765 ms		
17386 vw				13786 vw	
17926 w			18001 ms		
18473 vw				18473 vw	
19152 ms			19292 s		
20573 vw				20573 vw	
22070 m		22070 m			
23817 vs	23891 vs				
24574 m	24567 m				
24816 vw				24816 vw	
25654 w				25654 w	
26363 w				26363 w	
27223 m	27255 mw				
28900 w				28900 w	
29866 w				29866 w	
31073 mw			31093 m		
32530 mw	32577 w				
35237 ms	35266 m				
36117 w					
36763 vw					
37943 m	37982 m				
39799 m		39799 m			
41138 w		41138 w			
41855 m		41855 m			
43174 w	43348 mw				
43817 vw					
45981 ms	46000 ms				

* (a) See end of Appendix for annotations.

80% Zn - 20% Sr (Continued)

Observed Q Value	ASSIGNMENT:			Unassigned
	Phase I(b)	Phase II(c)	Phase III(d)	
47782 vw		47782 vw		
48667 vw	48704 w			
49022 m				49022 m
50676 w	50568 vw		50519 w	
51802 mw				51802 mw
53163 m				53163 m
54166 vw	53866 w			
54716 vw				54716 vw
56050 ms	56012 ms			
57252 m				57252 m
60052 mw			60123 m	
61273 m	61388 ms			
61650 w				61650 w
62928 w				62928 w
64541 ms	64708 ms			
67217 mw	67404 mw			
68610 w				68610 w
70055 m	69983 mw			
71117 w				71117 w
71795 w				71795 w
72425 ms		72425 ms		
77143 ms	77259 ms			
79194 w				79194 w
80465 mw	80532 w			
82275 w				82275 w
88001 ms	87934 ms			
88589 ms	88520 ms			
90106 w				90106 w
91328 ms		91328 ms		
93231 mw	93142 w			
96636 vw	96605 vw			
98379 w				98379 w
101893 mw	Remaining lines not assigned.			
103806 w				
109525 w				
119892 mw				
123407 vw				
128563 w				

80% Zn - 20% Sr (Continued)

Observed Q Value	ASSIGNMENT:			
	Phase I _(b)	Phase II _(c)	Phase III _(d)	Unassigned

Remaining lines not assigned.

130506 w
133446 ms
133854 ms
135811 mw
139045 w

141142 ms
141785 m
144490 s
146607 w
147426 w
149243 w
149728 ms

151757 w
152459 m

161948 w
162417 m
165665 s

70% Zn - 30% Sr

02931 vw

11235 mw
11717 w
12810 s
13281 ms
14411 ms
15301 mw
16666 mw
17835 m
19058 vs

02879 vw

11345 m
11866 mw

13229 ms
14493 ms
15413 mw

12836 vs
13401 m

16765 m
18001 ms
19292 s

20509 vw
21905 m
23817 ms
24574 ms
25479 w
26114 vw
26827 vw
28569 vw
29568 vw

23891 vs
24574 m

22070 m
23817 vs
24574 m

26007 mw
26827 vw

20509 vw

25479 w

28569 vw
29568 vw

30960 m
32801 w
34286 w
34998 w

31093 m
32801 mw
34345 ms

34998 w

70% Zn - 30% Sr (Continued)

Observed Q Value	ASSIGNMENT:			Unassigned
	Phase I (b)	Phase II (c)	Phase III (d)	
35616 vw				35616 vw
37800 vw				37800 vw
38414 vw				38414 vw
39654 mw		39799 m		
41054 w		41138 w		
41687 m		41855 m		
43602 w				43602 w
45328 ms			45503 ms	
47825 mw		47782 vw		
48778 m	48704 w			48778 m
50317 vw				50317 vw
51667 vw				51667 vw
53984 m	53866 w			53984 m
54371 w			54487 m	
57067 m				57067 m
59535 m			60123 m	
61556 m		61388 ms		
62714 w				62714 w
64375 w				64375 w

Remaining lines too diffuse to measure.

60% Zn - 40% Sr

Observed Q Value	ASSIGNMENT:		Unassigned
	Phase II (c)	Phase III (d)	
11272 vw	11345 m		
11816 vw	11866 mw		
12915 vs		12836 vs	
13414 m		13401 m	
14466 mw	14493 ms		
15440 w	15413 mw		
16882 ms		16765 ms	
17895 ms		18001 ms	
19339 s		19292 s	
22038 mw	22070 m		
23817 m	23817 vs		
24643 m	24574 m		
25831 w			25831 w
26220 mw		26007 mw	
26935 w		26827 vw	
28900 vw			28900 vw
29905 w			29905 w

60% Zn - 40% Sr (Continued)

Observed Q Value	ASSIGNMENT:		Unassigned
	Phase II(c)	Phase III(d)	
31187 ms		31093 m	
32994 m		32801 mw	
33344 w			33344 w
34445 ms		34345 ms	
35957 vw			35957 vw
40467 w			40467 w
41307 vw			41307 vw
41939 vw	41855 m		
42577 vw			42577 vw
44118 vw			44118 vw
45677 s		45503 ms	
48268 m		48179 ms	
49289 mw			49289 mw
50676 w		50519 w	
52663 ms		52618 m	
53163 w			53163 w
54623 mw		54487 m	
57299 w			57299 w
59910 m			59910 m
61830 w			61830 w
62784 w			62784 w
70394 w		70779 mw	
72280 mw	72425 ms		
77045 mw		77703 mw	
78509 w		78753 mw	
80416 m		80685 mw	
81981 w			81981 w

Remaining lines too diffuse to measure.

50% Zn - 50% Sr

Observed Q Value	ASSIGNMENT:		Unassigned
	Phase III(d)	Phase IV(e)	
08784 w		08731 mw	
10313 m		10278 s	
11308 w		11308 ms	
11802 vw			11802 vw
12169 vw			12169 vw
12836 vs	12836 vs	12745 ms	
13401 m	13401 m		
14549 mw		14700 mw	

50% Zn - 50% Sr (Continued)

Observed Q Value	ASSIGNMENT:		Unassigned
	Phase III(d)	Phase IV(e)	
15328 vw			15328 vw
16039 ms		16053 vs	
16765 m	16765 ms		
18001 ms	18001 ms		
18611 vw			18611 vw
19292 s	19292 s	19244 ms	
22669 vw			22669 vw
23852 vw			23852 vw
24503 vw			24503 vw
25338 vw			25338 vw
26007 w	26007 mw		
26827 w	26827 vw		
28422 w			28422 w
28919 vw			28919 vw
30280 m		30204 s	
31093 m	31093 m		
32181 m			32181 m
32801 w	32801 mw		
33539 m		33637 ms	
34345 m	34345 ms		
35278 vw			35278 vw
39197 vw			39197 vw
39799 m			39799 m
42662 m		42513 mw	
43260 mw	43260 vw		
44204 w			44204 w
45503 ms	45503 ms		
46375 vw			46375 vw
47649 vw			47649 vw
48179 ms	48179 ms		
49044 vw			49044 vw
50519 m	50519 w		
52618 ms	52618 m		
53823 m		54075 ms	
54487 m	54487 m		
56003 vw			56003 vw
58369 vw			58369 vw
60123 ms	60123 m		
61203 vw	61203 vw		
62100 w			62100 w
63045 vw			63045 vw
64851 mw	64851 w		
66355 vw			66355 vw
68004 w	68004 w		
69838 w			69838 w

50% Zn - 50% Sr (Continued)

Observed Q Value	ASSIGNMENT:		Unassigned
	Phase III(d)	Phase IV(e)	
70779 mw	70779 mw		
77703 w	77703 mw		
78753 mw	78753 mw		
80685 ms	80685 mw		
85211 w		85452 ms	
86876 ms		86752 ms	
89785 mw			89785 mw
91516 w			91516 w
93050 m			93050 m

Remaining lines too diffuse to measure.

40% Zn - 60% Sr

07976 vw			07976 vw
08731 w		08731 mw	
09450 vw		09506 w	
10242 ms		10278 s	
11345 ms		11308 ms	
11892 vw			11892 vw
12119 vw			12119 vw
12694 ms		12745 ms	
12926 vw	12836 vs		
13453 vw	13401 m		
13936 vw			13936 vw
14618 ms		14700 mw	
15343 vw			15343 vw
16097 ms		16053 vs	
16867 m	16765 m		
17865 w	18001 ms		
18489 w			18489 w
19245 s	19292 s	19244 ms	
23309 vw			23309 vw
23834 mw			23834 mw
24435 vw			24435 vw
26149 mw	26007 mw		
26701 m	26827 w		
28395 mw			28395 mw
29011 vw			29011 vw
29494 vw			29494 vw
30261 s		30204 s	
31093 w	31093 m		
32181 m			32181 m
32839 vw	32801 mw		

40% Zn - 60% Sr (Continued)

Observed Q Value	ASSIGNMENT:		Unassigned
	Phase III (d)	Phase IV (e)	
33539 m		33637 ms	
34286 w			34286 w
39281 w		39218 w	
40405 ms			40405 ms
41645 vw			41645 vw
42641 m		42513 mw	
43346 m		43494 w	
44398 w			44398 w
46637 vw		46528 w	
47671 ms			47671 ms
48002 mw		47958 ms	
49000 w		49200 mw	
50541 m	50519 w		
52527 mw	52618 m		
52867 w			52867 w
53870 ms		54075 ms	
54854 w			54854 w
58275 w			58275 w
59724 w			59724 w
60849 mw			60849 mw
64114 vw			64114 vw
66402 w			66402 w
68342 vw			68342 vw
70032 w			70032 w
73104 vw			73104 vw
74415 mw			74415 mw
75583 vw			75583 vw
78802 w	78753 mw		
85306 vw		85452 ms	
86825 ms		86752 ms	
89862 vw			89862 vw
91475 w			91475 w
94839 mw			94839 mw

Remaining lines too diffuse to measure.

30% Zn - 70% Sr

Observed Q Value	ASSIGNMENT:			
	Phase III(d)	Phase IV(e)	Sr(f)	Unassigned
08376 m			08175 vs	
08731 mw		08731 mw		
09506 w		09506 w		
10278 s		10278 s		
11308 ms		11308 ms		
11666 vw				11666 vw
12745 ms	12836 vs	12745 ms		
14700 mw		14700 mw		
15427 w				15427 w
16053 vs		16053 vs		
18688 vw				18688 vw
19244 ms	19292 s	19244 ms		
21939 w			21774 m	
23938 w				23938 w
26862 w	26827 vw			
28385 w				28385 w
30204 s		30204 s		
31434 vw				31434 vw
31683 ms				31683 ms
33637 ms		33637 ms		
39218 w		39218 w		
40676 w				40676 w
41875 w				41875 w
42513 mw		42513 mw		
43494 w		43494 w		
45567 w				45567 w
46528 w		46528		
47958 ms		47958 ms		
49200 mw		49200 mw		
50587 mw	50519 w			
52730 w	52618 mw			
54075 ms		54075 ms		
58159 ms		58159 ms		
62406 mw				62406 mw
63163 w				63163 w
64208 w				64208 w
65327 w				65327 w
66665 w		66665 w		
69862 w				69862 w

30% Zn - 70% Sr (Continued)

Observed Q Value	ASSIGNMENT:			Unassigned
	Phase III(d)	Phase IV(e)	Sr(f)	
71747 w				71747 w
72911 w				72911 w
74828 vw				74828 vw
75852 m				75852 m
85452 ms		85452 ms		
86752 ms		86752 ms		
91914 w				91914 w
104949 mw				104949 mw

Remaining lines too diffuse to measure.

20% Zn - 80% Sr

Observed Q Value	ASSIGNMENT:			Unassigned
	Phase IV(e)	Sr(f)		
08365 ms		08175 vs		
09506 ms	09506 w			
10360 mw	10278 s			
11272 w	11308 ms			
12926 vw				12926 vw
14631 vw				14631 vw
16053 s	16053 vs			
19277 m	19244 ms			
22137 ms				22137 ms
25937 vw				25937 vw
30354 vs	30204 s			
31453 mw				31453 mw
32220 w		32473 w		
34169 vw				34169 vw
37433 w				37433 w
48002 ms	47958 ms			
49557 w				49557 w
54440 mw		54235 w		

Remaining lines too diffuse to measure.

10% Zn - 90% Sr

Observed Q Value	ASSIGNMENT:		Unassigned
	Phase IV(e)	Sr(f)	
06593 vw			06593 vw
07384 w			07384 w
07996 ms			07996 ms
08292 s		08175 vs	
09193 m			09193 m
09474 s	09506 w		
10056 w	10278 s		
11150 mw	11308 ms		
15511 mw			15511 mw
15982 m	16053 vs		
18998 vw	19244 ms		
20541 vw			20541 vw
22005 ms		21774 m	
25584 mw			25584 mw
30129 s	30204 s	29829 m	
31187 mw			31187 mw
32473 vw		32473 w	
33405 vw			33405 vw
37250 w			37250 w
43153 vw			43153 vw
43688 vw			43688 vw
47605 mw	47958 ms		
49633 vw			49633 vw
52764 m			52764 m
54259 ms		54235 w	
57856 w			57856 w
61368 vw			61368 vw
65231 w			65231 w
68995 w		68995 vw	
71311 w			71311 w
73202 mw			73202 mw

Remaining lines too diffuse to measure.

ANNOTATIONS

- (a) The 90% Zn - 10% Sr data is reported in Table IV.
- (b) Observed values from 90% Zn - 10% Sr alloy.
- (c) Observed values from 80% Zn - 20% Sr alloy; selected from major lines remaining after assignments to phase I and phase III.

ANNOTATIONS (Continued)

- (d) Observed values from 50% Zn - 50% Sr alloy; selection made by comparison with photograph from powdered crystals of phase III; intensities from latter photograph.
- (e) From 30% Zn - 70% Sr alloy; excluding a few lines assigned to phase III and Sr.
- (f) Observed values from Sr powder photograph.

INTENSITIES -

vs	-	very strong
s	-	strong
ms	-	medium strong
m	-	medium
mw	-	medium weak
w	-	weak
vw	-	very weak

REFERENCES

1. H. K. Garner and H. J. Lucas, J. Am. Chem. Soc., 72, 5497 (1950).
2. G. Helmkamp and H. J. Lucas, ibid. 74, 952 (1952).
3. H. J. Lucas, Organic Chemistry p.52, American Book Co. (1935).
4. N. F. Mott and R. W. Gurney, Electronic Processes in Ionic Crystals 2nd ed. Oxford (1948).
5. F. Seitz, Rev. Mod. Phys. 18, 384 (1946).
6. J. P. Molnar, unpublished thesis, M.I.T. (1940).
7. F. Seitz, Rev. Mod. Phys. 26, sec. 2,6,9,12,23 (1954).
8. C. A. Hutchison, Phys. Rev. 75, 1769 (1949); 87, 1125 (1952);
A. F. Kip, et al., Phys. Rev. 83, 657 (1951); 91, 1066 (1953);
C. Kittell, Phys. Rev. 89, 316 (1953); 90, 238 (1953).
9. R. A. Levy, Table of Absorption Bands in Alkali Halides, unpublished compilation (Aug. 1953).
10. F. Seitz, ibid. sec 8.
11. A. G. Redfield, Phys. Rev. 94, 526,537 (1954);
J. R. McDonald, Phys. Rev. 95, 44 (1954); J. Chem. Phys., 23,
375 (1955).
12. K. Przibram, Verfärbung und Lumineszenz, p 27ff, Springer-Verlag,
Vienna (1953)
F. Seitz ibid p. 68
13. I. L. Mador, R. F. Wallis, et al. Phys. Rev. 96, 617 (1954).
14. Przibram, ibid, p. 38ff; Endeavour, 49 (Jan. 1954).
15. Przibram, ibid, p. 27
16. E. Burstein and J. J. Oberley, Phys. Rev. 76, 1254 (1949);
79, 903 (1950).
17. R. B. Gordon and A. S. Nowick, Phys. Rev. 101, 977 (1956).
18. M. Ishiguro et al., Phys. Rev. 95, 1347 (1954).
19. Seitz, ibid, p. 36 ff.
20. H. Siedentopf, Physik, Z. 6, 855 (1905); Gyulai, Z. Physik,
35, 411 (1925).
21. M. Savostianova, Z. Phys. 64, 262 (1930).

REFERENCES (continued)

22. E. Mollwo, Nachr. Akad Wiss Gott, 1932, 254 (1932).
23. A. B. Scott, et al., J. Phys. Chem. 57, 757 (1953) et priori.
24. D. R. Westervelt, Report NAA-SR-1050, North American Aviation Inc. (December 15, 1954).
25. A. B. Scott, private communication.
26. R. A. Levy, private communication.
27. Wardel and Thompson, Geo. Chem. et Cosmo Chem. Acta., 4, 169, (1954).
28. J. D. Buddhue, Mineralogist, p. 346 (1946).
29. C. Kittell, Introduction to Solid State Theory, p. 85, Wiley (1953).
30. Bull. Amer. Phys. Soc., p. 6 (Nov. 1954); H1 (Mar. 1955); UA1 (Apr. 1955).
31. C. Doelter, Wien, Ber. I, 138, 113, (1929).
32. Seitz, ibid., sec. X.
33. Pezibram, ibid., p. 34.
34. E. Jahoda, Wien, Ber. IIa 135, 675 (1926);
A. Smakula, Z. Phys., 45, 1 (1927).
35. Przibram, ibid., p. 100-200.
36. R. W. Pohl and E. Rupp, Ann. Phys. 81, 1161 (1926);
A. Arsenjewa, Z. Phys., 57, 163 (1929).
37. Seitz, ibid., p. 17 ff.
38. R. S. Alger and R. D. Jordan, Phys. Rev., 97, 277 (1955).
39. R. J. Gnaedinger, J. Chem. Phys., 21, 323 (1953).
40. Seitz, ibid., p. 91 ff.
41. H. C. Buckley, Crystal Growth, New York (1951).
42. S. Kyropoulos, Z anorg. Chem., 154, 308 (1926).
43. R. W. Pohl, Einführung in die Optik, Springer, Berlin (1943).
44. Seitz, ibid., p. 5 ff.
A. G. Reese, Chemistry of the Defect Solid State, Menthuen, London (1954).

REFERENCES (continued)

45. Seitz, ibid., p. 9.
46. D. L. Dexter and J. Schulman, J. Phys. Chem., 22, 1063 (1954).
47. A. G. Reese, ibid., p. 14.
48. A. Rose, Phys. Rev., 97, 322-333 (1955).
49. J. Ketelaar, J. Chem. Phys., 5, 668 (1937).
50. E. Zintl and W. Hauke, Nature, 25, 717 (1937).
51. D. Shoemaker, R. Marsh, F. Ewing, and L. Pauling, Acta Cryst., 5, 637 (1952).
52. L. Pauling, The Nature of The Chemical Bond, p. 410, Cornell (1948).
53. R. Wyckoff, Crystal Structures, v. 1, Chap. V, a 7, Interscience, (1951 et. seq.).
54. International Tables for X-ray Crystallography, v. I, Birmingham, England (1952).

PROPOSITIONS.

1. In order to account for the effect of abrasion, moisture, and hydrofluoric acid on the strength of glass, E. U. Condon and others have postulated the existence of surface "crevices". Electron microscope studies of glass have failed to reveal any such surface irregularities. It is proposed that all of these observed phenomena can be satisfactorily explained in terms of strained bonds, making the crevice assumption unnecessary.

2. When an ionic crystal (e.g. sodium chloride) is grown slowly from its melt, the partition of an impurity between the melt and the growing crystal may be expressed by the equation

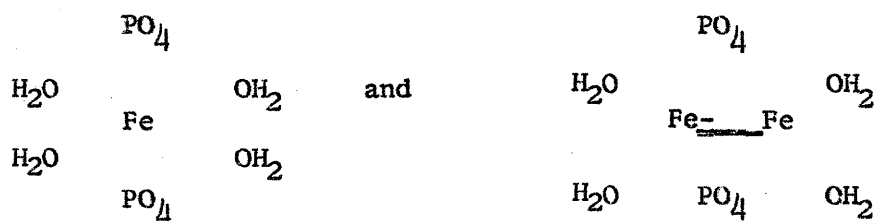
$$\frac{dI}{dx} = \frac{kI_0}{M^k} (M-X)^{k-1}$$

when M is the original weight of the melt, I_0 the total weight of impurity, x the weight of the growing crystal, I the total impurity in the crystal, and k the partition coefficient. This equation presupposes equilibrium conditions, which are not valid for the growth of a covalent crystal, such as germanium.

3. a) Although the digitalis-like drugs have two apparently different effects on the mammalian heart, it is proposed that both are caused by the same features of the drug molecule; the unsaturated lactone plus the configuration of the steroid nucleus are proposed as "toxiphores", the various OH and aldehyde groups as "auxitoxins". Despite opinions to the contrary (of. Fieser), the 14-hydroxyl group has not been shown to be necessary.

b) Using an "inverted saucepan" model for the drug molecule, it is suggested that the initial reaction involves a steric fit of the molecule onto a reactive site of the heart cell membrane, involving no subsequent penetration into the cell. The glycoside chain would seem to have no other role besides aiding this fit.

4. The iron atoms in the mineral Vivianite ($Fe_3(PO_4)_2 \cdot 8H_2O$) have the following arrangements (LC axis):



It is proposed that the blue pleochroic color found in some specimens is caused by a +1 oxidation of the two contiguous ferrous ions, i.e., $(Fe-Fe)^{+5}$.

PROPOSITIONS (continued)

5. The mineral cuprite is occasionally found in a hair-like modification known as chalcotrichite. It is proposed that the chalcotrichite corresponds to "whiskers" of the normal form of cuprite, i.e., crystals so perfect that they are capable only of one-dimensional growth.
6. With the sole exception of the M center, no alkali halide color centers have been shown to involve anion-cation vacancy groups. This can be explained in terms of recombination centers.
7. The observed secular variations and inclination of the earth's magnetic field can be satisfactorily explained only if it is assumed that the heat transfer from the core to the mantle is sufficient to cause a gradual change in the dimensions of the liquid-solid boundary within the core.
8. The mineral kunzite develops a pink color upon exposure to long-wave ultraviolet light and turns green when subjected to more energetic radiation. It is proposed that these colors are due to excited states of manganese ions present as impurities.
9. A continuous flow process for gas chromatography is impossible unless the liquid phase is in motion with respect to the point of injection. The weaknesses of such a process are discussed and it is proposed that the vortex tube would be a more successful means of large scale separations of vapor mixtures.
10. Tetramethyl dioxane can exist in seven isomeric forms including two pairs of enantiomorphs. It is proposed that all of these isomers can be synthesized in pure and unambiguous configurations from the various isomers of 2,3-butanediol.
11. It is proposed that the laws of nature are invariant with respect to the gender of the observer, and that the observed discrepancies are caused by masculine and feminine observers using different systems of units.